PRODUCTION OF HIGH PURITY SILICA FROM RICE HUSK AS A SOLID SUPPORT FOR HPLC AND GC COLUMN

DAMRONGSAK JADSADAPATTARAKUL

A THESIS SUBMITTED IN PARTIAL FULFILLMENT

OF THE REQUIEMENT FOR THE DEGREE OF

MASTER OF SCIENCE IN CHEMISTRY

SCHOOL OF GRADUATE STUDIES

KING MONGKUT'S INSTITUTE OF TECHNOLOGY LADKRABANG

2004

ISBN 974-9708-07-5

หัวข้อวิทยานิพนธ์	การผลิตซิลิกาความบริสุทธิ์สูงจากแกลบเพื่อใช้เป็นของแข็งยึดเกาะสำหรับคอลัมน์ HPLC และ GC
นักศึกษา	นายดำรงค์ศักดิ์ เจษฎาภัทรกุล
รหัสประจำตัว	44065505
ปริญญา	วิทยาศาสตรมหาบัณฑิต
สาขา	เคมี (เคมีวิเคราะห์)
พ.ศ.	2547
อาจารย์ผู้ควบคุมวิทยานิพนธ์	ผศ. คณิตา ดังคณานุรักษ์
อาจารย์ผู้ควบคุมวิทยานิพนธ์ร่วม	ดร.ชัญชณา ธนชยานนท์ (มีนกาญจน์)

บทคัดย่อ

การวิจัยครั้งนี้มีจุดมุ่งหมายเพื่อศึกษาความเป็นไปได้และข้อจำกัดของการใช้แกลบข้าวเป็นวัตถุดิบในการผลิตอนุภาคซิลิกาที่มีความบริสุทธิ์สูงสำหรับใช้ในคอลัมน์โครมาโทกราฟีแบบของเหลวสมรรถนะสูง (HPLC) และแบบแก๊ส (GC) เนื่องจากคอลัมน์ทั้งสองที่ผลิตขายเชิงการค้ามีราคาแพงมากและต้องนำเข้าจากต่างประเทศ งานวิจัยนี้จึงมุ่งหวังที่จะพัฒนากระบวนการผลิตอนุภาคซิลิกาที่ใช้สำหรับคอลัมน์โครมาโทกราฟีทั้งสองชนิดให้มีราคาถูกลง ทำโดยเผาแกลบข้าว 50 กรัมที่อุณหภูมิ 700°C เป็นระยะเวลา 1 ชั่วโมง จากนั้นจึงนำเถ้าแกลบที่ได้มารีฟลักซ์ กับสารละลายโซเดียมไฮดรอกไซด์ 10% (w/v) ที่อุณหภูมิ 80-85°C เป็นเวลา 1 ชั่วโมง กรองและปรับปริมาตรของสารละลายโซเดียมซิลิเกตให้มีความเข้มข้นประมาณ 1% (w/v) จากนั้นตกตะกอนสารละลายโซเดียมซิลิเกตด้วยกรดไฮโดรคลอริก และนำมาผลิตเป็นอนุภาคด้วยเทคนิคพ่นแห้ง (สำหรับคอลัมน์ HPLC) และเทคนิคบด (สำหรับคอลัมน์ GC) พบว่าซิลิกาที่ผลิตได้มีความบริสุทธิ์มากกว่า 99%, โครงสร้างเป็นแบบอสัญฐาน สำหรับคอลัมน์ HPLC ซิลิกาที่ผลิตได้มีลักษณะเป็นรูปทรงกลม ขนาดอนุภาคเฉลี่ย 21.52 μm, พื้นที่ผิวเฉลี่ย 307.28 m^2/g และมีขนาดรูพรุนสูงสุด 60 Å ซึ่งจะถูกนำมาสังเคราะห์เป็น silica-ODS (C18) และทำการคัดแยกขนาดอนุภาคอีกครั้งเพื่อให้ได้อนุภาคที่มีขนาดใกล้เคียงกับ 10 μm ในการบรรจุคอลัมน์ HPLC ใช้เทคนิคการบรรจุแบบเปียก สำหรับคอลัมน์ GC ซิลิกาที่ผลิตได้มีรูปร่างไม่แน่นอน, ขนาดอนุภาคอยู่ในช่วง 150-180 μm, พื้นที่ผิวเฉลี่ย 135.56 m^2/g และมีขนาดรูพรุนสูงสุด 300 Å ใช้อนุภาคซิลิกาที่ผลิตได้บรรจุลงในคอลัมน์ GC โดยตรงด้วยเทคนิคการบรรจุแบบแห้ง ผลการทดลอง สำหรับคอลัมน์ HPLC พบว่า carbon loading 17.72%, ขนาดอนุภาคเฉลี่ย 14.92 μm, ความหนาแน่นแท้จริง

เฉลี่ย 1.6519 g/cm^3 และมีค่าความสูงของเพลททางทฤษฎี (*H*) ต่ำสุด 0.0467 cm ที่อัตราการไหลของเฟสเคลื่อนที่เท่ากับ 0.3 ml/min (ทดสอบกับสารมาตรฐานฟีนอล 5000 ppm, ปริมาตร 1.0 µl และใช้เฟสเคลื่อนที่เป็นเมทานอล 100%) สำหรับกรณีคอลัมน์ GC พบว่ามีค่า *H* ต่ำสุด 0.100 cm ที่อัตราการไหลของแก๊สพาเท่ากับ 6.76 ml/min (ทดสอบกับสารมาตรฐาน n-pentane, ปริมาตร 0.2 µl, ใช้แก๊สพาเป็น N_2)

Thesis Title	PRODUCTION OF HIGH PURITY SILICA FROM RICE HUSK AS A SOLID SUPPORT FOR HPLC AND GC COLUMN
Student	Mr. Damrongsak Jadsadapattarakul
Student I.D.	44065505
Degree	Master of Science
Programme	Chemistry (Analytical Chemistry)
Year	2004
Thesis Advisor	Assistant Professor Kanita Tangkananurak
Thesis Co-advisor	Dr. Chanchana Thanachayanont (Meenakarn)

ABSTRACT

The aim of this research was to investigate possibilities and limitation in using rice husk to produce silica particles for high performance liquid chromatography (HPLC) and gas chromatography (GC). Because of commercial HPLC and GC columns were very expensive and could be imported from foreign countries, the main purpose of the present research work was to develop the chromatographic silica particle preparation process, which reduced cost of the two columns. The process started with burning 50 g of rice husk at 700°C for 1 hour. Then, rice husk ash was refluxed with 10% (w/v) sodium hydroxide solution at 80-85°C for 1 hour, and then precipitated with hydrochloric acid that produced the silica particulate form by spray drying (for HPLC column) and grinding (for GC column) technique. The obtained silica products have purity above 99% and amorphous form. For HPLC column, silica particles had spherical shape and average particle size of 21.52 μm, average surface area of 307.28 m^2/g and major pore size of 60 Å. After that, silica particles were synthesized into silica-ODS (C18) and particle size approximately of 10 μm (the popular particle size used and has the high efficiency for separation) were selected. The HPLC column packing was performed using wet packing (slurry packing) technique. For GC column, silica particles had irregular shape and particle size between 150 and 180 μm, average surface area of 135.56 m^2/g and major pore size of 300 Å. In the case of GC column, bare silica was directly packed into the column using dry packing technique. For HPLC column, carbon loading of 17.72%, average particle

size of 14.92 μm, average true density of 1.6519 g/cm^3 and theoretical plate height minimum value (*H*) of 0.0467 cm at 0.3 ml/min of 100% methanol (tested with standard phenol 5000 ppm and injection volume of 1.0 μl) were obtained. For the GC column, *H* minimum value of 0.100 cm at carrier gas flow-rate of 6.76 ml/min (tested with standard n-pentane, injection volume of 0.2 μl and carrier gas used as N_2)

ACKNOWLEDGEMENT

The author would like to express sincere thanks to my advisor, Asst. Prof. Kanita Tangkananurak and co-advisor, Dr. Chanchana Thanachayanont (Meenakarn), (Researcher, National Metal and Materials Technology Center (MTEC)) for their inspiration, encouraging and helpful suggestion throughout this research.

The extend many thanks to Assoc. Prof. Arunee Kongsakphaisal and Asst. Prof. Dr. Tawan Suknoi for useful advice and characterization instrument facility.

Appreciation is also extended to Mr. Srichalai Khunton, (Researcher, Metallurgy and Materials Science Research, Chulalongkorn University), Asst. Prof. Dr. Ladawan Padungtrab, (Department of Chemistry, Mahidol University), and Assoc. Prof. Dr. Surapote Wongyai, (Dean, Faculty of Oriental Medicine, Rangsit University).

Sincere thanks for assists from Miss Ubon Rerk-am, Miss Kadsirin Sonoum, Miss Luksana Jiramitmongkon, Miss Wonpen Prasittiwong, Miss Sirinlux Kerdsiri, Mr. Sanit Chaiya, Miss Siripan Chantrasakul, Miss Bunyachat Itdiwattana, Ms. Chatporn klaikeow, and everyone who has associated in this research. Furthermore, I was greatly indebted and gratitude to my family for their love, support and encouragement.

Finally, thanks to National Metal and Materials Technology Center (MTEC), National Science and Technology Development Agency (NSTDA) for financial support in this work (Budget year 2003).

DAMRONGSAK JADSADAPATTARAKUL

TABLE OF CONTENTS

TABLE OF CONTENTS (Continued)

TABLE OF CONTENTS (Continued)

TABLE OF CONTENTS (Continued)

LIST OF TABLES

LIST OF TABLES (continued)

LIST OF FIGURES

LIST OF FIGURES (continued)

LIST OF FIGURES (continued)

Figure No. Page

LIST OF FIGURES (continued)

LIST OF FIGURES (continued)

Figure No. Page

ABBREVIATIONS

HPLC	: High performance liquid chromatography
GC	: Gas chromatography
GLC	: Gas-liquid chromatography
GSC	: Gas-solid chromatography
Silica-ODS	: Chemically bonded phase of silica with octadecyltrichlorosilane
C18	: Octadecylsilane
H	: The theoretical plate height
N	: The theoretical plate number
t_r	: Retention time
W_b	: Peak width at based peak
$W_{0.1}$	: Peak width at 1/10 of plate high
CP-MAS	: Cross polarization – magic angle spinning
FTIR	: Fourier transform infrared spectroscopy
TGA	: Thermal gravimetric analysis
^{29}Si solid state NMR	: Silicon solid state nuclear magnetic resonance
SEM-EDS	: Scanning electron microscope – energy dispersive spectroscopy
XRD	: X-ray diffraction
XRF	: X-ray fluorescence

CHAPTER 1

INTRODUCTION

1.1 PROBLEM STATEMENT

Thailand is one of the largest rice producing countries in the world. Therefore, a large quantity of rice husk is generated as a by-product of rice milling. It has been estimated that 4.4-4.6 million tons of rice husk is produced every year and has the potential of heat (overall gross calorific value of rice husk is 2,900-4,560 kcal/kg) equal to crude oil of 1.46-1.53 million tons (calorific value is 9,900 kcal/kg) [1]. Rice husk can be used as fuel for the small electrical generator power plants that production power of 25-50 megawatt. Today in Thailand, a lot of electrical generator power plants that use rice husk as a fuel source are established increasing every year. So, the large quantities of by-product (rice husk ash) are generated. After burning of rice husk, 16-22% rice husk ash are obtained (>90% SiO_2). Furthermore generally, source of silica is sand which production of silica from this source was required the high energy and complicate specific equipment. From all reasons, rice husk has a high potential for silica production in order to save the energy consumption, money and increase agriculture product waste value. From previous study have found that rice husk consist of ash 20%, lignin 22%, cellulose 38%, pentosans 18%, and other organics 2%. After burning at 450-500°C, rice husk ash have silicon dioxide major component more than 90%, siloxane (Si-O-Si) structure, and silanol groups (Si-OH) [2].

1.2 OBJECTIVE OF THE STUDY

1. Find an optimum process for high purity silica production from rice husk.
2. Produce low cost high purity silica particles as a solid support of stationary phase for HPLC and GC column.
3. Produce the HPLC and GC low cost column.

1.3 SCOPE OF THE STUDY

1. Study of silica gel production process from rice husk, which has appropriate characteristics for usage in HPLC and GC column.
2. Synthesis of silica-ODS for HPLC and silica gel for GC application.
3. Study of characterization of silica and silica-ODS.
4. Study of HPLC and GC column packing techniques.
5. Evaluate of chromatographic column efficiencies.

1.4 PROCESS OF THE STUDY

1. Study of thermogravimetric analysis of rice husk
2. Study of optimum burning conditions of rice husk
3. Study of quantity and concentration of NaOH that used for dissolve of silica in rice husk ash into sodium silicate solution.
4. Study of high purity silica gel production process from sodium silicate solution.
5. Study of characterization of silica gel that produced.
6. Study of synthesis process of silica-ODS for HPLC.
7. Study of characterization of silica-bonded phase that produced.
8. Study of HPLC and GC column packing process.
9. Study of chromatographic column efficiency evaluation.

CHAPTER 2

THEORY AND LITERATURE REVIEWS

2.1 PROPERTIES OF RICE HUSK

The rice grain, commonly called a seed, consists of the true fruit or brown rice (caryopsis) and the hull, which encloses the brown rice. Brown rice consists mainly of the embryo and endosperm. The surface contains several thin layers of differentiated tissues that enclose the embryo and endosperm. The palea, lemmas, and rachilla constitute the hull of indica rices. In japonica rices, however, the hull usually includes rudimentary glumes and perhaps a portion of the pedicel. A single grain weighs about 10-45 mg at 0% moisture content. Grain length, width, and thickness vary widely among varieties. Hull weight averages about 20% of total grain weight [3].

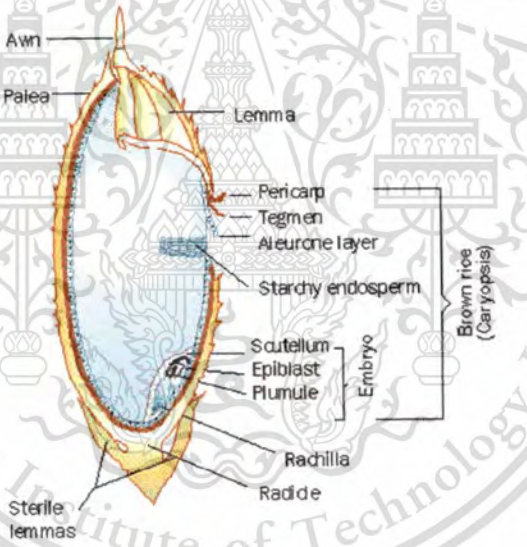

Fig. 2.1 Morphology of rice seed [3].

The overall gross calorific value of rice husk was 2,900-4,560 kcal/kg [1]. The composition of rice husk depends on agricultural, geographical and meteorological factors. Reported data may also be influenced by sample preparation and analysis method. From previous study have found that rice husk consists of ash 20%, lignin 22%, cellulose 38%, pentosans 18%, and other organics 2%. After burning at 450-500°C, rice husk ash have silicon dioxide major component more than 90% [2].

2.2 SILICA CHEMISTRY

The term silica denotes the compound silicon dioxide. Silicon dioxide is the most common binary compound of silicon and oxygen, the two elements of greatest terrestrial abundance. It constitutes *ca.* 60 wt. % of the earth's crust (in the form of sand), occurring either alone or combined with other oxides in silicates. It is thus a ubiquitous chemical substance and, owing to its rich chemistry, is of great geological importance. Commercially, it is the source of elemental silicon and is used in large quantities as a constituent of building materials.

Generally, silica is produced from reaction between sand (silica source) and soda ash at high temperature as shown in Fig. 2.2. Silica can be separated into two types, crystalline and amorphous, which both can be found in nature and synthesized for special uses. Both types have some common properties.

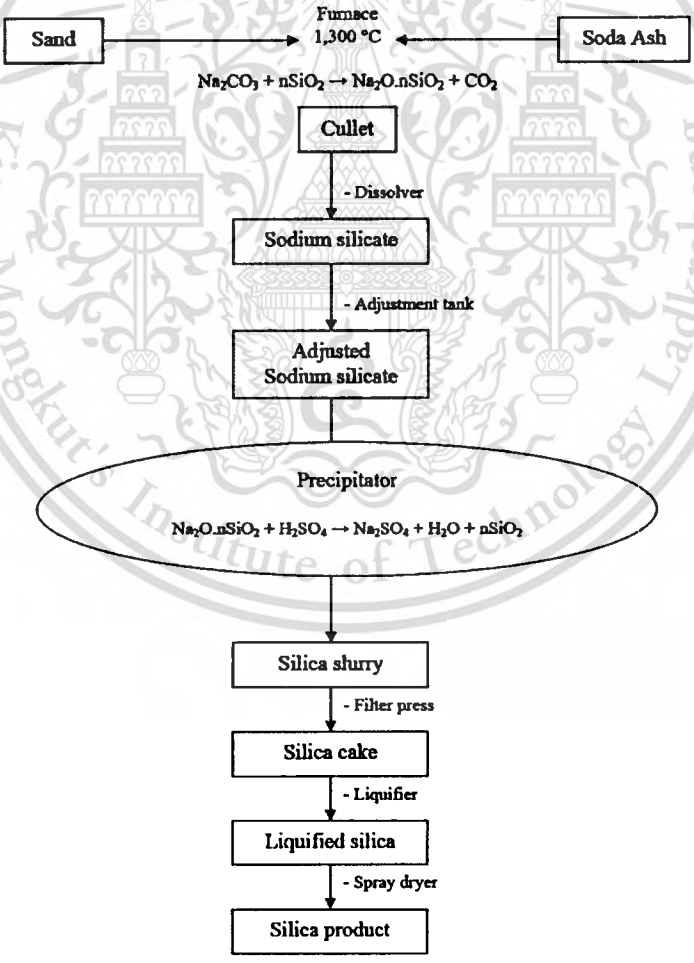

Fig. 2.2 Silica production process.

At ordinary temperatures, silica is chemically resistant to many common reagents. Acids do not attack silica, except for hydrofluoric acid which forms fluorosilicate anions, *i.e.*, SiF_6^{2-} or volatile SiF_4. The rate at which the various forms (low-T modifications) of silica are dissolved by aqueous HF decreases with increasing of density (ρ) in the sequence: vitreous silica (ρ = 2.2 g/cm^3) < tridymite (ρ = 2.22 g/cm^3) ≅ cristobalite (ρ = 2.33 g/cm^3) < quartz (ρ = 2.65 g/cm^3). Coesite (ρ = 3.01 g/cm^3) is practically insoluble in aqueous HF. Stishovite (ρ = 4.35 g/cm^3) is even less soluble. Phosphoric acid attacks vitreous silica at elevated temperatures, forming a crystalline silicophosphate. The solubility of silica is greater in dilute than concentrated aqueous phosphoric acid. Quartz and vitreous silica are affected only slightly by aqueous alkali at room temperature. The attack is faster at higher temperatures. Precipitated amorphous silica is more reactive than vitreous silica, which in turn is more reactive than quartz.

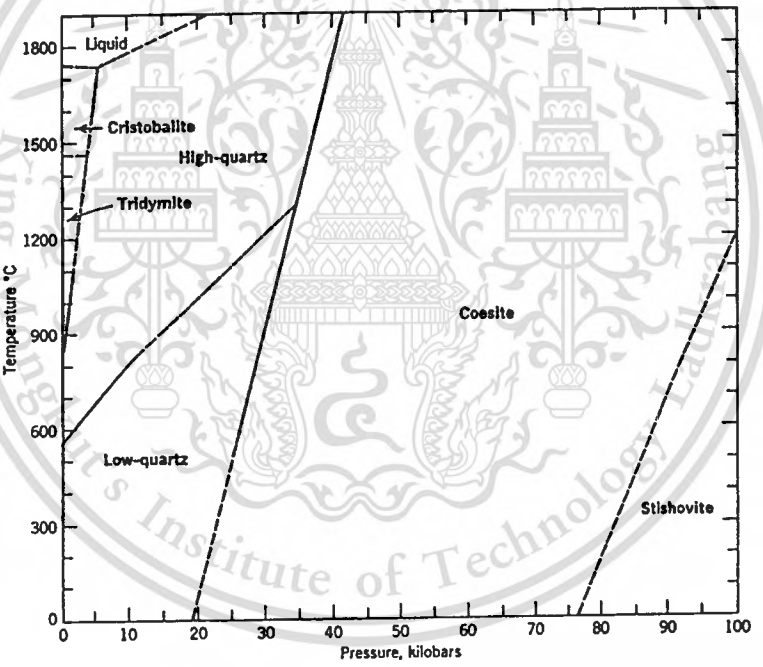

Fig. 2.3 Phase diagram of silica forms [4].

2.2.1 FORM OF SILICA

CRYSTALLINE SILICA: Silica exists in a variety of polymorphic crystalline forms. According to the conventional view of the polymorphism of silica, there are three main forms at atmospheric pressure: quartz, stable below 870°C; tridymite, stable from 870-1,470°C; and cristobalite, stable from 1,470°C to the melting point at 1,723°C. In all these forms, the

structures are based on [SiO_4] tetrahedral linked in such a way that every oxygen atom is shared between two silicon atoms. The structures, however, are quite different in detail.

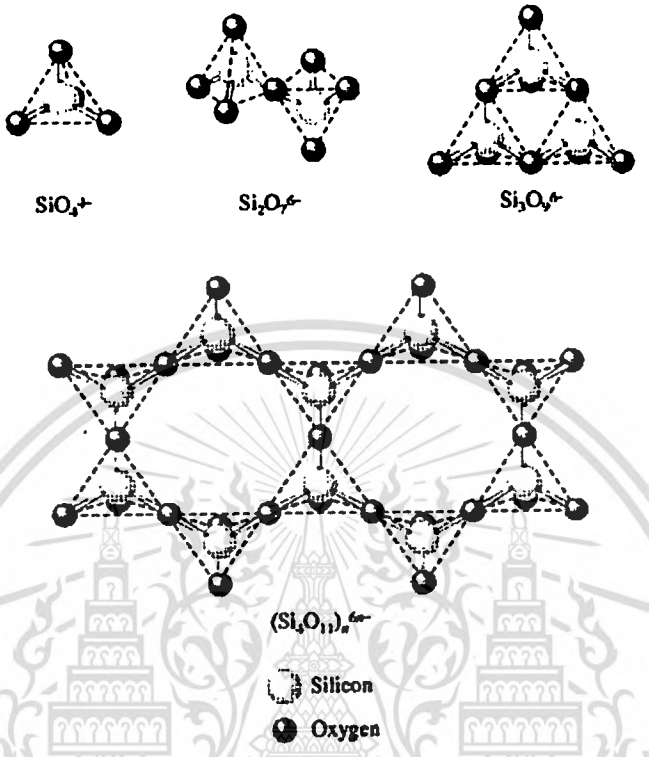

Fig. 2.4 The basic structure of SiO_4 tetrahedral bonds.

At the temperature limits of their stability ranges, these forms interconvert. The transformations involve a change in the secondary (non-nearest-neighbor) coordination and require the breaking and reforming of Si-O bonds. The transformation processes, known as reconstructive polymorphic transformations, are slow, as shown by the fact that the high temperature polymorphs can persist outside their normal stability range. The transformations are aided by or may require the presence of impurities or added mineralizer such as alkali metal oxides. Indeed, it has been suggested that tridymite cannot be formed at all in the absence of impurities, and some modern texts assert that pure SiO_2 occurs in only two forms, *i.e.*, quartz and cristobalite. In addition to the reconstructive transformations, each of the main forms of silica undergoes one or more transformations of a different sort, the so-called high-low, displacive, or martensitic transformations. These involve relatively small structural rearrangements such as minor rotations of the tetrahedra without bond-breaking. In general, they are quick and reversible.

The transformation among the principle crystalline forms of silica may thus be represented in simplified form:

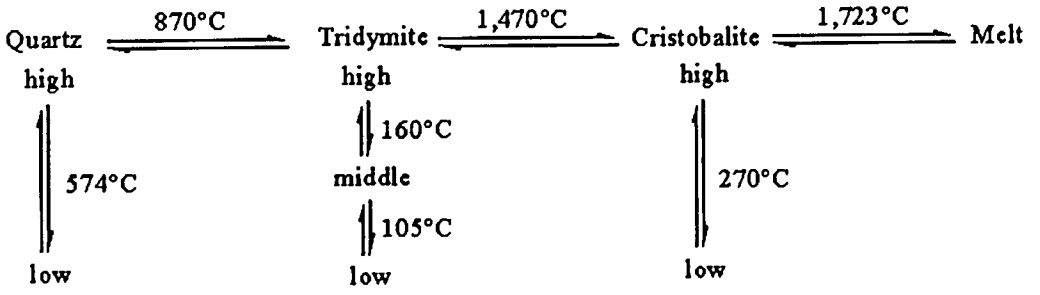

Fig. 2.5 The transformation of silica forms [5].

The vertical directions represent the quick, displacive polymorphic transitions, whereas the horizontal directions represent the sluggish reconstructive transitions.

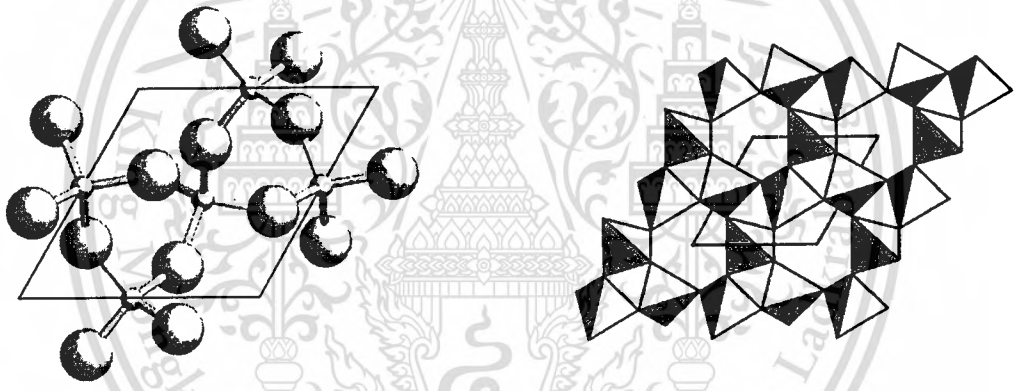

Fig. 2.6 Three-dimension structure of quartz in (a) molecular and (b) frame work [4].

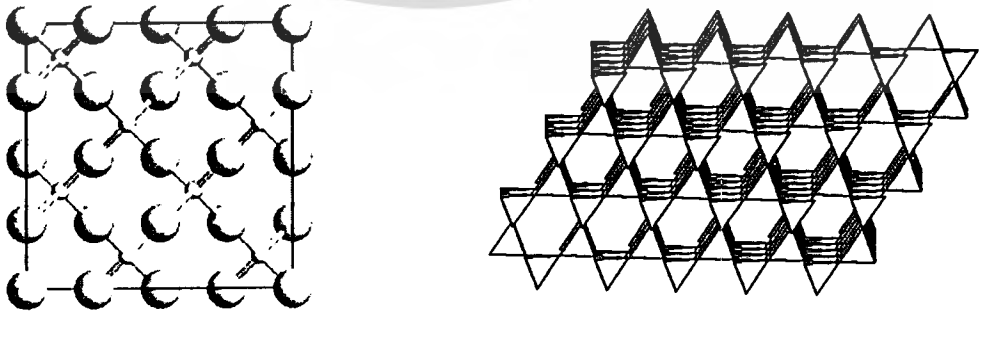

Fig. 2.7 Three-dimension structure of cristobalite in (a) molecular and (b) frame work [4].

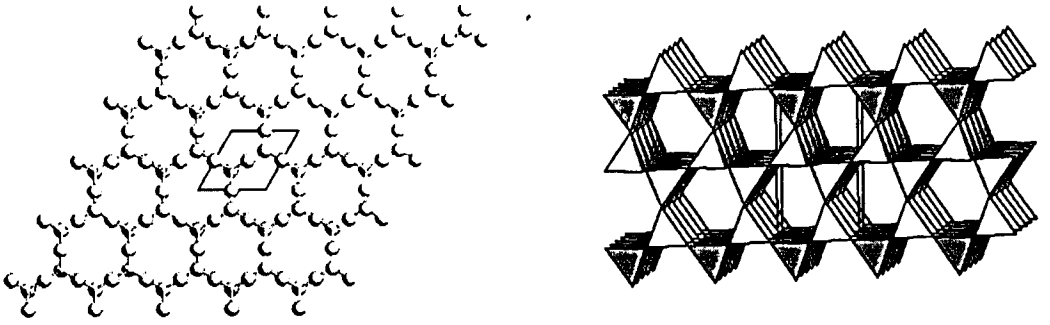

(a) (b)

Fig. 2.8 Three-dimension structure of tridymite in (a) molecular and (b) frame work [4].

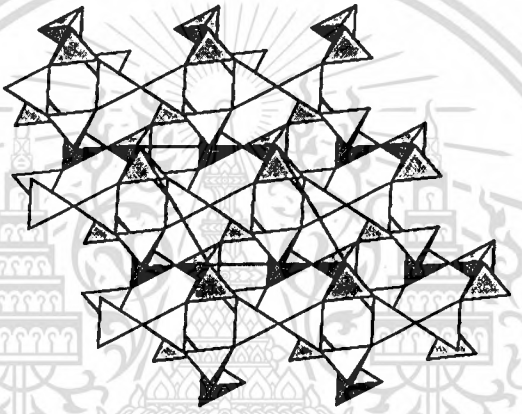

Fig. 2.9 Three-dimension structure of coesite in frame work [4].

NONCRYSTALLINE SILICA: The noncrystalline forms of silica include bulk vitreous silica and a variety of other amorphous types. Vitreous silica (silica glass) is essentially a super-cooled frozen-in liquid traditionally formed by fusion and subsequent cooling of crystalline silica. It is hardly found in nature except for some exotic species, *i.e.*, fused bodies resulting from lightning striking sand, or Libyan desert glass. Liquid silica is highly viscous, and freezing-in to the glassy form occurs readily at approximate 1,100°C. In practice, vitreous silica is prepared by fusion of crystalline quartz or quartz sand. Vitreous silica is also made by flame or plasma hydrolysis of silicon tetrachloride, by thermal decomposition of silicate esters, or by sputtering of SiO_2. Glasses are prepared by flame-fusion process may contain significant amounts (>1,000 ppm) of hydroxyl impurity which affect optical transmission as well as thermal and mechanical properties.

The structure of vitreous silica is a continuous network of [SiO_4] tetrahedra with a lower degree of order than the crystalline phases. The structure itself is subject to many speculations,

involving microcrystal theories and a complete random approach. The following is generally accepted: silica glass differs form crystalline silica in having a broader distribution of Si-O-Si bond angles, and a less negative Gibb's free energy of formation. As to the Gibb's free energy of formation, ΔG of vitreous silica is –849.05 kJ/mole; ΔG of low-T cristobalite is –849.76 kJ/mole; ΔG of low-T tridymite is –852.18 kJ/mole; ΔG of low-T quartz is –857.08 kJ/mole. This means silica glass and critobalite are closer to each other thermodynamicly than any other two silica species. From the width of the main broad diffraction peak in the glass diffraction pattern, the "crystallite size" in the case of silica glass was estimated at about 0.8 nm. Since the size of a unit cell of cristobalite is also about 0.8 nm, any crystallites would be only a single unit cell in extent; at such a scale, the terms amorphous and crystalline cease to make sense.

The properties of high quality vitreous silica which determine its uses include high chemical resistance, low coefficient of thermal expansion ($0.5\text{-}0.8 \times 10^{-6}\ K^{-1}$), high thermal shock resistance, high electrical resistivity, and high optical transmission, especially in the ultraviolet. Bulk vitreous silica is difficult to work because of the absence of network-modifying ions present in common glass. The traditional melting process requires temperatures of 2,000 $^{\circ}$C and more.

Amorphous silica exists also in a variety of forms, which are composed of small particles, possibly aggregated. Commonly encountered products include colloidal silica, silica gels, precipitated silica, and fumed or pyrogenic silica. Amorphous silicas are characterized by small ultimate particle size and high specific surface area. Their surfaces may be substantially anhydrous or may contain silanol (Si-OH) groups. They are frequently viewed as condensation polymers of silicic acid, $Si(OH)_4$. Colloidal silicas (silica sols) are stable dispersions of amorphous silica particles in water. Commercial products contain silica particles with diameters of *ca.* 3-100 nm, specific surface area of 50-270 m^2/g, with silica contents of 15-50 wt. %. They contain small amounts (<1 wt. %) of stabilizers, most commonly sodium ions.

Silica gels contain three-dimensional networks of aggregated silica particles of colloidal dimension. As formed, the pores are filled with the medium in which the gel is prepared. The medium gives the name to the product, e.g., hydrogel for water, alcogel for alcohols, etc. Simple removal of the liquid results in extensive shrinkage owing to surface-tension forces. Silica gels dried this way are termed xerogels. If the liquid in the pores is replaced by a substance which can be processed in the supercritical range (e.g., certain alcohols, or CO_2) and the gel is heated under pressure above the critical temperature of the liquid, resulting in the disappearance of the liquid-

vapor interface, surface-tension effects are absent and a very voluminous dry silica gel (aerogel) is obtained.

Precipitated silicas are powders obtained by coagulation of silica particles from an aqueous medium under the influence of high salt concentrations or other coagulants.

Fumed silicas (aerosils, pyrogenic silica) are produced by vapor-phase processes, generally by the vapor-phase hydrolysis of silicon tetrahalides. Other methods include vaporization of SiO_2, vaporization and oxidation of Si, and high temperature oxidation and hydrolysis of silicon compounds such as silicate esters.

Vaporization: silica vaporized principally by dissociation to gaseous SiO and O_2; these are the predominant vapor species, with some contribution from atomic oxygen and gaseous SiO_2. The total vapor pressure over the liquid at the melting point is in the range 1-10 Pa (10^{-5} – 10^{-4} bar). The boiling of silica is estimated as 2,797±75°C. The heat of vaporization of SiO_2 at the melting point is given as 560 kJ/mole, whereas the heat of the reaction is 750 kJ/mole.

$$SiO_2 (l) \rightarrow SiO + \tfrac{1}{2} O_2$$

Biogenic silicas are natural amorphous silicas. They occur from small organisms in water (diatom) and in plant cells. Dissolved silica is absorbed by the diatom or plant to form a silica skeleton. Diatomite (silica from diatom structure) is usually used as filler or filter medium. Silica in plant has little industrial used.

2.2.2 WATER SOLUBILITY

Water solubility highly depends on the crystalline or amorphous form of silica, and also on physico-chemical characteristics such as porosity, surface area and particle size. The water temperature, pressure and pH change the solubility of silica. The solubilization equation is

$$SiO_2 + 2H_2O \rightarrow Si(OH)_4 \qquad (2.1)$$

The solubility of crystalline and glass forms (amorphous) of silica is in the parts per million range (ppm = mg/l). The concentration of dissolved silica in rivers varies from 5 to 20 ppm [5].

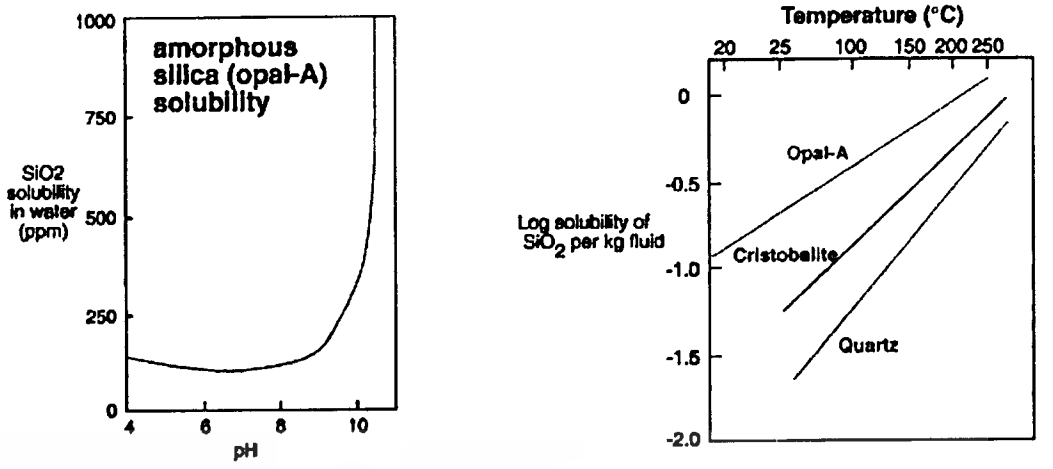

Fig. 2.10 Solubility of amorphous silica as a function of pH (a) and temperature (b) [5].

In seawater, the range is from 0.01 ppm in the Pacific ocean to 10 ppm in the Mediterranean sea [5]. The dissolved silica concentration is very sensitive to the presence and concentration of other salts.

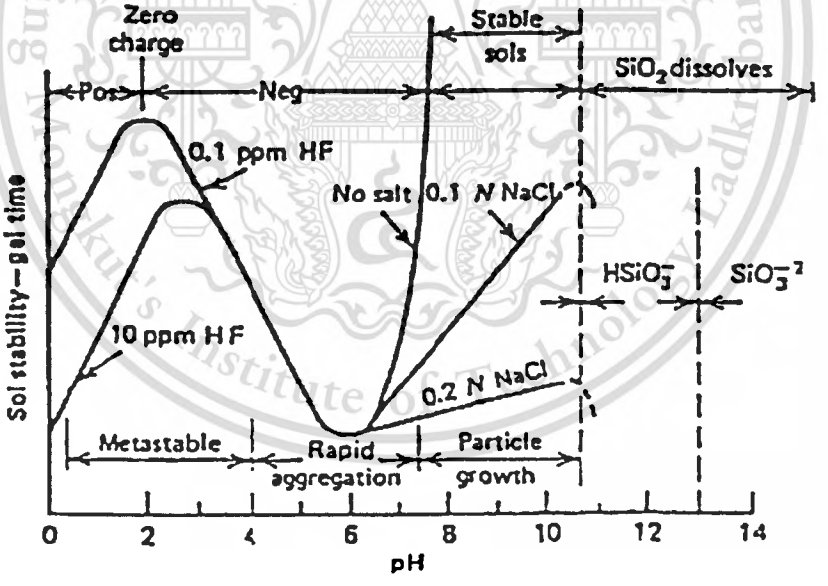

Fig. 2.11 Effect of pH in the colloidal silica-water system [5].

All living cell fluid contain a few ppm of dissolved silica. The solubility of silicic acid [$Si(OH)_4$] is greatly depends on the pH of the solution.

2.2.3 POLYMERIZATION OF SILICA GEL

The formation of silica gel can be regarded as taking place in two stages. In the first, initially formed $Si(OH)_4$ condenses to form colloidal particles. In dilute solution, a further slow increase in particle size is the only subsequent change, but at a concentration of about 1 percent silica, these primary particles are able to condense together to give a very open but continuous structure, extending throughout the medium, thus bestowing a certain degree of rigidity upon it. In both stages of polymerization, the mechanism is the same, that is, condensation to form Si-O-Si links, but in the first state, condensation leads to particles of massive silica, while in the second, since it is not possible to fit two particles accurately together over a common face, the number of Si-O-Si linkages between particles is fewer in number than those within the particles themselves. They are merely sufficient to bind adjacent particles together, in a fixed position relative to one another, and thereby lead to a rigid, highly porous, tangled network of branching chains [5].

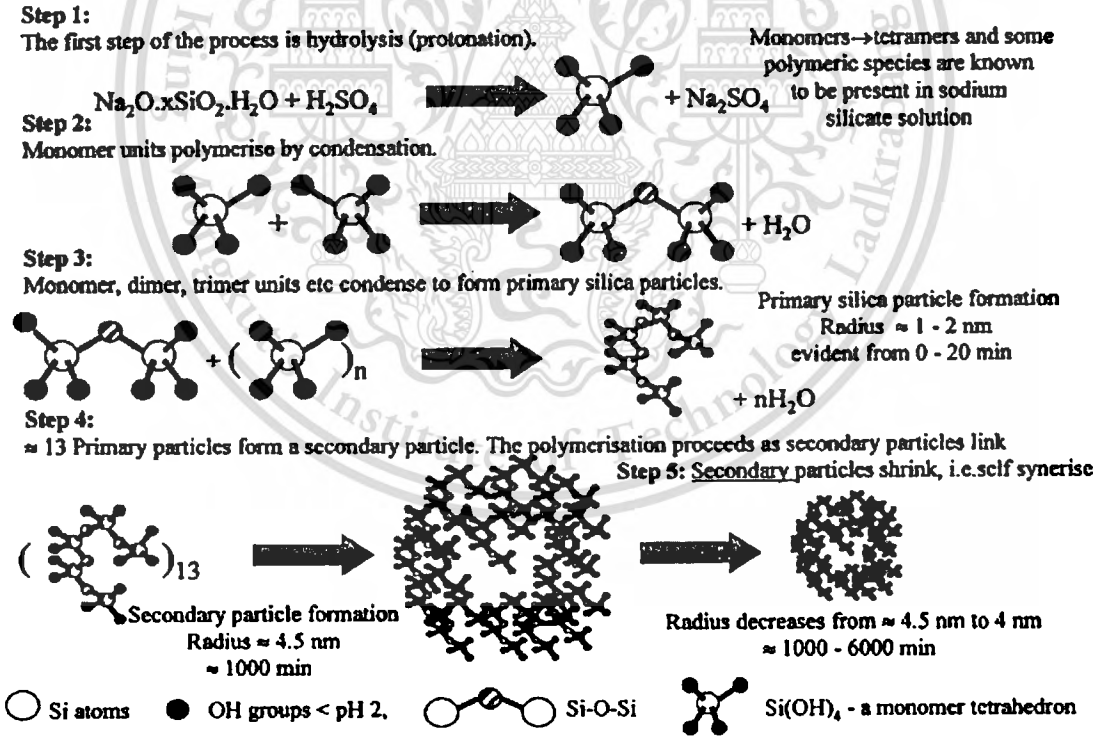

Fig. 2.12 The sequence of events leading up to silica hydrogel formation at low pH [6].

In polymerization process, there are many factors that can affect silica particle morphology such as temperature, concentration of the silicate solution, neutralizing acid solution, pH gradient, ionic strength, final pH, delay time for gel ageing, effect of additives (e.g., ammonia

acts as a coagulant) and the stirring energy or other external pressure or forces applied to the reactor [7].

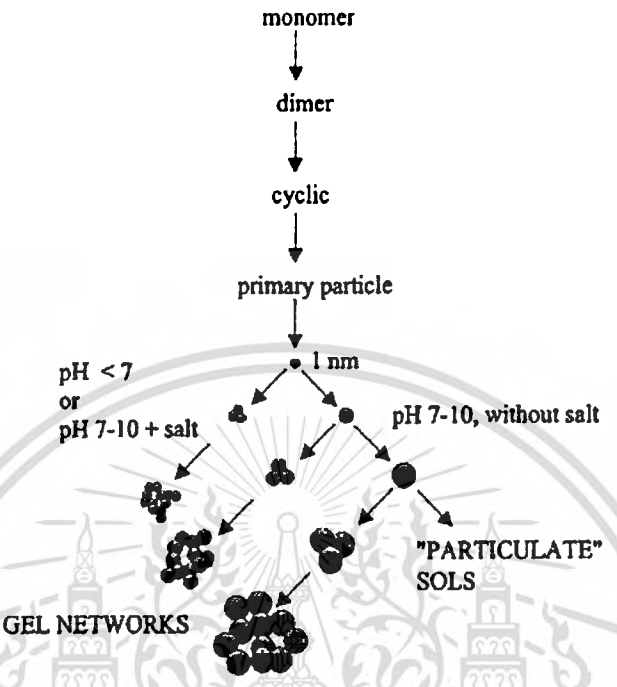

Fig. 2.13 Effect of ionic strength and pH gradient on the structure of silica obtained [5].

Fig. 2.13 illustrates the effect of two parameters, ionic strength and pH gradient. The pH value of sodium silicate is *ca.* 12. On addition of an acid, the pH can be rapidly lowered to 7 or slowly lowered to 10. A rapid decrease in pH induces very small microparticles, with diameters in the nanometer range. A gentle decrease in pH produces 100 times larger initial particles. A low ionic strength does not favour the three-dimensional organization and produces precipitates. A high ionic strength favours gel formation.

2.3 CHROMATOGRAPHIC THEORY

Chromatography is unique in the history of analytical methodology and is probably the most powerful and versatile technique available to the modern analyst. In a single procedure it can separate a mixture into its individual components and simultaneously determine quantitatively the amount of each component present. The samples may be gaseous, liquid or solid in nature and may range in complexity from a single substance to a multicomponent mixture containing widely differing chemical species. Furthermore, the analysis can be carried out, at one

extreme, on a very costly and complex instrument, and at the other, on a simple, inexpensive thin layer plate [8].

All chromatographic separations are carried out using a *mobile* and a *stationary* phase. As a result of this prerequisite, the primary classification of chromatography is based on the physical nature of the *mobile* phase. Thus, all separation processes that utilize a *gas* as the mobile phase are classed as gas chromatography. Conversely, all separation processes that utilize a *liquid* as the mobile phase are classified as liquid chromatography. In a similar manner the subclasses of chromatography are defined on a basis of the physical nature of the stationary phase. Consequently, if the mobile phase is a gas and the stationary phase is a liquid, then the technique is called gas-liquid chromatography (GLC) and if the mobile phase is a gas and the stationary phase is a solid, then the technique is called gas-solid chromatography (GSC). If the mobile phase is liquid, then there will be two complimentary sub-classes of liquid chromatography, that is, liquid-liquid chromatography (LLC) and liquid-solid chromatography (LSC). Table 2.1 shows the classification of chromatography in tabular form.

Table 2.1 Classification of chromatographic technique.

Mobile phase	Gas		Liquid	
Stationary phase	Liquid	Solid	Liquid	Solid
Chromatographic technique	**Gas-Liquid Chromatography**	**Gas-Solid Chromatography**	**Liquid-Liquid Chromatography**	**Liquid-Solid Chromatography**

2.3.1 DISTRIBUTION OF ANALYST BETWEEN PHASES

The distribution of analytes between phases can often be described quite simply. An analyte is in equilibrium between the two phases;

$$A_{Mobile} \rightleftharpoons A_{stationary}$$

The equilibrium constant, K, is termed the *partition coefficient*; defined as the molar concentration of analyte in the stationary phase divided by the molar concentration of the analyte in the mobile phase. The time between sample injection and an analyte peak reaching a detector at the end of the column is termed the *retention time* (t_R). Each analyte in a sample will have a

different retention time. The time taken for the mobile phase to pass through the column is called t_M [9].

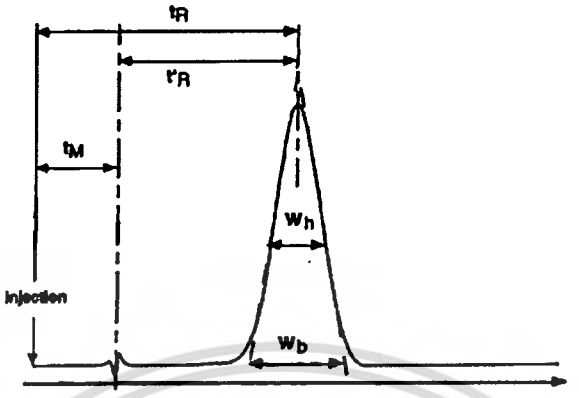

Fig. 2.14 Definitions of various chromatographic parameters [9].

A term called the *retention factor, k'*, is often used to describe the migration rate of an analyte on a column. You may also find it called the *capacity factor*. The retention factor for analyte *A* is defined as;

$$K'_A = \frac{(t_R - t_M)}{t_M} \tag{2.2}$$

t_R and t_M are easily obtained from a chromatogram. When an analytes retention factor is less than one, elution is so fast that accurate determination of the retention time is very difficult. High retention factors (greater than 20) mean that elution takes a very long time. Ideally, the retention factor for an analyte is between one and five. We define a quantity called the *selectivity factor*, α , which describes the separation of two species (A and B) on the column;

$$\alpha = \frac{k'_B}{k'_A} \tag{2.3}$$

When calculating the selectivity factor, species A elutes faster than species B. The selectivity factor is always greater than one.

2.3.2 BAND BROADENING AND COLUMN EFFICIENCY

To obtain optimal separations, sharp, symmetrical chromatographic peaks must be obtained. This means that band broadening must be limited. It is also beneficial to measure the efficiency of the column.

THE THEORECTICAL PLATE MODEL OF CHROMATOGRAPHY:

The plate model supposes that the chromatographic column is contains a large number of separate layers, called *theoretical plates*. Separate equilibrations of the sample between the stationary and mobile phase occur in these "plates". The analyte moves down the column by transfer of equilibrated mobile phase from one plate to the next.

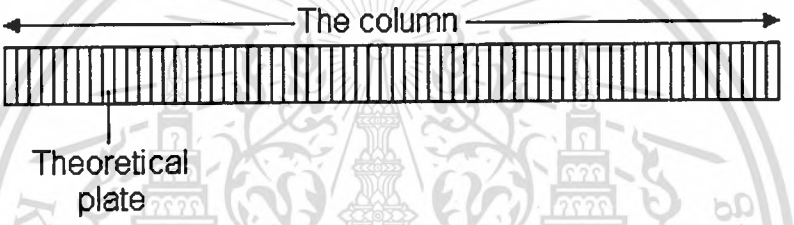

Fig. 2.15 Theoretical plate model [9].

It is important to remember that the plates do not really exist; they are a figment of the imagination that helps us understand the processes at work in the column. They also serve as a way of measuring column efficiency, either by stating the number of theoretical plates in a column, N (the more plates the better), or by stating the plate height; the *Height Equivalent to a Theoretical Plate* (the smaller the better). If the length of the column is L, then the *HETP* is

$$HETP = \frac{L}{N} \tag{2.4}$$

The number of theoretical plates that a real column possesses can be found by examining a chromatographic peak after elution;

$$N = \frac{5.55\, t_R^{\,2}}{w_{1/2}^{\,2}} = \frac{16\, t_R^{\,2}}{w_b^{\,2}} \tag{2.5}$$

Where $w_{1/2}$ and w_b are the peak width at half-height and at base peak respectively. As can be seen from this equation, columns behave as if they have different numbers of plates for different solutes in a mixture.

In case of asymmetric chromatographic peak, N can be estimated from [10]:

$$N = \frac{41.7\left(\frac{t_R}{w_{0.1}}\right)^2}{\left(\frac{A}{B}\right) + 1.25} \tag{2.6}$$

Where $w_{0.1}$ is peak width at 1/10 height = A + B. Draw a horizontal line across the peak at a height equal to 1/10 of the maximum height.

THE RATE THEORY OF CHROMATOGRAPHY

A more realistic description of the processes at work inside a column takes account of the time taken for the solute to equilibrate between the stationary and mobile phase (unlike the plate model, which assumes that equilibration is infinitely fast). The resulting band shape of a chromatographic peak is therefore affected by the rate of elution. It is also affected by the different paths available to solute molecules as they travel between particles of stationary phase. If we consider the various mechanisms which contribute to band broadening, we arrive at the Van Deemter equation for plate height;

$$HETP = A + B/u + Cu \tag{2.7}$$

Where u is the average velocity of the mobile phase. A, B, and C are factors which contribute to band broadening.

A – Eddy diffusion

The mobile phase moves through the column which is packed with stationary phase. Solute molecules will take different paths through the stationary phase at random. This will cause broadening of the solute band, because different paths are of different lengths.

***B* - Longitudinal diffusion**

The concentration of analyte is less at the edges of the band than at the center. Analyte diffuses out from the center to the edges. This causes band broadening. If the velocity of the mobile phase is high then the analyte spends less time on the column, which decreases the effects of longitudinal diffusion.

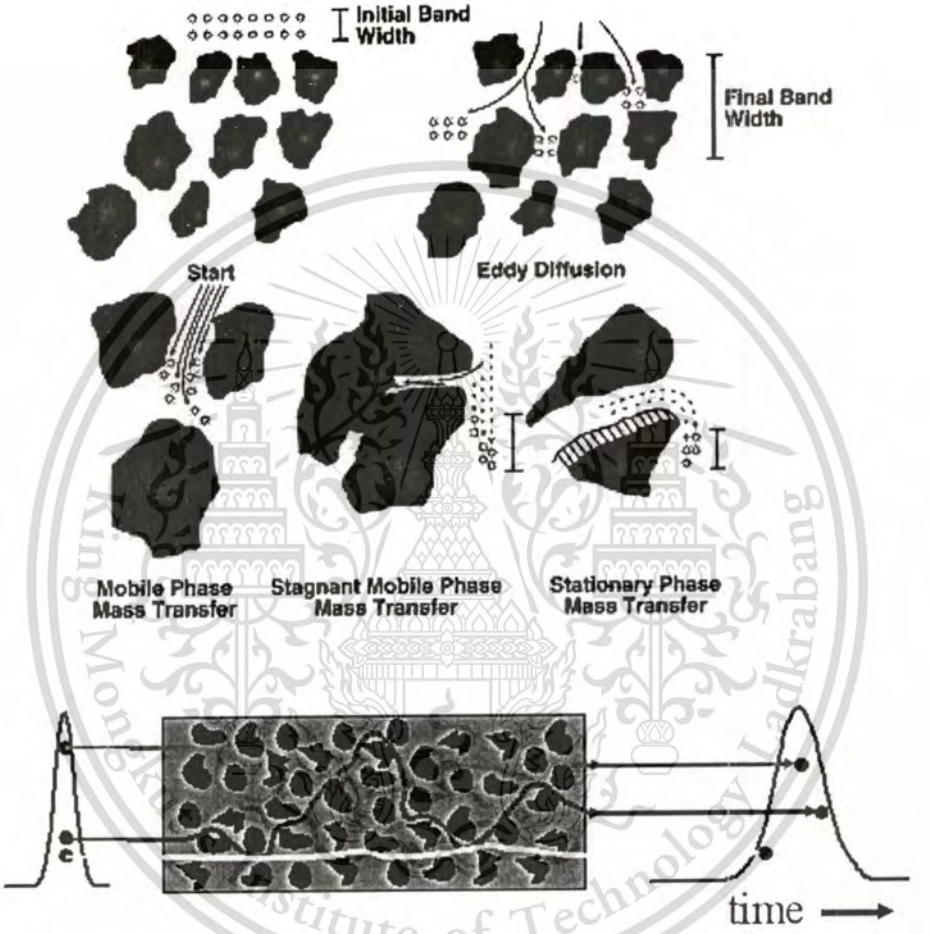

Fig. 2.16 Eddy diffusion model [11].

***C* - Resistance to mass transfer**

The analyte takes a certain amount of time to equilibrate between the stationary and mobile phase. If the velocity of the mobile phase is high, and the analyte has a strong affinity for the stationary phase, then the analyte in the mobile phase will move ahead of the analyte in the stationary phase. The band of analyte is broadened. The higher velocity of mobile phase, the worse the broadening becomes.

VAN DEEMTER PLOTS

A plot of plate height vs. average linear velocity of mobile phase. Such plots are of considerable use in determining the optimum mobile phase flow rate.

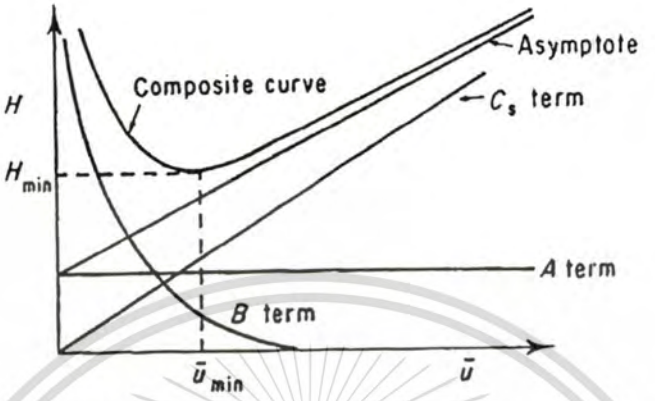

Fig. 2.17 A typical of Van Deemter plot [8].

RESOLUTION

Although the selectivity factor, α, describes the separation of band centres, it does not take into account peak widths. Another measure of how well species have been separated is provided by measurement of the *resolution*. The resolution of two species, A and B, is defined as

$$R = \frac{2\left[(t_R)_B - (t_R)_A\right]}{w_A + w_B} \tag{2.8}$$

Baseline resolution is achieved when $R = 1.5$. It is useful to relate the resolution to the number of plates in the column, the selectivity factor and the retention factors of the two solutes;

$$R = \frac{\sqrt{N}}{4}\left(\frac{\alpha - 1}{\alpha}\right)\left(\frac{1 + k'_B}{k'_B}\right) \tag{2.9}$$

To obtain high resolution, the three terms must be maximised. An increase in N, the number of theoretical plates, by lengthening the column leads to an increase in retention time and increased band broadening - which may not be desirable. Instead, to increase the number of plates, the height equivalent to a theoretical plate can be reduced by reducing the size of the stationary phase particles. It is often found that by controlling the capacity factor, k', separations

can be greatly improved. This can be achieved by changing the temperature (in Gas Chromatography) or the composition of the mobile phase (in Liquid Chromatography).

The selectivity factor, α, can also be manipulated to improve separations. When α is close to unity, optimising k' and increasing N is not sufficient to give good separation in a reasonable time. In these cases, k' is optimised first, and then a is increased by one of the following procedures:

1) Changing mobile phase composition in LC
2) Changing column temperature in GC
3) Changing composition of stationary phase
4) Using special chemical effects (such as incorporating a species which complexes with one of the solutes into the stationary phase)

2.4 HIGH PERFORMANCE LIQUID CHROMATOGRAPHY

High Performance Liquid Chromatography (HPLC) is by far the most common analytical separation technique. HPLC encompasses five main techniques;

ADSORPTION CHROMATOGRAPHY

Adsorption chromatography, often referred to as liquid-solid chromatography (LSC), is based on interactions between the solute and fixed active sites on a solid adsorbent used as the stationary phase. The adsorbent can be packed in a column, spread on a plan, or impregnated into a porous paper. The adsorbent is generally an active, porous solid with a large surface area, such as silica gel, alumina, or charcoal. The active sites, such as the surface silanol groups of silica gel, generally interact with the polar functional groups of the compounds to be separated. The nonpolar (e.g., hydrocarbon) portion of a molecule has only a compounds (e.g., separating alcohols from aromatic hydrocarbons) [12].

PARTITION CHROMATOGRAPHY

In partition chromatography, also referred to as liquid-liquid chromatography, the solute molecules distribute themselves between two immiscible liquid phases, the stationary phase and the mobile phase, according to their relative solubilities. The stationary phase is uniformly spread on an inert porous support or nonporous particulate solid or porous paper (paper chromatography). To avoid mixing of the two phases, the two partitioning liquids must differ

greatly in polarity. If the stationary liquid is polar (e.g., ethylene glycol) and the mobile phase is nonpolar (e.g., hexane), then polar components are retained more strongly; this is the usual mode of operation. On the other hand, if the stationary liquid is nonpolar (e.g., decane) and the mobile phase polar (e.g., water), polar components favor the mobile phase and elute faster. The latter technique (which has a reversed polarity) is referred to as reverse-phase LLC. Because of the subtle effects of solubility differences, LLC is well suited for separating homologs and isomers [12].

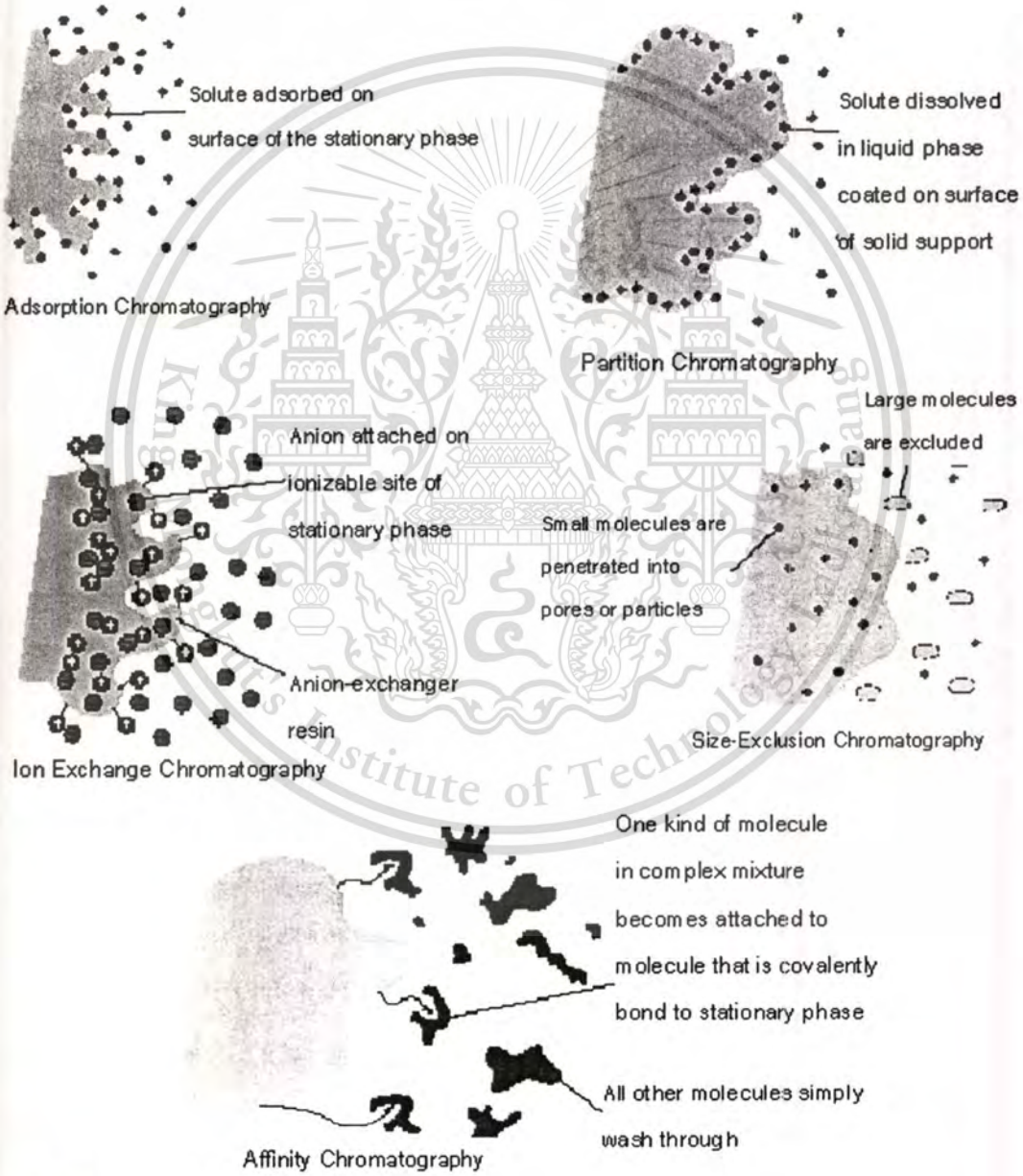

Fig. 2.18 Types of chromatography [11].

Most often, the stationary phase in LLC is chemically bonded to the support material rather than mechanically applied to it. This is referred to as bonded-phase chromatography (BPC). The separation mechanism of this technique is not clear, but both partition and adsorption mechanism may be involved, depending on experimental conditions. In HPLC, the use of BPC dominates all other modes [12].

ION-EXCHANGE CHROMATOGRAPHY

Ion-exchange chromatography, depicted in Fig. 2.18, is based on the affinity of ions in solution for oppositely charged ions on the stationary phase. Ion-exchange packings consist of a porous solid phase, usually a resin, onto which ionic groups are chemically bonded. The mobile phase is usually a buffered aqueous solution containing a counter ion whose charge is opposite to that of the surface groups-that is, it has the same charge as the solute-but which is in charge equilibrium with the resin in the form of an ion pair. Competition between the solute and the counter ion for the ionic site governs chromatographic retention. Ion-exchange chromatography has found wide application in inorganic chemistry for separating metallic ions, and in biological systems for separating water-soluble ionic compounds such as proteins, nucleotides, and amino acids [12].

SIZE-EXCLUSION CHROMATOGRAPHY

The mechanism of size-exclusion chromatography, also referred to as gel-permeation or gel-filtration chromatography, is shown in Fig. 2.18. Here, the stationary phase should be chemically inert. Size-exclusion chromatography involves selectivity diffusing solute molecules into and out of mobile phase-filled pores in a three-dimensional network, which may be a gel or a porous inorganic solid. The degree of retention depends on the size of the solvated solute molecule relative to the size of the pore. Small molecules will permeate the smaller pores, intermediate-sized molecules will permeate only part of the pores and be excluded from others, and the very large molecules will be completely excluded. The larger molecules will travel faster through the stationary phase and elute from the column first. Thus, size-exclusion chromatography is especially useful in separating high-molecular-weight organic compounds (e.g., polymers) and biopolymers from smaller molecules [12].

AFFINITY CHROMATOGRAPHY

In this case, highly specific biochemical interactions provide the means of separation. The stationary phase contains specific groups of molecules which can only adsorb the sample if certain steric and charge-related conditions are satisfied (cf. Interaction between antigens an antibodies). Affinity chromatography can be used to isolate proteins (enzymes as well as structural proteins), lipids, etc., from complex mixtures without involving any great expenditure [13].

2.4.1 HPLC INSTRUMENTATION

To facilitate acceptable mobile-phase flow rates, through packings of particle size in the range of 3 to 10 μm, pumping pressures in the order of 70 – 350 atm. are required. Equipment for HPLC is therefore more expensive than for other types of chromatography. Have a look at this schematic diagram of a "typical" HPLC setup.

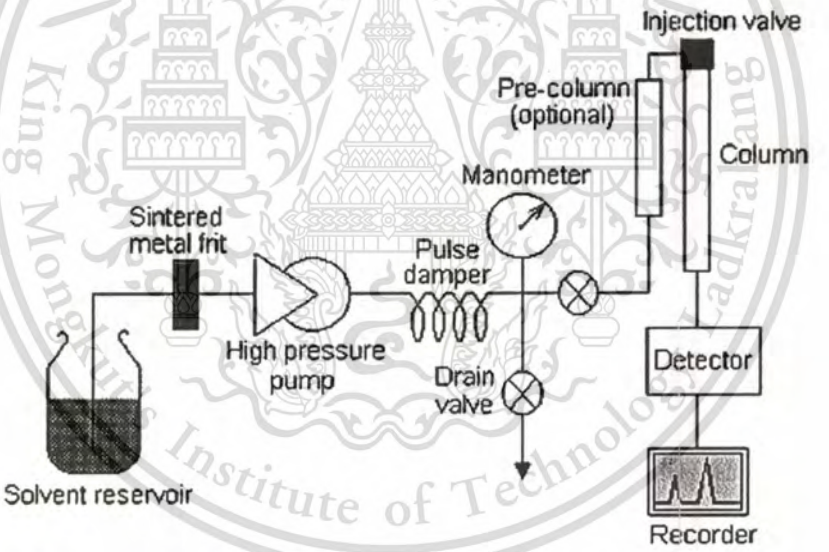

Fig. 2.19 HPLC instrumentation setup [14].

2.4.2 COLUMN FOR HPLC

Most HPLC columns are made of 316-grade stainless steel, which is austenitic chromium-nickel-molybdenum steel, USA standard AISI, resistant to the usual HPLC pressure and also relatively inert to chemical corrosion (chloride ions and lithium ions at low pH being important exceptions). The inside of the column should have no rough surfaces, grooves or microporous structures, so the steel tubes must be either precision drilled or polished or electropolished after common manufacturing, e.g. by drawing.

Columns, of i.d. 2-5 mm are generally used for analytical purposes. Wider columns of i.d. between 10 mm and 1 in (25.4 mm) may be used for preparative work. Some companies even market preparative columns of i.d. 30 cm and more.

Columns 5, 10, 15 or 25 cm long are common if microparticulate stationary phases of 10 μm or less are used. If higher plate numbers are needed it is usually better to use a packing with smaller particles than to lengthen the column. A longer column increases the retention volume, thus decreasing the concentration of the peak in the eluate and impairing the detection limit.

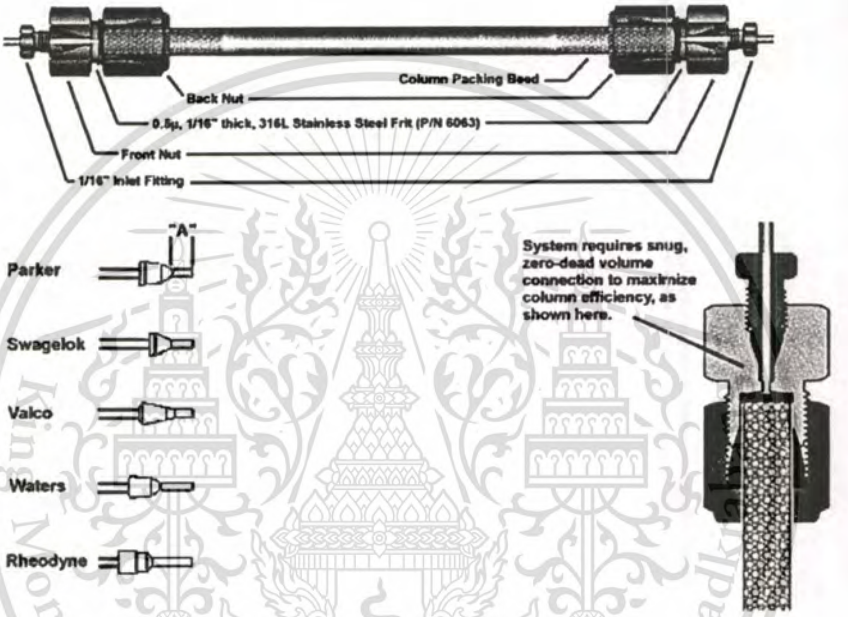

Fig. 2.20 Standard HPLC column hardware and fittings [15].

The column is closed off with steel frits of smaller pore size than the particle diameter of the column packing. The standard pore diameter is 2 μm but packings with particles of 3.5 μm or finer need 0.5 μm frits. If a frit is clogged it is bast to replace it; if you cannot afford this, try ultrasonic cleaning [13].

2.4.3 GENERAL PROPERTIES OF COLUMN PACKINGS

A large number of theoretical plates can only be achieved by ensuring short diffusion paths in the stationary phase pores; hence HPLC tends to favour microparticles. A sample molecule cannot penetrate more than 2.5 μm into a 5 μm particle. The particle size distribution should be as narrow as possible (with a ratio of diameters of the smallest and the largest particles of 1:1.5 or 1:2, as already mentioned). This is because the smallest particles determine the column permeability and the largest particles fix the plate number. Small particles produce a high flow

resistance and large particles are responsible for a high degree of band broadening. For this reason, a particle size analysis accompanies many products. But it says nothing about how large or how small the particles are at the two extremes. This particle size distribution representation may appear unusual, but is based on practical particle size analysis methods such as sieving, air separation, sedimentation, optical methods and the Coulter counter.

The properties of packing materials may vary from batch to batch of the same product, so a large amount of one batch should be bought for series analysis over a long period of time.

Various types of stationary phases are in use: porous particles, non-porous particles of small diameter, porous layer beads, perfusive particles, and monolithic materials [13].

POROUS PARTICLES

This is the usual type of HPLC stationary phase. These materials are 3, 3.5, 5 or 10 μm in size. As a rule of thumb, their performance, i.e. the plate number per unit length, doubles each time from 10 to 5 and 3 μm, whereas the pressure drop increases each time by a factor of four. Their internal structure is fully porous and can best be compared with the appearance of a sponge (however, in contrast to a sponge, the structure is very rigid). Within the pores the mobile phase (and the analytes) dose not flow but moves only by diffusion [13].

NON-POROUS, SMALL-DIAMETER PARTICLES

If the stationary phase is non-porous, the mass-transfer component of band broadening, the so-called *C* term of the van Deemter curve disappears or becomes very small because diffusion within pores does not occur. As a consequence, the curve becomes very flat to the right of its minimum and fast chromatography is possible without a loss in separation performance [13].

POROUS LAYER BEADS (PLB'S)

These are large particles with a diameter in the 30 μm range which allows to pack them dry. They consist of a non-porous core (e.g. from glass) which is covered with a 1-3 μm thick layer of a chromatographically active material. PLB's are rarely used nowadays but can be found in guard columns or as repair material for deteriorated columns with collapsed packing [13].

PERFUSIVE PARTICLES

In analogy to the non-porous phases the perfusive packings have also been developed for the fast separation of biopolymers. They consist of highly cross-linked styrene-divinylbenzene with two types of pores: very large throughpores with a diameter of 600-800 nm and narrow diffusion pores of 80-150 nm. The active stationary phase (e.g. a reversed phase, ion exchanger or affinity phase) fully covers the external and internal surface of the particles. The throughpores are wide enough to allow the mobile phase to flow through, whereas it stagnates in the diffusion pores. The analytes are rapidly transported in and out by the flowing eluent and diffusion paths in the narrow pores are short, therefore separation is fast and the van Deemter curve is very favourable. It is not necessary (and also not possible) to prepare really small particles: the typical diameter of perfusive particles is 20 μm. Their flow resistance is very low.

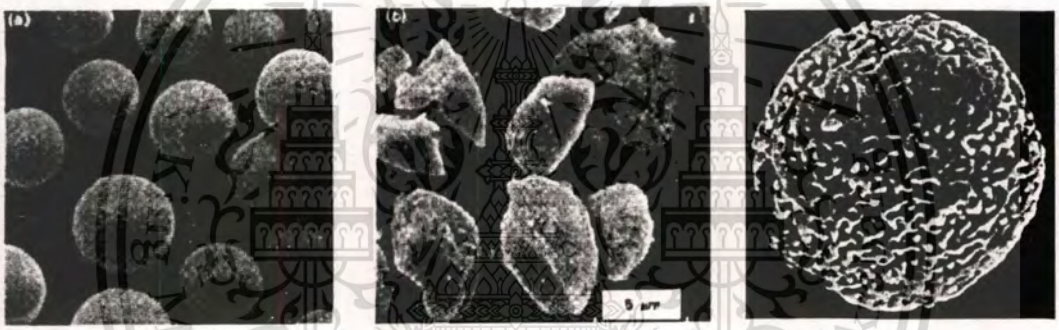

(a) (b) (c)

Fig. 2.21 Electron microphotographs of spherical (a), irregular (b) [16] and macro porous spherical (c) silica particle [17].

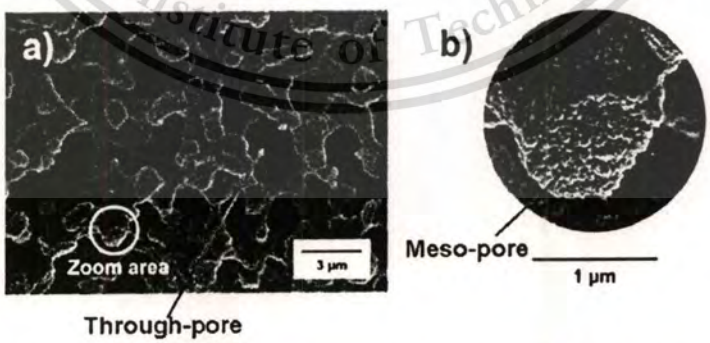

Fig. 2.22 Scanning electron micrographs of a monolithic column. (a) through-pore or marco-pore, (b) meso-pore [13].

MONOLITHIC STATIONARY PHASES

It is possible to synthesize stationary phases which consist of one single piece of porous material such as organic polymers or silica. With this concept, the chromatographic bed is not a packing of particles but a porous rod which totally fills the cylindrical volume of the column. The diameter of the large pores (where the mobile phase flows through) is e.g. 2 μm, the mean diameter of the skeleton structure is e.g. 1.6 μm, and the diameter of the mesopores is e.g. 12 nm. Such materials have a porosity of more than 0.8, their separation performance is similar to packed beds, and their van Deemter curve is very favourable [13].

2.4.4 SILICA

Silica is an adsorbent with outstanding properties. It may also be used for size-exclusion chromatography and forms the basic of numerous chemically bonded stationary phases. It consists of silicon atoms bridged three-dimensionally by oxygen atoms. Fig. 2.23 shows that the lattice is saturated at the surface with OH groups, the so-called silanol groups. Because the material is amorphous with a heterogeneous surface it is not easy to synthesize well-defined silicas.

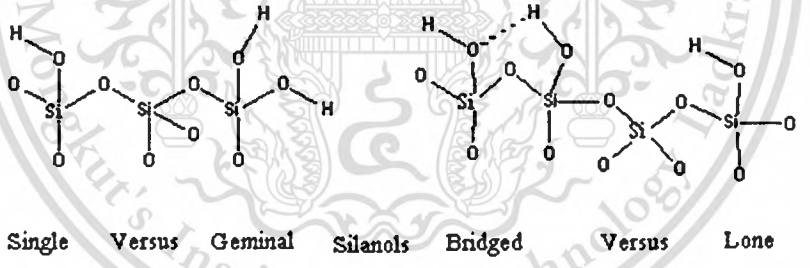

Fig. 2.23 Chemical structure of silica [20].

Although all functional groups at the surface act as adsorptive centers, the various types have different properties:

(a) Free silanols are slightly acidic, therefore basic compounds will preferably adsorb here. This effect can give rise to chemical tailing.

(b) Geminal silanols are not acidic.

(c) Associated silanols are not acidic. Compounds with OH groups tend to adsorb here.

(d) Silanols near metal cations are strongly acidic. They increase the heterogeneity of the surface and can badly affect the separation of basic compounds.

(e) Siloxanes are the product from the condensation of associated silanols. Heat treatment of silica increases the amount of siloxanes and decreases the silanol concentration.

Table 2.2 Comparison of various types of packing material [19].

Choosing the Right Base Material				
	Silica	**Alumina**	**Styrene-divinylbenzene**	**Methacrylate**
Organic Solvents	+++	+++	++	++
pH Range	+	++	+++	++
Swelling/Shrinking	+++	+++	+	+
Pressure Capability	+++	+++	++	+
Surface Chemistries	+++	+	++	+++
Efficiency	+++	++	+	+

+++Good ++Average +Poor

Silica can be produced by a number of different syntheses such as the complete hydrolysis of sodium silicate or the polymerization of emulsified polyethoxysiloxane, followed by dehydration. The gels obtained are irregular or spherical in shape, depending on the process.

IRREGULAR SHAPE

Irregular-shaped particles are obtained by milling and sizing of large particles. The original high-performance chromatographic packings were prepared by this technology. Many standard analytical methods are based on these materials. Irregular-shaped packings are available in larger sizes than spherical packings, but are not usually available less than 5 μm in diameter. A few have higher specific surface areas than those found in spherical particles. In general, irregular particles are more difficult to pack than spherical particles. Columns packed with small irregular particles may exhibit poorer packed bed stability than those prepared from spherical particles of the same size. However, the range of larger particle sizes and surface areas as well as their lower price makes irregular particles more attractive for larger scale preparative applications [19].

SPHERICAL SHAPE

The majority of currently available analytical packings are spherical. They are easier to pack than irregular packings. High performance, good column stability and low backpressure can be achieved reproducibly. Spherical materials are available with particle sizes from 3 μm to over 20 μm. The most popular particle size for analytical columns is 5 μm, but the use of short 3 μm columns is increasing. This is due to the fact that the technology for the preparation of 3 μm columns has improved over the last few years. Today, short 3 μm columns achieve the same column life time and performance as 5 μm columns, but provide the benefit of shorter analysis times. For reproducibility and high stability, spherical packings offer the best choice for analytical applications. The availability of larger particle sizes at reduced cost makes irregular-shaped packings attractive for preparative applications [19].

Table 2.3 Comparison between irregular and spherical types [19].

	Comparison	
	Irregular	**Spherical**
Stability	+	+++
Particle size range	+++	++
Analytical	+	+++
Preparative	+++	+

+++Good ++Average +Poor

Moreover, the properties of the end product depend on the reaction conditions (pH, concentration, additives, and even on stirring speed and vessel size). One of the most important parameters is the metal content of the starting materials because this will determine the concentration of acidic silanols. "Conventional" silicas are contaminated with up to 250 ppm sodium and 150 ppm aluminium besides other cations. Their surface reaction can even be basic, depending on the type and concentration of embedded ions. "Modern", low-metal silicas have not more than 1 ppm of sodium, calcium, magnesium and aluminium, plus slightly higher contents of iron. Only these materials are suited for the separation of basic compounds in both the normal-phase mode (as silicas) or the reversed-phase mode (as chemically bonded silicas).

Besides the shape (irregular or spherical), other physical properties can also vary between different brands:

(a) Pore width: It should be larger than 5 nm (50 Å). Macromolecules must be separated on wide-pore materials (30 nm = 300 Å or more).

(b) Specific surface area: This is inversely proportional to the pore width and is specified in m^2g^{-1}. The smaller the specific surface area, the lower are the retention factors at constant chromatographic conditions.

(c) Pore width distribution: a narrow pore width distribution is essential for symmetrical peaks.

(d) Density: The density of silica is ca. 2.2 g cm^{-3}; the packing density in the column varies according to the product within the range 0.3-0.6 g cm^{-3}.

The pH stability of silicas and silica-based bonded phases is restricted to the range of approximately pH 1-8. Silicas with pore widths up to 400 nm (an a particle size of 10 μm) are produced for use in size-exclusion chromatography. These stationary phases must have a well-defined pore width and pore-width distribution and no adsorptive properties.

SURFACE AREA AND PORE SIZE

The specific surface area of a packing is determined by the size of the structural elements that form its skeleton. This size is in turn closely linked to the pore size of the packing. Therefore there is a fundamental relationship between the specific surface area of a packing and the size of its pores, especially at constant specific pore volume. Packings with a small pore size have a large specific surface area, packings with a larger pore size have a small specific surface area. For example, packings with a specific pore volume of about 1 mL/g and a pore size of 10 nm (100 Å) have a specific surface area of 300 m^2/g, while a packing with the same specific pore volume and a pore size of 30 nm (300 Å) has a specific surface area of 100 m^2/g. You can use the following rule of thumb for the relationship between specific surface area, pore size and specific pore volume [19]:

$$SA \approx 3 \times \frac{SV}{PD} \tag{2.10}$$

SA is the specific surface area, *SV* is the specific pore volume and *PD* is the pore diameter.

PORE SIZE DISTRIBUTION

The pore-size distribution and the specific surface area can be determined by the same methods, that is, nitrogen adsorption and mercury porosimetry. The average pore size can also be determined by an inverted size-exclusion method, but a true pore-size distribution can not be established by this method. However, due to problems with the other methods, the inverted size-exclusion method might nevertheless be the method of choice for polymeric packings. The pore size is given either in nm or in Å. The values for the average pore size are nominal, and different manufacturers make different assignments. Therefore, one manufacturer's designation of 10 nm (100 Å) might be identical to another manufacturer's designation of 8 nm (80 Å) or 12 nm (120 Å) [19].

PORE SIZE AND MOLECULAR WEIGHT

The size of analyte molecules increases with molecular weight. If the size of the molecule is about one third of the pore size or larger, mass transport in the pores is severely hindered and low efficiency and peak broadening result. Under these circumstances, packings with a larger pore size should be used. For all standard analytical problems, packings with pore sizes between about 6 nm (60 Å) and 13 nm (130 Å) are typically used. The larger pore size packings can also be used for peptide separations. For analytes with a larger molecular weight, for example proteins, packings with a 30 nm (300 Å) pore size are more suitable. But these packings do not work well with smaller molecules due to the reduced surface area. For analytes with a molecular weight of less than 3,000, the smaller pore size should be used. If the molecular weight is larger than 10,000, packings with a pore size of 30 nm should be used. For analytes with a molecular weight between 3,000 and 10,000, both packings may give satisfactory results [19].

NONPOROUS PACKINGS

Nonporous packings can be used for analytes with a very high molecular weight that exhibit restricted diffusion in large-pore packings. However, only a limited surface area is available [19].

Table 2.4 Choosing the right pore size [19].

Choosing the Right Pore Size	
Analyte Molecular Weight	**Recommended Pore Size of Packing**
< 3,000	6 nm (60Å)-13 nm(130Å)
3,000-10,000	10 nm (100Å)
> 10,000 (for example, proteins)	30 nm (300Å)-100 nm (1000Å)
very large molecules	non-porous

SPECIFIC PORE VOLUME

The same techniques used for the measurement of the specific surface area and the pore size distribution yield results for the specific pore volume of a packing. However, it can be determined by other techniques as well, for example size exclusion chromatography or titration. It is reported in mL/g [19].

SPECIFIC PORE VOLUME AND PARTICLE STRENGTH

The specific pore volume is a measure of the empty space in a particle. The larger the specific pore volume, the smaller is the fraction of the particle that is occupied by the particle skeleton. Therefore, particles with a large specific pore volume are less strong than particles with a small specific pore volume. Silicas with a specific pore volume of 0.5 mL/g or less are mechanically extremely rugged. Many HPLC-grade silicas have a specific pore volume of 1 mL/g, which is generally sufficient for most applications [19].

SPECIFIC PORE VOLUME AND SIZE EXCLUSION CHROMATOGRAPHY

In size-exclusion chromatography, the particle porosity is one of the key parameters that determines the usefulness of a packing. The particle porosity increases with increasing specific pore volume. If silica-based packings are used for size-exclusion chromatography, packings with a specific pore volume of about 1 mL/g or higher are preferred [19].

Table 2.5 Comparison of various parameters between pore size and specific pore volume [19].

	Comparison	
	Pore Size	**Specific Pore Volume**
Retentivity	small	-
Capacity	small	-
Strength	small	small
Mass Transfer	large	-
Size Exclusion	-	large
Large Analytes	large	-

For retentivity, capacity and strength, packings with a small pore size should be selected. The lower limit is determined by mass transfer in the pores. For analytes with a larger molecular weight, packings with a larger pore size should be selected. For size-exclusion chromatography, packings with a large specific pore volume should be chosen.

BONDED PHASE AND MODE OF SEPARATION

Most analytical chromatography is carried out using packings whose sorption properties have been modified by attaching a covalently bonded phase to the surface of silica. Alternatively, the surface of a packing can be modified by coating it with a chemically stable adsorptive layer. Chemically stable bonds between the packing and the ligands that are responsible for retention are only available for silica and polymeric packings. The surface of the silica can easily be derivatized through silanization. The most commonly used HPLC packing is obtained by derivatization of the surface of a silica sorbent with a long-chain aliphatic silane. The aliphatic chain is 18 carbons long, and the packing is called C18 or ODS (for octadecyl silane). However, several other surface derivatizations of silica are available which result in packings with widely varying properties. Also polymeric packings with a similar range of surface properties are used in HPLC. In the following, we will briefly discuss the available packings based on the mode of separation [19].

NORMAL PHASE CHROMATOGRAPHY

Normal-phase chromatography is the classical form of chromatography using polar stationary phases and non-polar mobile phases. The solute is retained by the interaction of its polar functional groups with the polar groups on the surface of the packing. Classically, unbonded silica and alumina have been used for this application, but today polar bonded phases can be used with the following advantages: bonded phases equilibrate faster, are less sensitive to minute concentrations of water in the mobile phase, and yield different selectivities [19].

Table 2.6 Choosing a normal phase packings for various applications [19].

Choosing a Normal Phase Packing	
Packing	**Application**
Silica	general purpose sorbent
Alumina	general purpose sorbent, more retentive than silica; group separation of aromatic hydrocarbons
Diol	less polar than silica, equilibrates quickly
CN	least retentive normal phase sorbent
NH_2	most polar bonded phase; different selectivity than silica; group separation of aromatic hydrocarbons

REVERSED-PHASE CHROMATOGRAPHY

Reversed-phase chromatography has become the most popular mode of chromatography. In reversed-phase chromatography, the stationary phase is non-polar and the mobile phase is polar. Typical mobile phases are mixtures of water or aqueous buffer with methanol, acetonitrile or tetrahydrofuran. Typical stationary phases are silica-based bonded phases with aliphatic hydrocarbons as ligands. Other packings for reversed-phase chromatography are graphitized carbon and styrenedivinylbenzene packings. The performance of reversed-phase bonded phases depends also on the activity of residual silanols. Silanols interact with the polar functional group of the solutes. Therefore, packings exhibit different selectivities depending on the activity of the silanols. Also, tailing peaks are often observed for basic compounds on packings with a high level of silanol activity. One way of modifying silanol activity is by end-capping, that is reaction with a silanization reagent that converts the silanols to trimethylsilyl groups. Nevertheless, the surface concentration of residual silanols is always higher than the total concentration of bonded ligand

including the end-capping ligand. Silanol activity also depends on the pretreatment of the silica ("base-deactivation") and the purity of the silica. Fully end-capped bonded phases based on high-purity silicas are recommended for the chromatography of basic analytes. Non-end-capped packings can be used with advantage in many other applications to obtain a different selectivity [19].

2.4.5 CHEMICALLY MODIFIED SILICA

Silica carries OH groups (silanol groups) on its surface and may be chemically modified at these points to give stationary phases with specific properties.

(I) The silanol group can be esterified with an alcohol, ROH, where R may be an alkyl or any other functional group. For steric reasons, reaction is confined to the silica surface (this obviously includes the 'inner' surface of the pores) and does not involve the solid body interior, so that the bonded residues project from the silica, like tails, or 'brushes'.

Esterified silica is prone to hydrolysis and so cannot be used with mobile phases containing water or alcohol, products with Si-O-Si-C bonds generally being preferred.

(II) Reaction with thionyl chloride, $SOCl_2$, produces chlorides which combine with amines to give an Si-N bond. R can be chosen at random. These products have better hydrolytic stability.

(III) Silicas in which the function group is bonded by an Si-O-Si-C bond (reaction with mono- or dichlorosilane) are the most stable of all.

Octadecylsilane ODS, in which R = $-(CH_2)_{17}CH_3$, is the most widely used of these chemically modified products. It is extremely non-polar and is the preferred choice for use in reversed-phase chromatography.

Method for the production of chemically bonded phases: 100 ml of dry toluene + 4 g of dried silica + 2.5 ml of dry pyridine are mixed with a fourfold excess of silane compound $RSi(CH_3)_2Cl$ (calculated for silica with a surface coverage of 2.4 groups per nm^2). The temperature is maintained at 10°C below that of the boiling point of the most volatile component for between 40 and 150 hours (depending on the R-group). The mixture is carefully shaken from time to time. Finally, the gel is filtered, washed and dried.

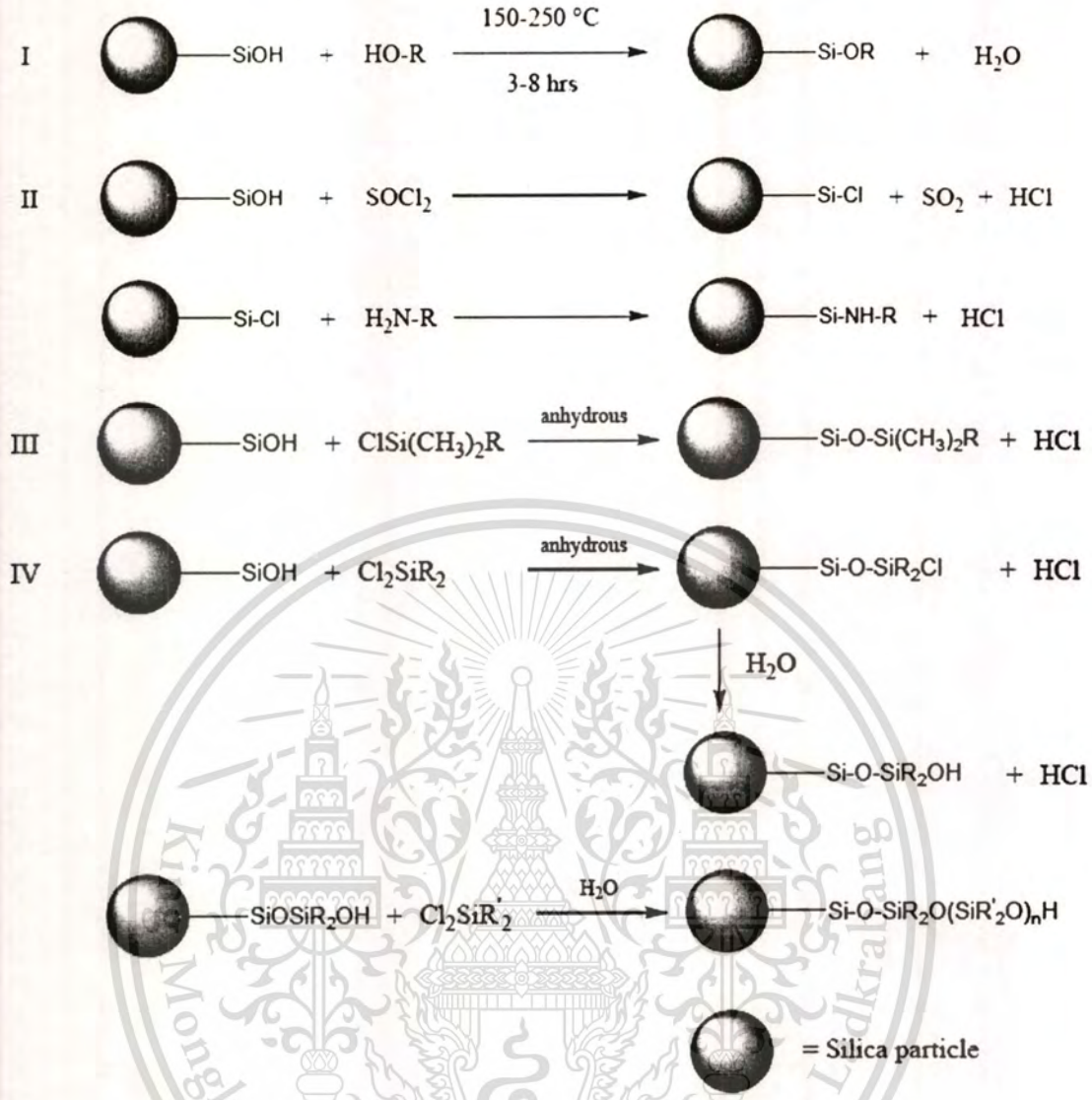

Fig. 2.24 Chemical modification of silica [13].

Subsequent treatment with trimethylchlorosilane may reduce the number of silanol groups that remain unreacted for steric reasons, this being known as end-capping.

(IV) These and similar reactions produce polymer structures (not brushes), which are, in fact, bonded silicone oils known as polysiloxanes. Any cross-linked polymer layer thickness can be chosen. Multifarious methods of synthesis are known. Very advantageous is the shielding of the silica backbone by the polymeric layer, leading to good pH stability.

Available functional groups are listed in Table 2.7. Silica can also be functionalized with groups suitable for ion exchange, affinity chromatography or the separation of enantiomers. The choice of special phases for the separation of biopolymers is immense use.

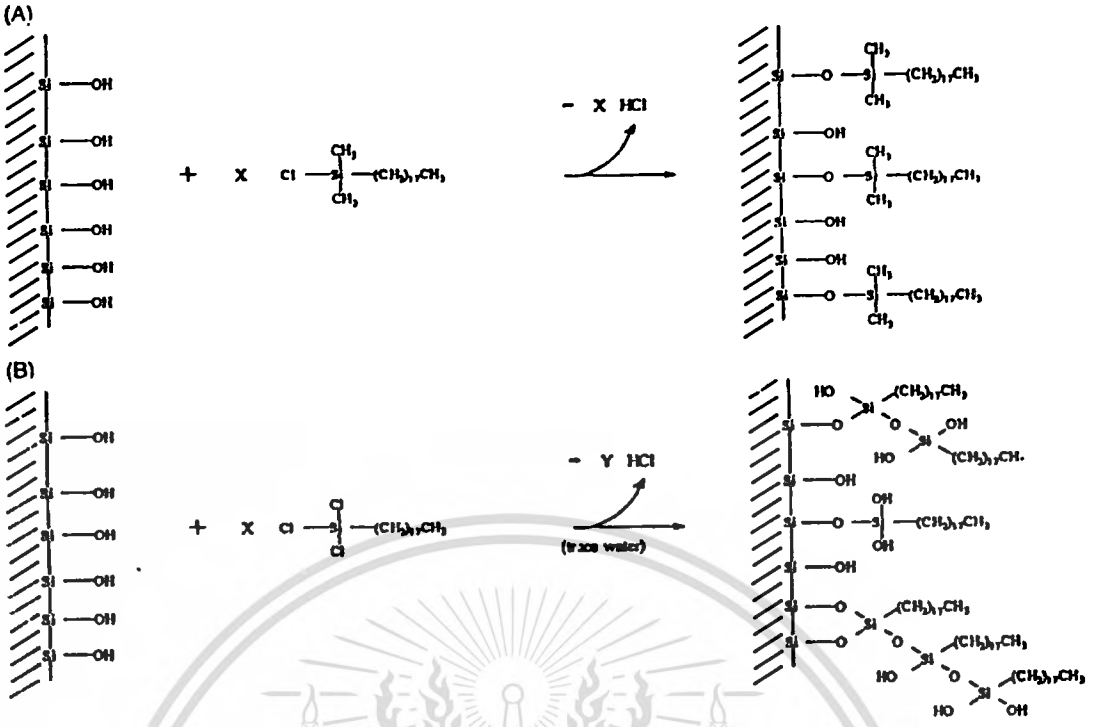

Fig. 2.25 Silica reaction with (A) Monofunctional ODS (B) trifunctional ODS [20].

Table 2.7 Functional groups in chemically modified silicas [13].

Group	Formula	Group	Formula
Triacontyl	$-(CH_2)_{29}CH_3$	Amino	$-NH_2$
Docosyl	$-(CH_2)_{21}CH_3$	Nitro	$-NO_2$
Octadecyl	$-(CH_2)_{17}CH_3$	Nitrile	$-C\equiv N$
Octyl	$-(CH_2)_7CH_3$	Oxypropionitrile	$-OCH_2CH_2C\equiv N$
Hexyl	$-(CH_2)_5CH_3$	Vic-Hydroxyl (diol)	$-CH(OH)-CH_2(OH)$
Trimethyl	$-Si(CH_3)_3$	Fluoroalkyl	$-(CF_2)_nCF_3$
Alkylcarbamate	$-CO(CO)NH-(CH_2)_nCH_3$	Polycaprolactam	$-[NH(CH_2)_5C=O]_n-$
Cyclohexyl	$-C_6H_{11}$	(polyamide, nylon)	
Phenyl	$-C_6H_5$		
Diphenyl	$(-C_6H_5)_2$		
Dimethylamino	$-N(CH_3)_2$		

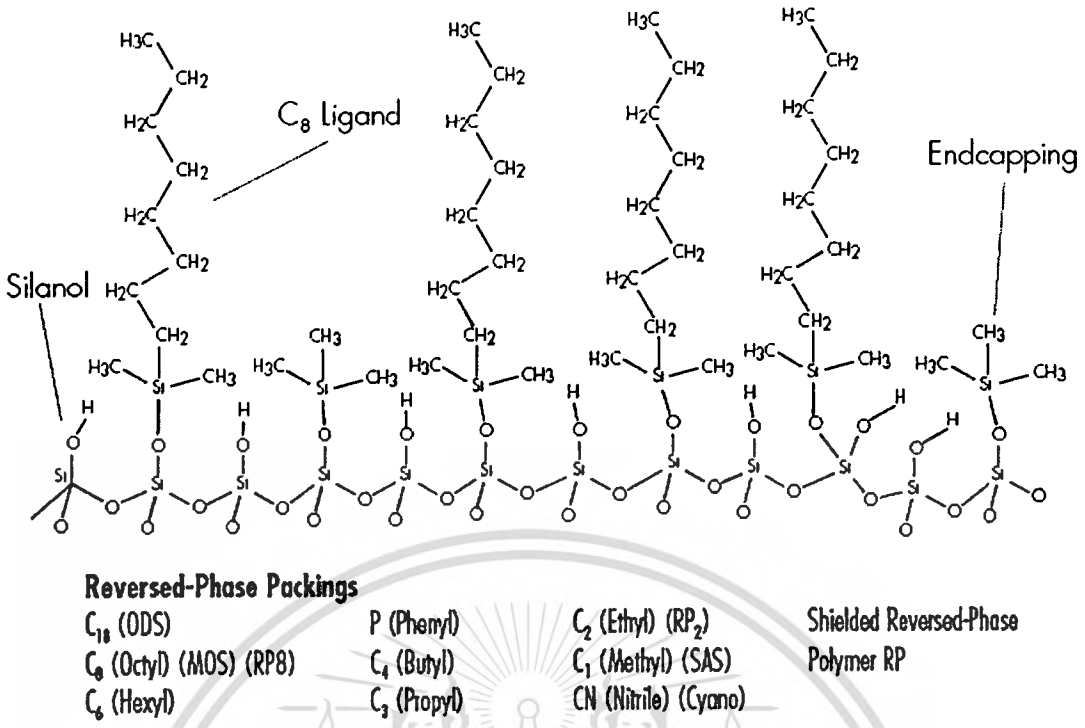

Fig. 2.26 Surface of a typical reversed-phase packing [19].

THE NATURE OF BONDED PHASES

CARBON LOAD AND LIGAND DENSITY

The carbon content of a packing is determined by elemental analysis. Often the results are reported directly as the carbon load of a packing. From this value and with the knowledge of the specific surface area of the packing and the molecular weight of the bonded ligand, the ligand density can be calculated. The ligand density is usually expressed in $\mu mol/m^2$. It is also sometimes called the surface coverage. The ligand density is a very important measure of the composition of the surface of the bonded phase, and is one of the important parameters determining the selectivity of a packing [19].

CARBON LOAD

At equal ligand density on the same base silica, packings with larger ligands have a higher carbon load that is, C18 phases have a higher carbon load than C1 phases. For the same ligand on the same silica, the carbon load increases with surface coverage. For the same ligand at equal surface coverage on packings with different pore sizes, the carbon load decreases with increasing pore size, such as decreasing specific surface area. From this discussion, we can see that carbon load alone is not a good measure for the retentivity or the selectivity of a packing [19].

LIGAND DENSITY

Ligand density, also called surface coverage, χ, is a much better measure of the characteristic properties of a packing. It is calculated using the following equation [19]:

$$\chi = \frac{\%C}{100 \bullet SA \bullet nC \bullet 12 \quad (1 - \frac{\%C}{100} \bullet \frac{MW - 1}{nC \bullet 12})} \tag{2.11}$$

SA is the specific surface area, *%C* is the carbon load, *MW* is the molecular weight of the ligand and *nC* is the number of carbon atoms in the molecule.

The higher this number, the higher is the density of the primary ligand on the surface of the packing. It is also a measure of the reduction of the density of silanols on the surface. On a fully hydroxylated silica, the surface concentration of silanols is around 8 μmol/m^2. Ligand densities of the primary ligand vary between 0.5 to 4 μmol/m^2 for different bonded phases based on monofunctional ligands. The reproducibility of the ligand density is of utmost importance for the reproducibility of the retentivity and selectivity of a packing. In addition, packings with a high ligand density tend to be hydrolytically more stable than packings with a low ligand density [19].

TYPE OF BONDED PHASE AND ENDCAPPING

Bonded phases are produced by the chemical reaction of an organosilane with the silica surface. The target is to achieve a uniform monomolecular layer. There are different types of silanes that are used for this bonding reaction. The silanes are characterized as mono-, di-, or trifunctional silanes depending on the number of groups on the silane that can react with the silica surface. With monofunctional silanes, the ligand density does not exceed 4 μmol/m^2 due to steric hindrance. With multifunctional silanes, higher ligand densities can be achieved. Often, packings with these higher ligand densities are referred to as polymeric packings, although there is little evidence for the formation of a polymer. Conversely, packings with a low ligand density are referred to as monomeric. The selectivity of a packing depends on the ligand density. Especially different shape selectivities have been demonstrated for polyaromatic hydrocarbons at different ligand densities. The majority of commercially available bonded phases have a ligand density under 4 μmol/m^2 and are therefore of the monomeric type. Monofunctional ligands give a more predictable coverage of the silica since complicating side reactions of the second reactive group are not possible. However, only one bond is made with the surface, which can result in an

accelerated hydrolysis compared with phases prepared from multifunctional ligands. Trifunctional ligands are more difficult to bond reproducibly to the surface. On the average, two bonds are made with the surface, which increases the resistance to hydrolysis. Trifunctional ligands are preferred when low pH mobile phases are used. Manufacturers do not always reveal their bonding chemistries. However most will indicate if a C18 phase is monofunctional. More recently introduced reversed-phase packings are usually of that type because bonded phases can be produced with a higher reproducibility using monofunctional silanes. For applications in hydrolyzing conditions of high or low pH and high aqueous content, it is best to select a robust silica with trifunctional bonding. All silica-based ion-exchangers are trifunctional. If nitrile packings are being used for reversed-phase chromatography, the better packings are based on a robust silica (low pore volume) and a trifunctional silane. Some manufacturers produce a nitrile bonding specifically for use in reversed-phase chromatography [19].

ENDCAPPING

For many reversed-phase packings, a secondary bonding step is carried out to cover unreacted silanol sites on the silica surface. A small silane, usually trimethylchlorosilane (TMCS), is used to produce a maximum coverage. This process is called endcapping. Endcapping is applied to most bonded phases used in reversed-phase chromatography. Phases used in normal-phase chromatography or other modes of chromatography are not endcapped. Reversed-phase packings that are not endcapped often exhibit a significantly different selectivity than endcapped packings. However, basic analytes tail on non-endcapped reversed-phase packings. Trimethylsilyl groups (endcapping groups) are subject to hydrolysis in acidic conditions. Therefore, endcapped packings should not be used at pH < 2.

2.5 GAS CHROMATOGRAPHY

Gas-chromatographic instrumentation differs very little from that used for other forms of column chromatography. The chromatographic system is composed of the chromatograph and a recorder for plotting chromatograms or a data station for generation and evaluation of chromatograms. The chromatograph consists of the sample injector, gas supplies, oven with temperature control for the chromatographic column and the detector [18].

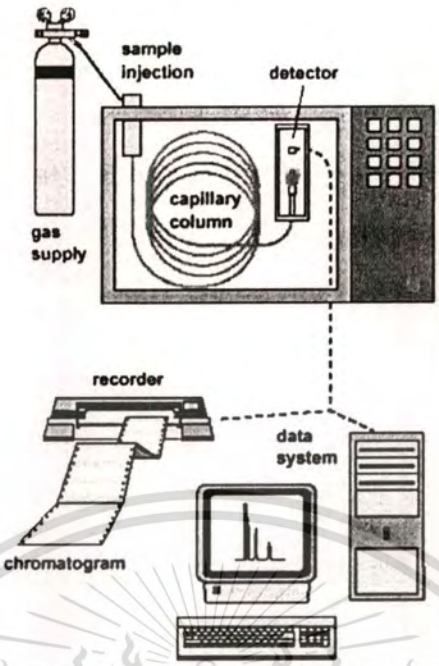

Fig. 2.27 Schematic presentation of a GC system [18].

2.5.1 COLUMN FOR GAS CHROMATOGRAPHY

The most commonly used gas-chromatographic column consists of a tube filled with solid particles of fairly uniform size; the particles are coated with the liquid stationary phase. Perhaps the most commonly used support is marine diatomite (e.g., Johns-Manville Chromosorb®). The choice of tubing material depends on the experiment. Aluminum and copper are commonly used, but may have chromatographically and catalytically active oxide films that make them undesirable for sensitive compounds (e.g., steroids); in such cases, stainless steel or glass is used (the latter is more inert, but is less conveniently manipulated) [12].

2.5.2 CHROMATOGRAPHIC SUPPORT MATERIALS

The function of a chromatographic support is to hold the stationary phase. One useful type of support is provided by the marine diatomites, which are the skeletons of tiny unicellular algae (diatoms) and consist chiefly of amorphous hydrated silica with traces of metal-oxide impurities. This material has the advantages of high porosity and large surface area. Some properties of a variety of diatomite supports are given in Table 2.8. Chromosorb P, for example, is prepared from one particular grade of firebrick and is a pink (hence P), calcined diatomite that is relatively hard and not easily friable [12].

Table 2.8 Properties of some diatomite supports [12].

Properties	Chromosorb®			
	A	G	P	W
Color	Pink,	Oyster White	Pink,	White,
Type	Flux-Calcined	Flux-Calcined	Calcined	Flux-Calcined
Density, g/cm^3				
(i) Loose weight	0.40	0.47	0.38	0.18
(ii) Packed	0.48	0.58	0.47	0.24
Surface area, m^2/g	2.7	0.5	4.0	1.0
Surface area, m^2/cm^3	1.3	0.29	1.88	0.29
Maximum liquid-phase Loading	25%	5%	30%	15%
pH	7.1	8.5	6.5	8.5
Handling characteristics	Good	Good	Good	Slightly Friable

Source: Courtesy of Johns-Manville Corporation.

It is used mainly with solutes of low to moderate polarity (e.g., hydrocarbons). It is a relatively good adsorbent, a quality that can be an interference. If there were no liquid phase at all, the support would act as an adsorbent, and gas-solid chromatography could be carried out. The effect of placing a thin film of liquid on an active adsorbent is to moderate the gas-solid activity, but not to eliminate it. It has been shown that even 20% by weight liquid loading does not eliminate this activity. Several techniques are used to reduce the activity-for instance, acid washing, and "silanizing" the active silica sites with dimethyldichlorosilane to displace the hydrogen [12].

2.5.3 PACKING MATERIALS AND COATING PROCEDURE

Uniformity of particle size is achieved by using a narrow range of mesh size, by carefully removing any fines (particles of very small size), and by not producing more fines by rough handling in the coating and packing processes. For analytical columns of 2 to 3 mm i.d., a mesh size of 100 to 120 is desirable.

Coating the support can be carried out by many methods; the least desirable is using a rotary evaporator in the drying step, which tends to agitate the packing and produce fines. A reliable method is as follows:

(i) Dissolve the liquid phase in a solvent in a flask. (A suitable solvent can be found in many of the suppliers' catalogs. Select one that does not boil under the vacuum to be used.)

(ii) Add the cooled solution to the support, swirling gently to ensure wetting.

(iii) Stopper, and apply vacuum to remove air from the pores of the support. When no more air bubbles escape, seal the vacuum and hold for 5 mins.

(iv) Release the vacuum, transfer the support to either a glass funnel with a coarse porosity frit in the neck or to a fluidized-bed dryer, and immediately suck the solution off.

(v) When the solution ceases to drip out, fluidize the bed of coated packing and dry with a gentle flow of hot nitrogen gas. (The packing is dry and ready for filling into the column when no odor of solvent remains.)

2.6 PACKING OF COLUMN

DRY PACKING: methods for packings with a particle size > 20 μm.

The dry packing material is filled into the vertically clamped column in small amounts and helped to deposit by tapping the wall and/or vibrating the column. Individual portions of packing should be adjusted to increase the level in the column by a few millimeters only. It is recommended that the column be unclamped now and then and tapped on a firm surface (e.g. bench top) to obtain dense and reproducible packings. The following values might provide a useful guide: a well packed column (particle size 30 to 40 μm) with a linear elution velocity of 2 cm/s and completely porous stationary phase will give a plate height in the region of 1 mm. With porous layer beads (PLB) under identical condiitons lower plate heights (0.2 to 0.5 mm) can be obtained [21].

Table 2.9 Properties of some slurry-packing solvents [22].

Slurry Solvent Data Chart		
Solvent	**Density (g/mL)**	**Viscosity (cP)**
Diiodometane	3.3	2.9
Tetrabromoethane	3.0	-
Dibromomethane	2.5	1.0
Iodomethane	2.3	0.5
Tetrachloroethylene	1.6	0.9
Carbon Tetrachloride	1.6	1.0
Chloroform	1.5	0.6
Trichloroethylene	1.5	0.6
Bromoethane	1.5	0.4
Dichloromethane	1.3	0.4
n-Butanol	0.8	3.0
n-Propanol	0.8	2.3
Ethanol	0.8	1.2
Methanol	0.8	0.6
Cyclohexane	0.8	1.0
n-Heptane	0.7	0.4

WET OR SLURRY PACKING: methods for packings with a particle size < 20 μm.

While packing is in progress the suspension must remain stable, sedimentation of the solid particles or agglomeration being avoided. Ultrasonic tratment of suspensions is recommended. The balanced density method has been treated by several authors and suitable packing apparatus have been described. For the suspension of silica gel with a density of 2.2 g/cm^3, however, only halogenated hydrocarbons can be used. Now almost exclusively the viscosity method is used to pack analytical columns. The suspension is prepared with a high viscosity liquid. The filling process for both methods is identical. In some instances a combination of both processes (balanced density and viscosity) can be used. Virtually all stationary phases can be packed by one of these methods or a combination of both. However stability of the suspension during the time span of the packing process remains a factor of the

utmost importance. Aluminium oxide and pre-swollen stationary phases for size exclusion chromatography can also be packed by the same method. Only packings coated with liquid stationary phases for partition chromatography cannot be packes in this way as the liquid phase would be washed out during packing or during conditioning of the column. Particles in the 10 μm range are easier to pack reproduciby than 5 μm particles. With 10 μm particles and eluent linear velocities of 1 cm/s, plate heights below 0.05 mm are easily obtained, while well packed 5 μm particles and eluent linear velocities of 0.5 cm/s will give plate heights below 0.025 mm. However, these numbers should be considered as orienting values, since the measured plate heights depend on the type of interactions involved and on the chromatogrpahic conditions [21].

2.7 LITERATURE REVIEWS

D.M. IBRAHIM and M. HELMY (1981) studied an effect of temperature of firing and time of annealing on crystallite size of silica. The work was conducted by burning boiled rice husk. X-ray broadening technique was used in the investigation. Their results showed that nuclei of disordered cristobalite were present in ash silica, and crystallite growth was governed by two processes, namely nucleation and growth taking place simultaneously with a rate varying with the temperature of treatment. The nucleation process manifested itself in the low temperature range of 800-900^{o}C, while growth was more pronounced in the temperature range of 1000-1100^{o}C, occurring with different activation energies of 81.3 and 52.4 cal mole^{-1}, respectively. Both processes occurred with the same intensity at 964^{o}C. An activation energy of the growth process and crystal perfection was found to be 36.8 cal mole^{-1} [23].

J. JAMES and M. SUBBA RAO (1986) studied thermal decomposition characteristics of rice husk using dynamic thermoanalytical techniques: DTA, TG, DTG and isothermal heating. The observed thermal behavior was explained on the basis of a superposition of the decomposition of cellulose and lignin, which are the major organic constituents of rice husk. Morphological features of silica in husk as well as the ash were examined by scanning electron microscopy. Silica in the residual ash was characterized by X-ray diffraction and infrared spectroscopy. Controlled thermal decomposition of rice husk was found to be a convenient method for the liberation of silica [2].

U. LEELA-ADISORN (1992) studied potential and limits of rice husk to become a competitive source of nano-structured silica. Husk samples were submitted to a chemical pre-treatment using cellulase enzyme and different inorganic acids. Subsequently, samples were incinerated at 600°C for 6 hours under static atmosphere. The product was characterized in terms of silica content, particle size distributions at the different levels of agglomeration, and specific surface area (BET, N_2). With pre-treatment acids, (HCl (1:4) or H_2SO_4 (1:4)) a product with properties intermediate to those of fumed silica and xerogel was obtained. The size distribution for secondary particles follows a log-normal distribution with d_{50}=26 nm and d_{84}/d_{16}=2. Tertiary agglomerates range from 0.3 to 30 μm. The specific surface area was determined by the primary particle and reach values of 250 m^2/g. Purity was 99.4% silica [24].

S. KHUNTHON, S. TANGWIWAT and S. ROENGSUMRAN (1997) studied effective method of silica production from rice husk ash by using a chemical process so-called sodium silicate solution route. By refluxing the ground rice husk ash with sodium hydroxide solution, silica with 80% yield could be obtained. The advantages, compared with the method of purification of rice hulls with acid before ignition, are that amorphous silica product, obtained from this method, contains with higher purity and produces an increase in surface area. It was also showed that silica content obtained from this experiment is amorphous silica with 99.91±2% purity and give 600 m^2/g specific surface area thus this can be properly used as stationary phase for thin layer chromatography [25].

S. LIMPANART, K. SIRALERTMUKUL and S. KHUNTHON (2000) studied silica filter production process from domestic rice husk ash. As a preliminary raw material, the ash was chemically synthesized and then spray dried to produce silica powder with a specific density of 2.098 g/cm^3 and a purity of 99.8%. The formation of filters was achieved by using a gel casting process accompanying acrylamide polymerization, in which ratios of initiator, catalyst and silica contents were varied. In this study, it was found that the best ratio of those is 1% initiator, 3.8 ml/L catalyst and 50% Vol. Silica, leading to the gelation time of 30 minutes. After sintering at different temperatures and times, samples without cracking were acquired when sintered at 1300° C for an hour [26].

U. KALAPATHY, A PROCTOR and J SHULTZ (2000) studied silica xerogels production from rice hull ash (RHA), structure, density and mechanical strength of the gel. Silica was extracted as sodium silicate from RHA using 1M NaOH. This silicate solution was concentrated by volume reduction and used to obtain silica concentrations of 0.04, 0.06, 0.08, 0.10, and 0.12 g cm^{-3}. The pH values of these silicate solutions were adjusted to 9.0, 10.0, 10.5, or 11.0 to produce silica gels. The silica gels produced were then dried at 80°C for 24 hours. X-ray diffraction demonstrated the amorphous nature of silica gels. Diffuse reflectance Fourier Transform Infrared (FTIR) spectroscopy was used to investigate the effect of gelation pH, and silica concentration on the chemical structure of the xerogel and concomitant effect on density and mechanical strength of xerogel. The FTIR spectra demonstrated that at higher pH of gelation, siloxane bonding was the primary network in the xerogel. As the pH of gelation decreased, the silica gel structure network became the major interaction in the silica xerogel. At each gelation pH, the silica gel network increased with increase in silica concentration. The higher pH led to condensed glassy solids, while higher silica concentration produced highly porous silica xerogel. Hence, gelation pH and silica concentration of gel-forming solution had significant effects on the density and the mechanical strength of xerogels produced from rice hull silica [27].

M.F. DE SOUZA, P.S. BATISTA, I. REGIANT, J.B.L. LIBORIO and D.P.F. DE SOUZA (2000) studied silica production from rice hulls by three processing routes, starting with acid treatment followed by burning and milling. The amorphous white silica powder showed a surface area of 260 to 480 m^2/g, purity above 99% and average particle size of 2.0 to 0.6 mm. This silica is suitable for the preparation of mullite whiskers employing the rare earth aluminosilicate glass technique. Due to its highly pozzolanic reaction, this prepared silica is used as an additive in high performance concrete [28].

W. NAKBANPOTE, P. THIRAVETYAN and C. KALAMBAHETI (2000) studied and developed a new, efficient adsorbent of gold-thiourea complex, $[Au(CS(NH_2)_2]^+$. In this experiment, rice husk was heated at three different temperature: 300°C, 400°C and 500°C. Rice husk ash heated at 300°C adsorbed gold thiourea complex, whereas rice husk ash heated at 400 °C and 500°C did not. The structure of rice husk ash heated at 300°C had specific silanol groups and oxygen functional groups of carbon, while rice husk ash heated at 400°C and 500°C contained siloxane groups. Maximum gold adsorption of rice husk ash heated at 300°C and

activated carbon, was 21.12 and 33.27 mg Au/g adsorbent, respectively. However, rice husk ash absorbed 0.072 mg thiourea/g adsorbent, which was less than activated carbon adsorbed (0.377 mg thiourea/g adsorbent). In addition, the adsorbed gold could be eluted from this rice husk ash by sodiumthiosulfate more easily than from activated carbon. The results revealed that rice husk ash heated at 300^{o}C can be used as a new adsorbent for gold thiourea complex [29].

CHAPTER 3

EXPERIMENTAL

3.1 CHEMICALS

1. Sodium hydroxide (NaOH), >99.0% (w/w), A.R. grade, ANALYTICAL SCIENCES (LAB_SCAN).
2. Hydrochloric acid (HCl), 37% (w/v), A.R. grade, ANALYTICAL SCIENCES (LAB_SCAN).
3. Octadecyltrichlorosilane ($C_{18}H_{37}SiCl_3$), >85 % (GC), Fluka Chemika.
4. Trimethylchlorosilane (C_3H_9SiCl), >99.0 % (GC), puriss, Fluka Chemika.
5. 1,1,2-trichloroethane, 97 %, ALDRICH.
6. Pyridine, 99.7 % (GLC), For analysis, ACS.
7. Methanol, Low in water, For analysis, CARLO ERBA REAGENTI (RPE).
8. Methanol, HPLC grade, ANALYTICAL SCIENCES (LAB_SCAN).
9. Methanol, commercial grade, ZEN POINT.
10. Parafin oil, CARLO ERBA REAGENTI (RPH).
11. Dichloromethane, commercial grade, ZEN POINT.
12. Toluene, commercial grade, BDH.
13. Chloroform, for analysis, CARLO ERBA REAGENTI (RPE).
14. Phenol, >99.5 %, A.R. grade, CARLO ERBA REAGENTI.
15. 2-nitrophenol, >99.5 %, A.R. grade, CARLO ERBA REAGENTI (RPH).
16. n-Hexane, commercial grade, ZEN POINT.
17. n-Pentane, commercial grade, ZEN POINT.
18. Silane-treated glass wool.
19. Distillation water and demineralized water.

3.2 EQUIPMENTS

1.	High temperature furnace	: CSF 1200, Carbolite Furnaces.
2.	X-ray fluorescent	: SRS 3400, Bruker AG.
3.	X-ray diffractometer	: D8 Advance, Bruker AG.
4.	Surface area analyzer	: AUTOSORB-1, Quanta Chrome.
5.	Particle size analyzer	: Masterzizer X, MALY≡RN.
6.	Scanning electron microscope	: 1455VP / EDAX®, LEO.
7.	Fourier transforms infrared spectrometer	: FTIR Spectrum GX, Perkin Elmer.
8.	Thermogravimetric analyzer	: Pyris 1 TGA, Perkin Elmer.
9.	Solid state Nuclear magnetic resonance	: AVANCE DPX_{300}, BRUKER.
10.	Spray dryer	: L-8, Ohkawara Kakohki Co., Ltd.
11.	High performance liquid chromatograph	: Waters 510 HPLC pump / Waters 486 Tunable absorbance detector, MILLIPORE.
12.	Gas chromatograph	: 910 Gas Chromatograph, BUCK Scientific.
13.	HPLC column packing pump	: Pneumatic HPLC pump, KNAUSER.
14.	Motor stirrer and U-shape propeller	: SL 2400, StedFast™ Stirrer.
15.	HPLC column	: 316 stainless steel tubing (i.d. 4.6 x 250 mm).
16.	GC column	: 316 stainless steel tubing (o.d. 1/8 inc. x 6 ft.).
17.	True density analyzer	: Ultrapycnometer 1000, Quanta Chrome.

3.3 RESEARCH METHODOLOGY

Step 1: Synthesis of high purity silica from rice husk.

- Study of effects of temperature and time for burning of rice husk.
- Study of optimum sodium hydroxide quantity that can dissolve the silica in rice husk ash.
- Study of suitable silica production routes (e.g., particle size, pore size and surface area) to be used as a solid support of HPLC and GC column.
- Silica characterization (e.g., purity, morphology, etc.).

Step 2: Synthesis of silica-ODS.

- Study of silica-ODS synthesis.
- Study of silica-ODS characterization (e.g., carbon loading, true density, etc.).

Step 3: Column packing process.

- Study of wet (or slurry) and dry packing for HPLC and GC column.

Step 4: Chromatographic evaluations.

- Study of column efficiencies for HPLC column (e.g., theoretical plate number, linearity (or dynamic range), etc.) by analysis of standards and compared with commercial column.
- Study of column efficiency for GC column (theoretical plate number and mixture separation).

Step 5: Conclusion.

3.4 PROCEDURES

3.4.1 OPTIMIZATION OF RICE HUSK BURNING PROCESS

3.4.1.1 THERMOGRAVIMETRIC ANALYSIS

Raw rice husk was treated before measurement by washing with water, sieving and drying in an oven at 60°C for 6 hours. Then, this rice husk was analyzed using thermogravimetric analysis (TGA) technique.

Conditions:

Gas type: N_2 Temperature scan range: 50-800°C

Heating rate: 10°C/min Sample weight: ≈ 10-30 mg.

3.4.1.2 BURNING PROCESS

The weight of rice husk was fixed at 50 g in ceramic crucible (because of limitation of furnace and crucible) and putted into the furnace. The temperature was fixed at optimum temperature obtained step from 3.4.1.1 and varied the burning time for 1, 1.5 and 2 hours. The amount of silica in rice husk ash was determined using XRF technique.

3.4.2 SYNTHESIS OF SODIUM SILICATE

Rice husk ash was crushed with a mortar and sieved with test sieve aperture 35 mesh (500 μm, ASTM) before reacted with sodium hydroxide solution (ΔH_{sol} –416 kJ/mol).

Weighed rice husk ash at *X* g, stirred and refluxed with 10% NaOH solution (optimum concentration [25]) at 80-85°C for 1 hour. The amount of NaOH that sufficient for complete the reaction (3.1) can be calculated by:

$$SiO_2 + 2NaOH \longrightarrow Na_2SiO_3 + H_2O \quad (3.1)$$

$$\text{NaOH (required)} = \left[\frac{X \times (\frac{Y\%}{100})}{M.W._{SiO_2}}\right] \times 2(M.W._{NaOH}) \quad (3.2)$$

Where *X* is weight (g) of rice husk ash, *Y* is percent (%) of silica in rice husk ash, $M.W._{SiO2}$ and $M.W._{NaOH}$ are molecular weight of silica and sodium hydroxide respectively. After refluxed, the orange-brown colour solution can be obtained. Filtered and adjusted the volume that gives the concentration of Na_2SiO_3 about 1% (w/v).

3.4.3 SYNTHESIS OF HIGH PURITY SILICA GEL

High purity silica gel particle was obtained by two routes: (i) precipitating and crushing for GC application and (ii) precipitating and spray drying for HPLC application, all both cases of gel forming at room temperature.

$$Na_2SiO_3 + 2HCl \longrightarrow H_2SiO_3 + 2NaCl \quad (3.3)$$

3.4.3.1 SILICA PARTICLE FOR GC COLUMN

The sodium silicate solution was stirred with a U-shape propeller stirrer at speed of 2.5-3 and slowly adjusted the pH into 10.0 with 15% (v/v) HCl. A few minutes after the pH at 10.0, the solution was cloudy and the soft gel occurred. The solution was continuing stirred and added more of HCl into solution until the pH is 7.0 for neutralization. After a few minute of gel forming, the silica soft gel was precipitated, filtered, washed several times with hot distillation water and dried at 150°C for 24 hours.

The silica gel was crushed with a mortar and sieved by using test sieve aperture 80 and 100 mesh (180 and 150 μm, ASTM). After that, the silica powder form was washed with conc. HCl and hot demineralized water. Then, the high purity silica powder form was dried at 180°C for 24 hours before directly packing into GC column.

3.4.3.2 SILICA PARTICLE FOR HPLC COLUMN

The precipitation of silica soft gel was similar to the upper processes. But for this case, the silica soft gel was resuspended into demineralized water to make the slurry gel. The slurry gel was then introduced into the spray dryer by using peristaltic pump. The spray drier conditions were:

Atomizer: 50 Hz	Atomizer speed set: 4
Cyclone P.G.: 50 mm H_2O	Pump speed: 45
Inlet temperature: 180°C	Exhaust temperature: 133°C

The silica gel powder was sieved for particle size selection by using test sieve aperture 400 mesh (38 μm, ASTM). After that, the silica powder was washed with conc. HCl and hot demineralized water. Then, the high purity silica powder was dried at 180°C for 24 hours before silanization with octadecyltrichlorosilane for silica-ODS synthesis.

3.4.3.3 CHARACTERIZATION OF SILICA GEL

Purity and crystal structure of silica powder were characterized using XRF and XRD respectively. Surface area and pore size distribution were measured using AUTOSORB-1. Particle size distribution was measured using Masterzizer X. The functional groups and chemical structure of silica powder were measured using FTIR and solid state ^{29}Si NMR respectively. The morphology of silica particle was determined using SEM.

3.4.4 SYNTHESIS OF SILICA-ODS WITH END-CAPPING

Silica gel 25 g was putted into three-neck round bottom flask, added 1,1,2-trichloroethane 200 ml and distilled the mixture at azeotropic temperature, until obtained volume of the liquid was 50 ml, stopped the distillation. Added octadecyltrichlorosilane (ODTCS) 15.5 ml, stirred for 5 mins then added pyridine 22.4 ml and stirred for 3 hours. The product was filtered and washed with 1,1,2-trichloroethane, methanol, water-methanol (70:30), methanol and dried in vacuum oven at 60°C for 12 hours. Silica-ODS was putted into the three-neck round bottom flask, added 1,1,2-trichloroethane 200 ml and distilled the mixture at azeotropic temperature until obtained volume of the liquid was 50 ml. Then stopped the distillation, cooled down at room temperature, added trimethylchlorosilane (TMCS) 0.4 ml and stirred for 1 hour. After that, added dried methanol 50 ml and stirred for 30 mins. The product was filtered, washed with water-methanol (70:30), methanol and dried in vacuum oven at 60°C for 12 hours [30].

For steric reasons, it is not possible to fix an organic derivative on every hydroxyl group. Of the 9 μmol/m^2 initial silanol concentration, only 50% can be derivatized. The maximum bonding density is about 4.5 μmol/m^2 [7]. Therefore, the required amount of ODTCS can be calculated by:

$$\text{ODTCS (required)} = 4.5 \times 10^{-6}\ \text{mol/m}^2 \times M.W._{(\text{ODTCS})} \times S.A._{(\text{SiO2})} \qquad (3.5)$$

Where, $M.W._{(\text{ODTCS})}$ is molecular weight (g) of Octadecyl trichlorosilane and $S.A._{(\text{SiO2})}$ is specific surface area (m^2) of silica gel.

3.4.5 SELECTION OF USEFUL PARTICLE SIZE FOR HPLC COLUMN

Suspend silica-ODS in methanol and pour into the sedimentation cone. After a few minute, the silica-ODS was settled down on the bottom of the sedimentation cone. Use the spatula to collect silica-ODS on top and medium of sedimentation cone. The collected silica-ODS was resuspended in methanol and using the centrifugal process for select the particle size. Repeat this step until the average particle size was nearly 10 μm (for conventional used).

3.4.6 CHARACTERIZATION OF SILICA-ODS

The particle size distribution was determined using Masterzizer X. The functional groups and bonded-phase structure were determined using FTIR and solid state ^{29}Si NMR respectively. The surface morphology of silica-ODS was characterized using SEM. Carbon loading (%) and

elemental distribution on silica-ODS surface were determined using SEM-EDS. True density was determined using Ultrapycnometer 100.

3.4.7 PACKING OF CHROMATOGRAPHIC COLUMN

3.4.7.1 HPLC COLUMN PACKING

HPLC (i.d. 4.6 x 250 mm) was 316 stainless steel tube with inner surface already polished. The silica-ODS was packed using the conventional slurry packing technique. Thus, an amount of 2 g of silica-ODS was added into 20 ml of chloroform (10% slurry), and the slurry was dispersed for 5 hours by mechanical stirring and also sonicated for 30 mins. Then, the slurry was poured into the reservoir of the packing system, an additional volume of chloroform was added and the system was topped off. The column was downward packed at 700 bar (10,152.66 p.s.i.) using a pneumatic HPLC packing pump with methanol as propulsion solvent. After packing, a few minutes were allowed to reduce pressure inside the column to return to atmospheric pressure. The packed column was disconnected from the packing system, the excess of stationary phase on the top of the column was carefully removed and finally the inlet frit and end-fritting were installed and the ends plugged. The column was conditioned for 5 hours with a methanol mobile phase at a flow rate of 0.5 ml/min.

3.4.7.2 GC COLUMN PACKING

GC column (o.d. 1/8" x 6') was 316 stainless steel tube. The silica gel was packed using the conventional dry packing technique. Outlet side of column was plugged by using small amount of silane-treated glass wool (for preventing lost of the solid support). Inlet side was connected with the funnel (for pour silica gel into column). Small amount of silica gel was poured into the column for each time and disconnected the funnel from column. Connect the column with high-pressure gas source (N_2 gas). The column was pressured at 25 psi and vibrated using mechanical vibrator. Repeated this step until column was complete filled. The inlet side of column was plugged with silane-treated glass wool. After that, the column should be treated for removed any volatile contaminants from the packing material that are adsorbed during the packing procedure. If the packing is not properly conditioned, these contaminates will slowly elute off the column during your analysis causing baseline disturbances and a high background signal. Heating the packing for extended periods expedites this elution process.

GC column conditioning process [31]

1) Installed the column into the gas chromatograph at the injection side only. (Do not connect the column to the detector during conditioning stage. Any column bleed might foul the detector so it would be best to plug the port off as well).

2) Established a carrier gas flow through the column at ambient temperature for 30 mins. (Use 30 ml/min for an 1/8" column).

3) Heated the column at a rate of 5°C/min to the conditioning temperature (This temperature should be at least 25°C higher than the analysis temperature, but 25°C lower than the maximum operating temperature recommended for the liquid phase). and maintained this temperature for 8-12 hours with carrier gas flow.

4) Cooled the column slowly and connected the column to the detector.

3.4.8 DETERMINATION OF CHROMATOGRAPHIC PARAMETERS

3.4.8.1 HPLC COLUMN TESTING

The chromatographic tests were performed using a modular HPLC system with a Waters 510 pump and a Waters 486 tunable wavelength absorbance detector. All experiments were carried out at room temperature, with detection at 280 nm (for phenol) and 254 nm (for three mixed standard, toluene/phenol/2-nitrophenol). For column efficiency testing, the injection volume was 1 µl. For linearity (or dynamic range) testing, the injection volume was 5 µl. All solvents were filtered and degassed before use. The column was tested with standard phenol, mixed three standards (toluene/phenol/2-nitrophenol) and compared with a commercial HiQ sil C18V column (particle size of 5 µm, i.d. 4.6 x 150 mm).

3.4.8.2 GC COLUMN TESTING

The chromatographic tests were performed using a 910 Gas Chromatograph with flame ionization detector (FID). The injection volume was 0.2 µl. The column was tested with standard n-pentane (for Van Deemter's plot) and mixed two standards (n-pentane/n-hexane) (for mixture separation testing), respectively.

The all of experimental processes are summarized as a flow chart and showed in Appendix D.

CHAPTER 4

RESULTS AND DISCUSSIONS

4.1 OPTIMIZATION OF RICE HUSK BURNING PROCESS

4.1.1 DETERMINATION OF OPTIMUM BURNING TEMPERATURE

The thermal decomposition characteristics of rice husk have been investigated by thermogravimetric analysis (TGA). Thermogram of rice husk in static nitrogen atmosphere is shown in Fig. 4.1.

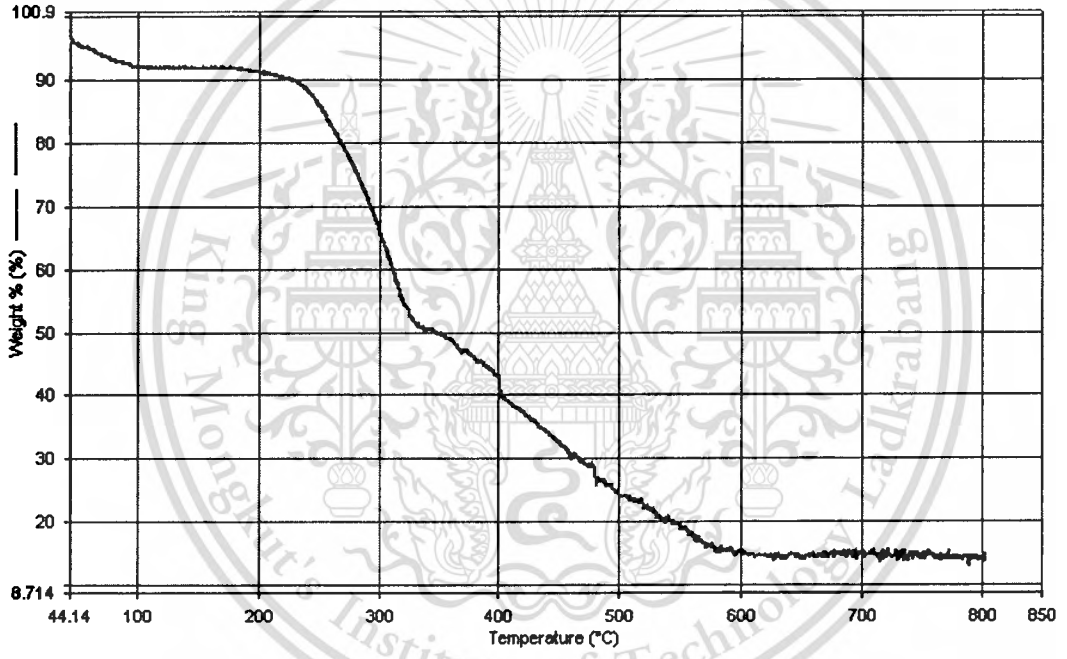

Fig. 4.1 TGA graph for the combustion of rice husk: heating rate at 10°C/min., under N_2 atmosphere.

Fig. 4.1 illustrates two major steps of weight losses at 230-330°C and 350-600°C; after 700°C, weight of rice husk is remained constant. These weight losses are due to elimination of organic matters (cellulose, hemicellulose and lignin) in rice husk. Cellulose materials can be broken down thermally by two mechanisms, a) dehydration followed by charring and b) depolymerization and volatilization of hydrocarbons [2]. With too high temperature and too low soaking time, crystallization occurs after a collapse of pore size smaller than 10 nm. To preserve

amorphous nanostructure, burning temperature at below 700°C is recommended [23]. Therefore, an optimum burning temperature was chosen at 700°C.

4.1.2 DETERMINATION OF OPTIMUM BURNING TIME

After burning process was finished, the percentage of silica and other components in rice husk ash were determined using XRF. The results are summarized in Table 4.1 and Table 4.2, respectively.

Table 4.1 Percentage of ash in rice husk after burning at 700 °C for 1, 1.5 and 2 hours.

Hour	Weight of rice husk (gram)	Weight of ash (gram)	Percent of ash (%)
1	50.0346	8.5291	17.05
1.5	50.0366	8.4955	16.98
2	50.1081	8.4606	16.88

Table 4.2 Percentage of components were contained in rice husk 50 g after burning at 700 °C for 1, 1.5 and 2 hours determined by XRF.

Hr.	SiO_2 (%)	K_2O (%)	P_2O_5 (%)	CaO (%)	SO_3 (%)	MgO (%)	Cl (%)	Na_2O (%)	MnO (%)	Al_2O_3 (%)	Fe_2O_3 (%)	TiO_2 (%)	etc. (%)
1	94.2	2.25	1.03	0.857	0.369	0.491	0.199	0.130	0.184	0.097	0.058	0.012	0.123
1.5	94.3	2.20	1.04	0.841	0.408	0.371	0.222	0.122	0.176	0.100	0.057	0.010	0.153
2	94.6	2.14	0.962	0.807	0.363	0.351	0.244	0.125	0.165	0.080	0.058	-	0.105

From the results, percent of silica contains in rice husk ash after burning at 700°C for 1, 1.5 and 2 hours were not different. Therefore, an optimum burning time was chosen at 1 hour.

4.2 SILICA PRODUCTION PROCESS

4.2.1 SYNTHESIS OF SODIUM SILICATE

From result in Table 4.2, silica was contained in rice husk ash at less 94%, then the quantity of sodium hydroxide that required for completed the reaction (3.1) can be calculated from equation (3.2):

$$NaOH_{(Estimate)} \approx 1.25X \text{ gram}$$

4.2.2 SYNTHESIS OF SILICA

After sieving, acid washing and drying process. The white silica powder was measured using XRF technique to determine the % purity, as shown in Table 4.3.

Table 4.3 Chemical compositions in silica gel after acid washed determined by XRF technique.

SiO_2 (%)	Al_2O_3 (%)	Fe_2O_3 (%)	etc. (%)
99.5	-	0.154	0.346

4.2.2.1 CHARACTERIZATION OF SILICA FOR HPLC COLUMN

The silica morphology was determined using XRD technique. Fig. 4.2 shows an XRD pattern of silica for HPLC column. From this XRD pattern, silica was contaminated with sodium chloride salt from neutralization process between sodium hydroxide and hydrochloric acid. All of sharp peaks were matched with XRD pattern of NaCl (as shown in appendix A).

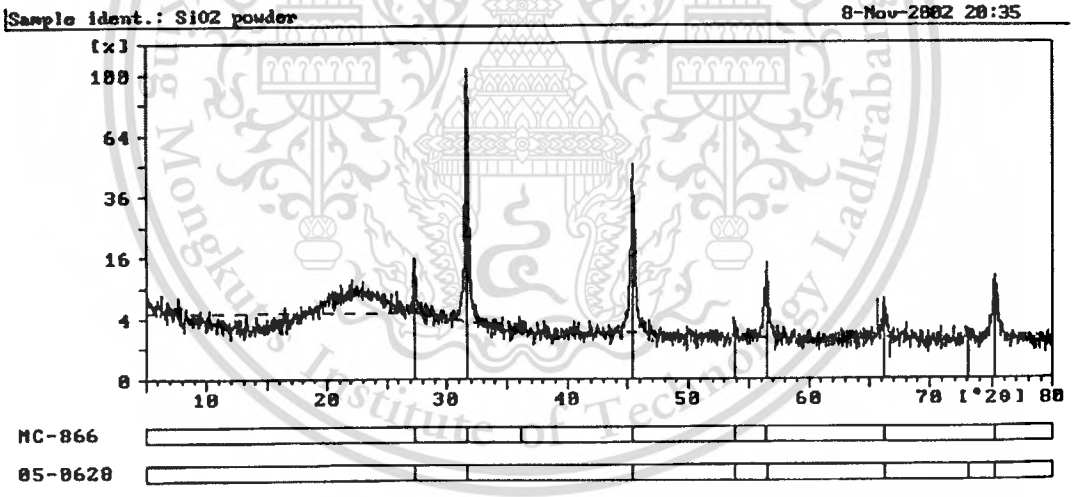

Fig. 4.2 XRD spectra of silica for HPLC column before acid washed.

After acid washed, the XRD pattern is shown in Fig. 4.3. Fig. 4.3 shows silica amorphous form [23, 25]. After sieving with test sieve aperture 400 mesh (38 μm, ASTM), the particle size distribution and particle shape of this silica were determined using light scattering analysis technique (Mastersizer X) and scanning electron microscope (SEM) as shown in Fig. 4.4 and Fig. 4.5, respectively.

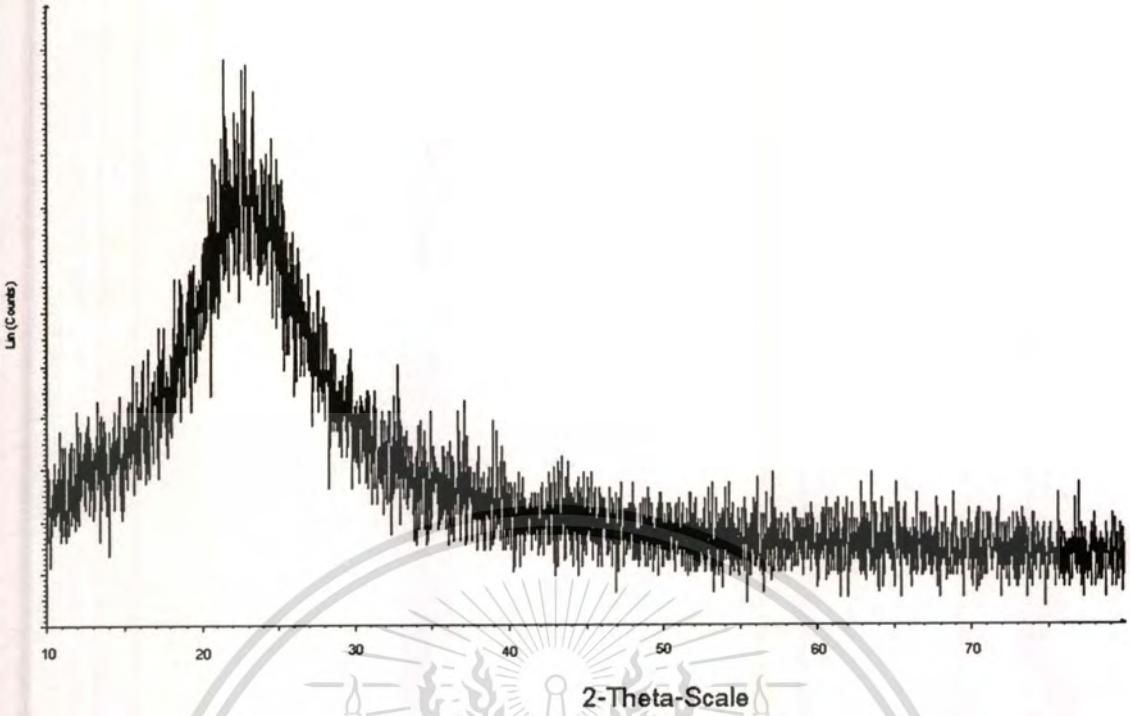

Fig. 4.3 XRD spectra of silica for HPLC column after acid washed.

From the results for particle size distribution and morphology, the average particle size of the silica was 21.52 μm and spherical shape. However, the results from SEM and Mastersizer were shown the silica particle into two size ranges (about 10-60 μm and 2-10 μm)

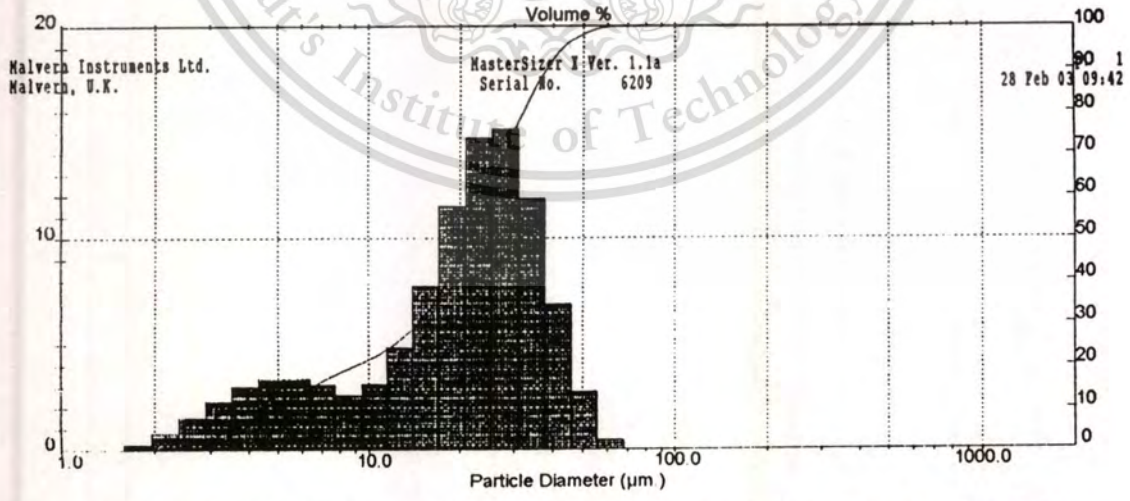

Fig. 4.4 Particle size distribution of silica powder after sieving with test sieve aperture of 400 mesh.

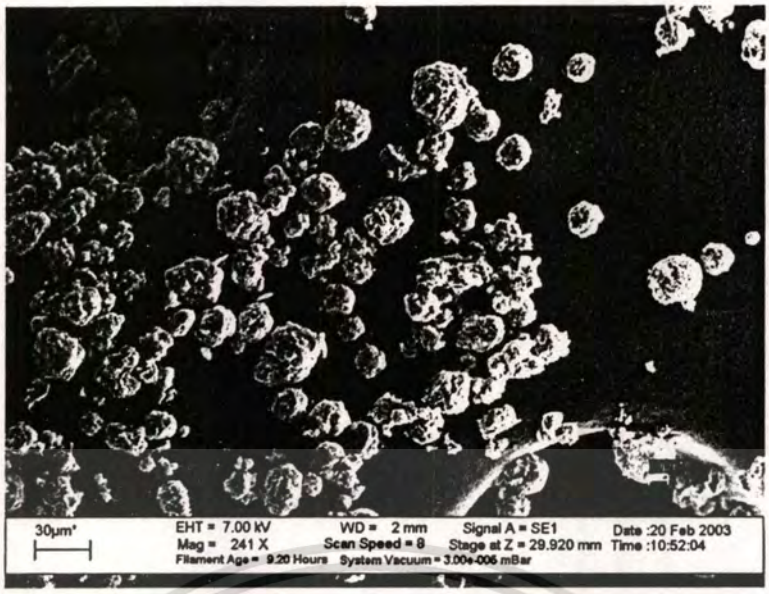

Fig. 4.5 SEM picture of silica particle after washed with conc. HCl and pass through test sieve aperture of 400 mesh.

Surface area and pore size distribution of silica powder were measured using Brunauer-Emmett-Teller (BET) method (Autosorb-1). Unwashed silica was having surface area of 188.58 m^2/g, that lower than washed silica that having 307.28 m^2/g. Because of the salt was covered on the silica surface, therefore the absorbate gas can not be absorbed on this surface. Washed silica was having major pore size of 60 Å. Fig. 4.6 was shown pore size distribution of silica for HPLC column.

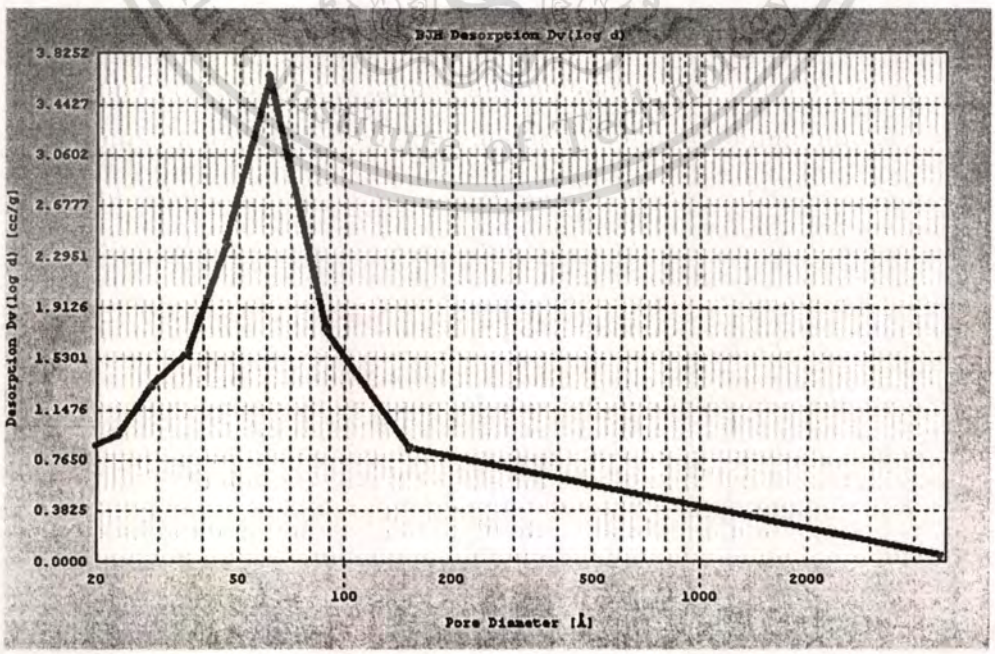

Fig. 4.6 Pore size distribution of silica for HPLC column: BJH desorption Dv (log d) plot.

The functional groups and chemical structures on silica surface were determined using FTIR and ^{29}Si solid state: CP/MAS techniques, respectively.

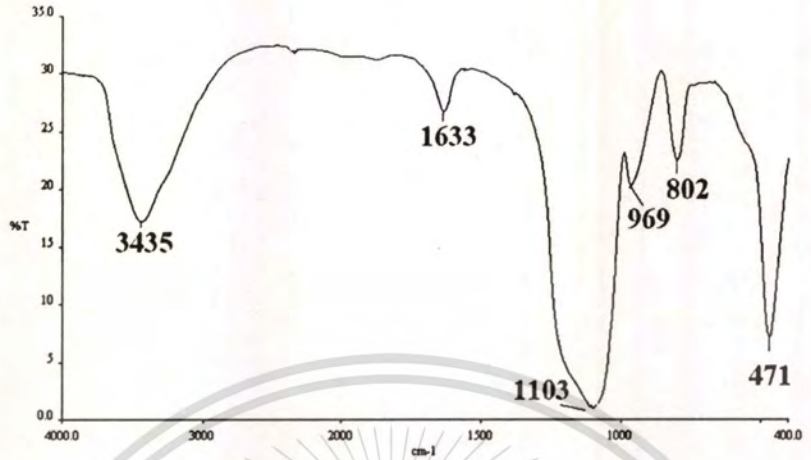

Fig. 4.7 FTIR spectrogram of silica for HPLC column.

Fig. 4.7 shows the FTIR spectra of silica for HPLC column. A strong, broad absorbance band was usually observed at ~3500 cm^{-1}, due to O-H stretching vibrations. A weaker O-H bending vibration band was seen at ~1600 cm^{-1}. Both adsorbed water and surface -OH groups contribute to these bands. The Si-O-Si fundamental vibration gives the strong band at ~1100 cm^{-1} [32, 38-39].

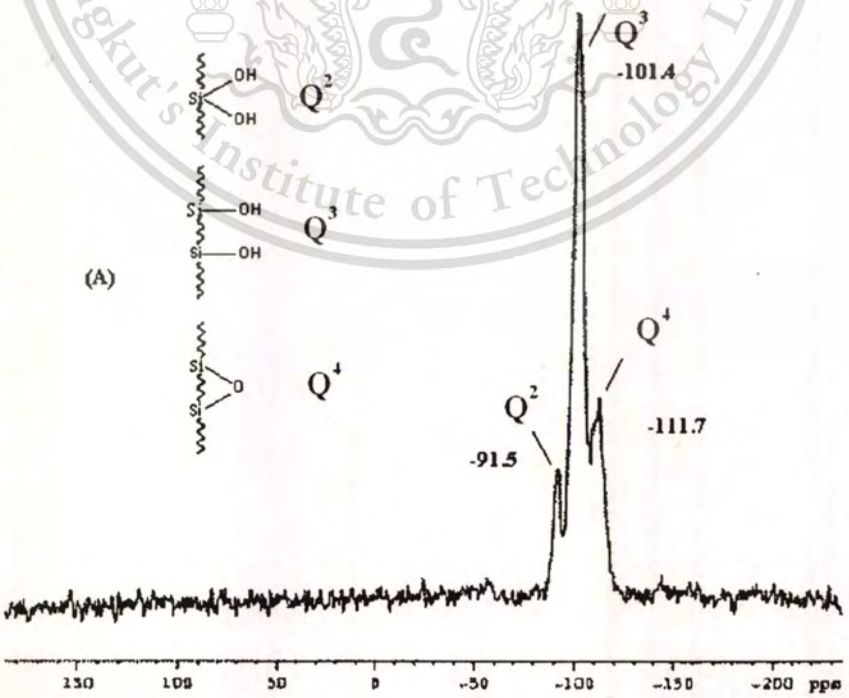

Fig. 4.8 Solid state ^{29}Si CP-MAS-NMR of silica gel for HPLC column.

Fig. 4.8 shows ^{29}Si CP-MAS-NMR spectra of the silica for HPLC column. The species found on the surface, described as the Q^n species, are related to the number of oxygen (geminal silanol Q^2, silanol Q^3, siloxanes Q^4) atoms bound to the silicon atom [33, 36-38]. In the spectrum of silica, the Q^4, Q^3 and Q^2 species were detected at -111.7, -101.4 and -91.5 ppm, respectively. These three peaks were exhibited to structural of bare silica gel as showed in Fig. 4.8.

4.2.2.2 CHARACTERIZATION OF SILICA FOR GC COLUMN

The XRD spectra of silica for GC column was represented to amorphous form similar to XRD spectra of silica for HPLC column, because of this silica was formed by sol-gel technique and drying temperature was not higher than transformation temperature between amorphous and another crystalline forms.

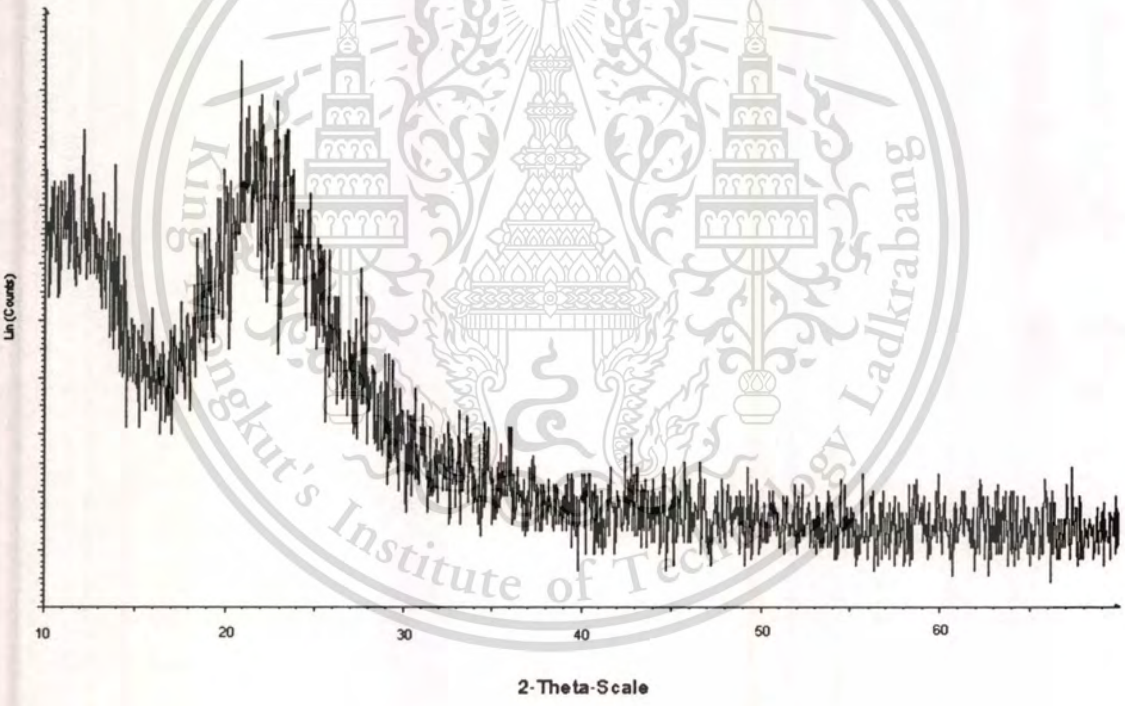

Fig. 4.9 XRD spectra of silica for GC column after acid washed.

The shape and particle size of silica for GC column were investigated using SEM technique and this results were shown in Fig. 4.10. From the SEM picture, the shape of silica particle for GC column was irregular shape and particle size diameter about 150-180 μm. Surface

area and pore size distribution of silica for GC column were determined using BET method. Fig. 4.11 shows pore size distribution of silica for GC column that has a major pore size of 300 Å.

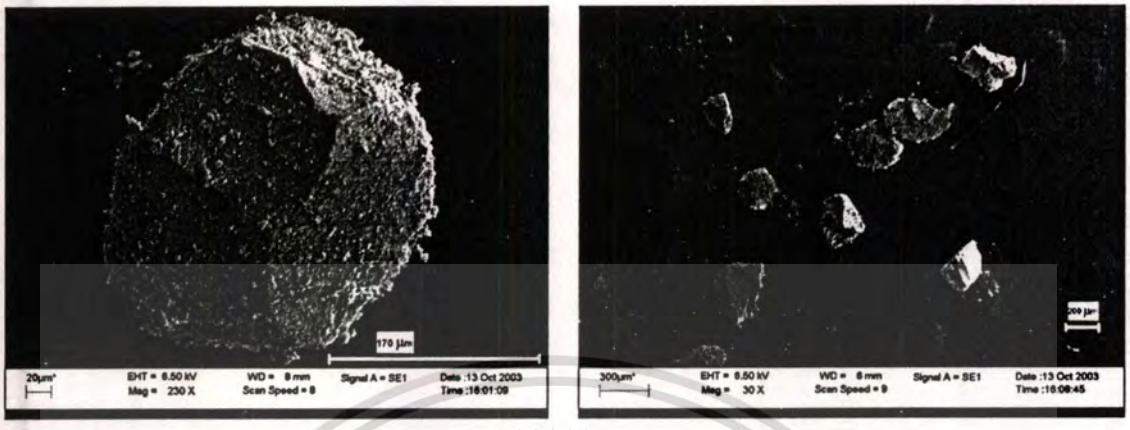

(a) (b)

Fig. 4.10 SEM photograph of silica for GC column. (a) 230X magnification: scale bar is 170 µm and (b) 30X magnification: scale bar is 200 µm.

The surface area of silica for GC is 135.56 m^2/g.

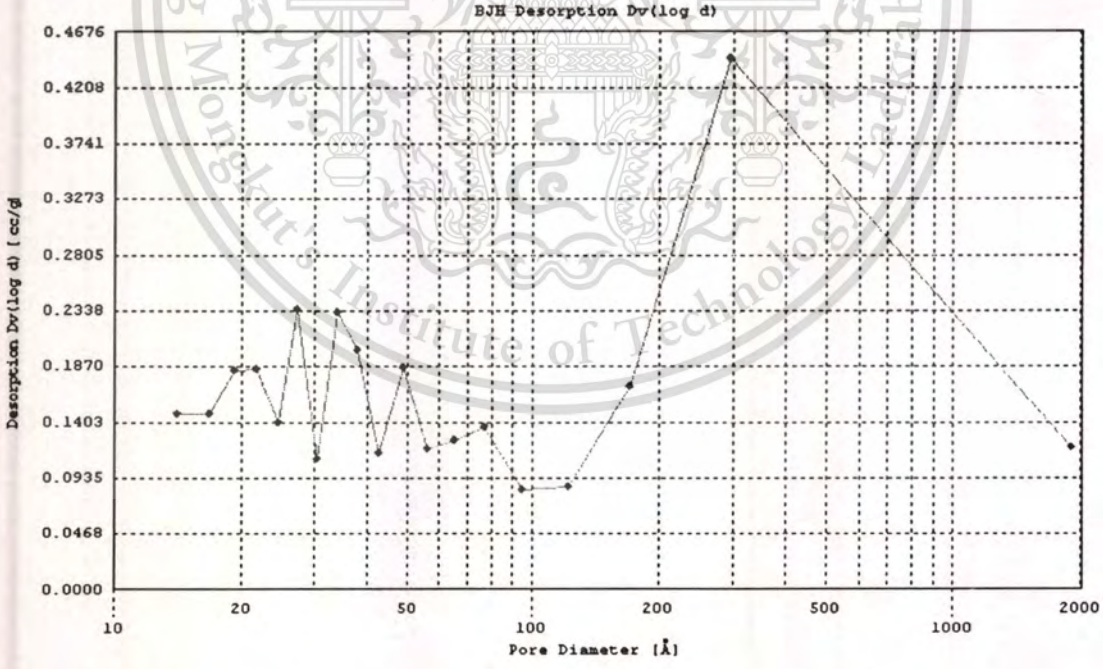

Fig. 4.11 Pore size distribution of silica for GC column: BJH desorption Dv (log d) plot.

4.3 SYNTHESIS OF SILICA-ODS WITH ENDCAPPING

4.3.1 CHARACTERIZATION OF SILICA-ODS

Physical and chemical properties of silica-ODS were characterized by using various instruments. In order to selects the optimum particle size that have high efficiency for HPLC using, the particle size should be uniform shape in range of 3-10 μm [19]. Fig. 4.12 shows the particle size distribution of silica-ODS particles. The silica-ODS has an average particle size of 14.92 μm. For this particle selection process, it was difficult for select the particle size in range of 3-10 μm. As a result, this process can not properly eliminate the smaller and bigger particles from useful particles.

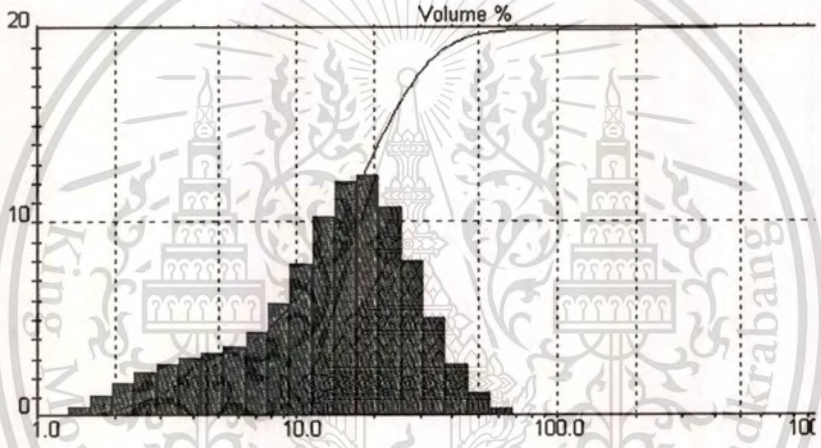

Fig. 4.12 Particle size distribution of silica-ODS after selected using sedimentation cone and centrifugation process.

The morphology, percent of carbon loading and elemental distribution on the silica-ODS surface were measurement using SEM and SEM-EDS techniques, respectively. Fig. 4.13 shows the morphology of silica-ODS.

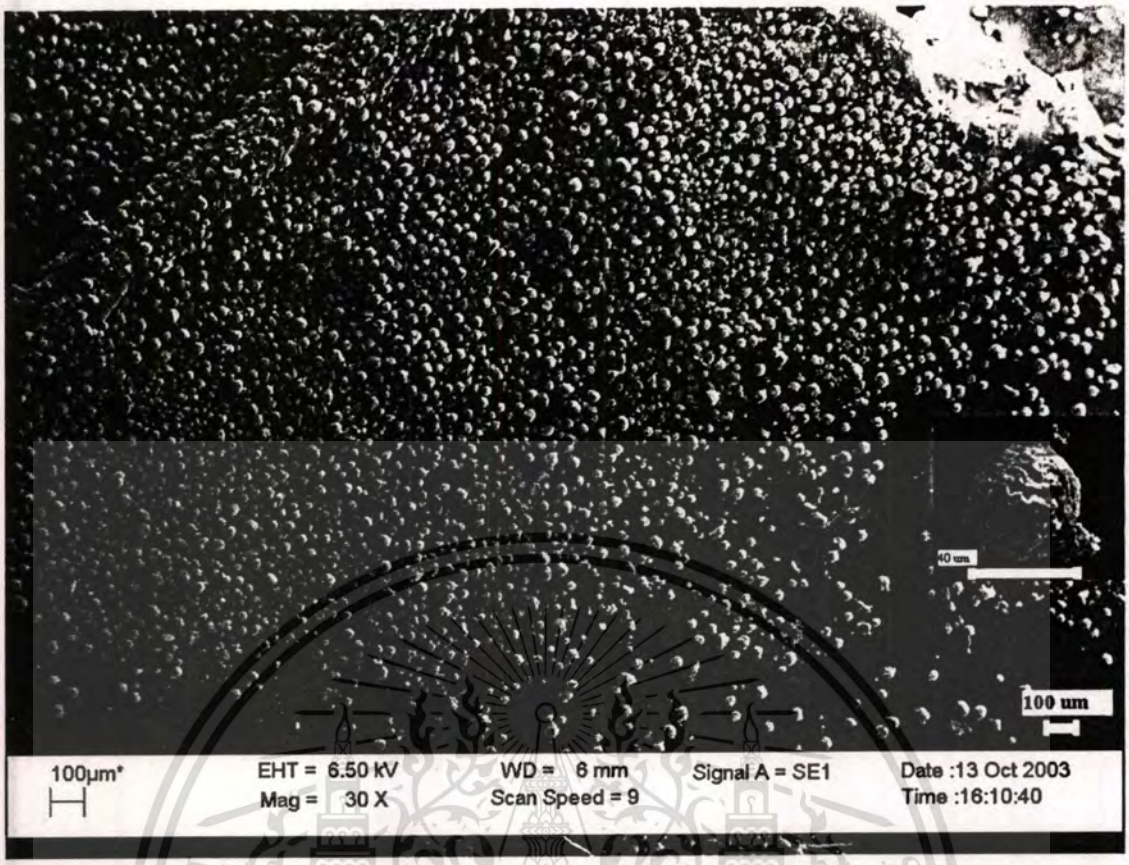

Fig. 4.13 SEM photographs of silica-ODS. Larger scale bar is 40 µm and smaller scale bar is 100 µm.

For SEM-EDS, chemical analysis in the scanning electron microscope (SEM) was performed by measuring the energy or wavelength and intensity distribution of X-ray signal generated by a focused electron beam on the specimen. With the attachment of the energy dispersive spectrometer (EDS) or wavelength dispersive spectrometers (WDS), the precise elemental composition of materials can be obtained with high spatial resolution. SEM very precise accurate chemical analyses (relative error 1-2%) can be obtained from larger areas of the solid (0.5-3 micrometer diameter) using an EDS [34]. The elemental distribution of carbon, oxygen and silicon on silica-ODS surface was shown in Fig. 4.14. Table 4.4 shows the percent of carbon loading and surface coverage (χ). The results were shown smooth carbon distribution on silica-ODS particle.

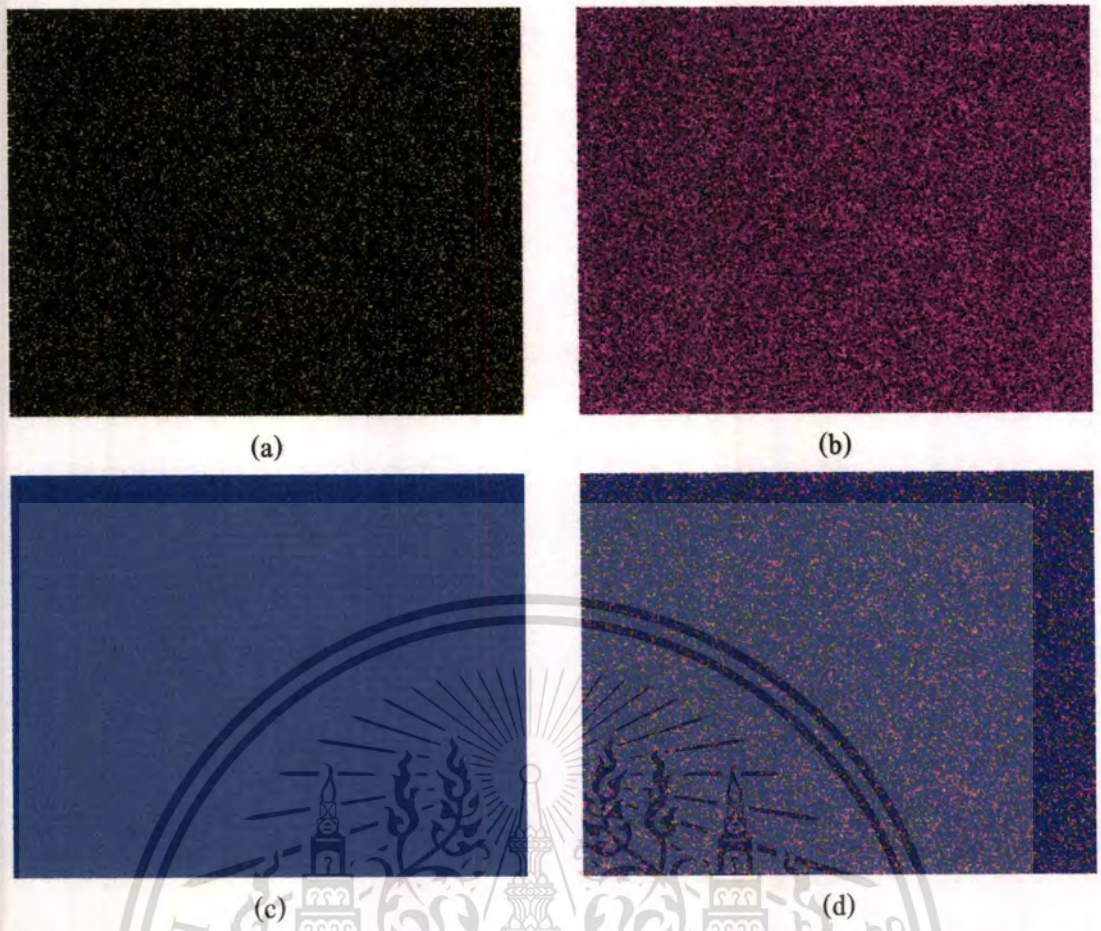

Fig. 4.14 Elemental distribution of (a) carbon, (b) oxygen, (c) silicon and (d) mixed of carbon, oxygen and silicon on the silica-ODS surface, measurement area is 1 x 1 μm^2.

Table 4.4 Percent carbon loading (*%C*) and surface coverage (χ) of ligand on silica bonded phase.

Percent carbon loading (*%C*)	Surface coverage (χ) ($\mu mol/m^2$)
17.72 ± 2.90*	3.70 ± 0.81*

* Note: These values are calculated from eleven raw data of percent carbon loading, which measured from 1 x 1 μm^2.

An average true density of silica-ODS was determined using He-ultrapycnometer and the results were reported in Table 4.5. This result was used for select the liquid medium of slurry preparation for HPLC column packing. Silica-ODS has an average of true density of 1.6519 g/cc and could be select the liquid dispersion medium into chloroform (balance density packing technique).

Table 4.5 Average true density of silica-ODS.

Average true density of silica-ODS (g/cc)
1.6519 ± 0.0105*

* Note: This value is calculated from five raw data of true density.

The silica-ODS was characterized by FTIR and solid-state ^{29}Si NMR using cross polarization and magic angle spinning (CP-MAS). Fig. 4.15 shows the FTIR spectrogram of silica-ODS. For comparison with the spectrum of the starting silica gel, two new absorption bands appear in the spectrum of the silica-ODS. The addition peaks at 2924 cm^{-1} and 2853 cm^{-1} are asymmetric stretching vibration and symmetric stretching vibration of $-CH_2-$, respectively [32, 39].

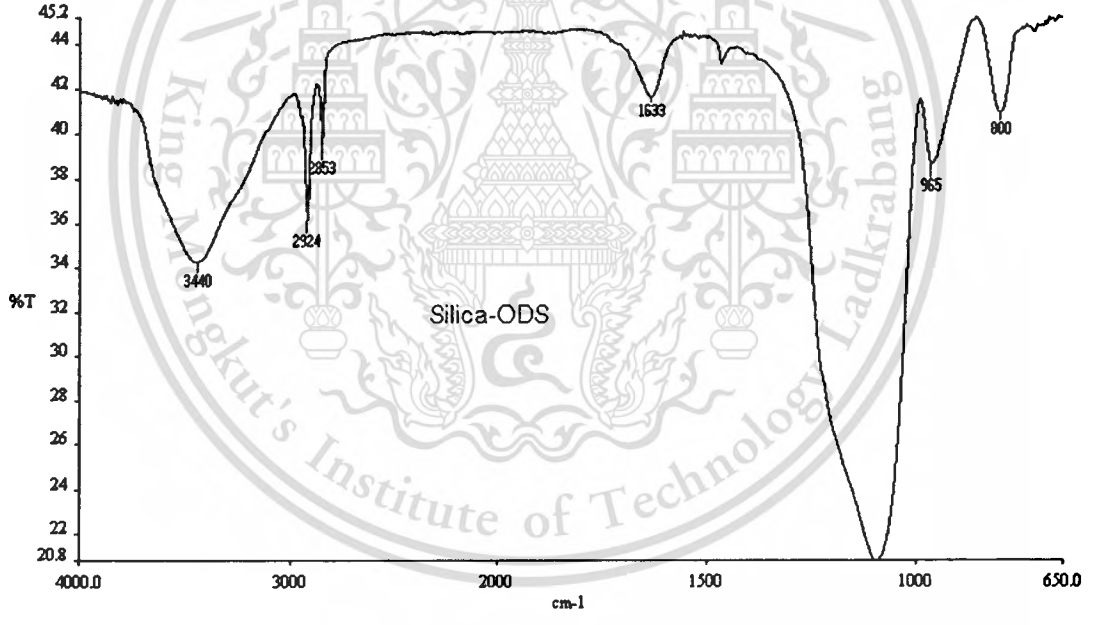

Fig. 4.15 FTIR spectrogram of silica-ODS.

Fig. 4.16 shows the ^{29}Si CP-MAS-NMR spectra of the silica-ODS. The species found on the surface, described as the T^n species. In the spectrum of silica-ODS and bare silica, the Q^4, Q^3 and Q^2 species were detected at -111.7, -101.4 and -91.5 ppm, respectively. These three peaks exhibit structure of bare silica gel as showed in Fig. 4.16. After bonded phase and end-capping, the additional three peaks at +12.2 ppm, -57.2 ppm and -65.4 ppm were detected. The peaks at -

57.2 ppm and -65.4 ppm are represented to the T^2 and T^3 species and are also shown in Fig. 4.16. The last one peak at +12.2 ppm was represented to the M species [33, 36].

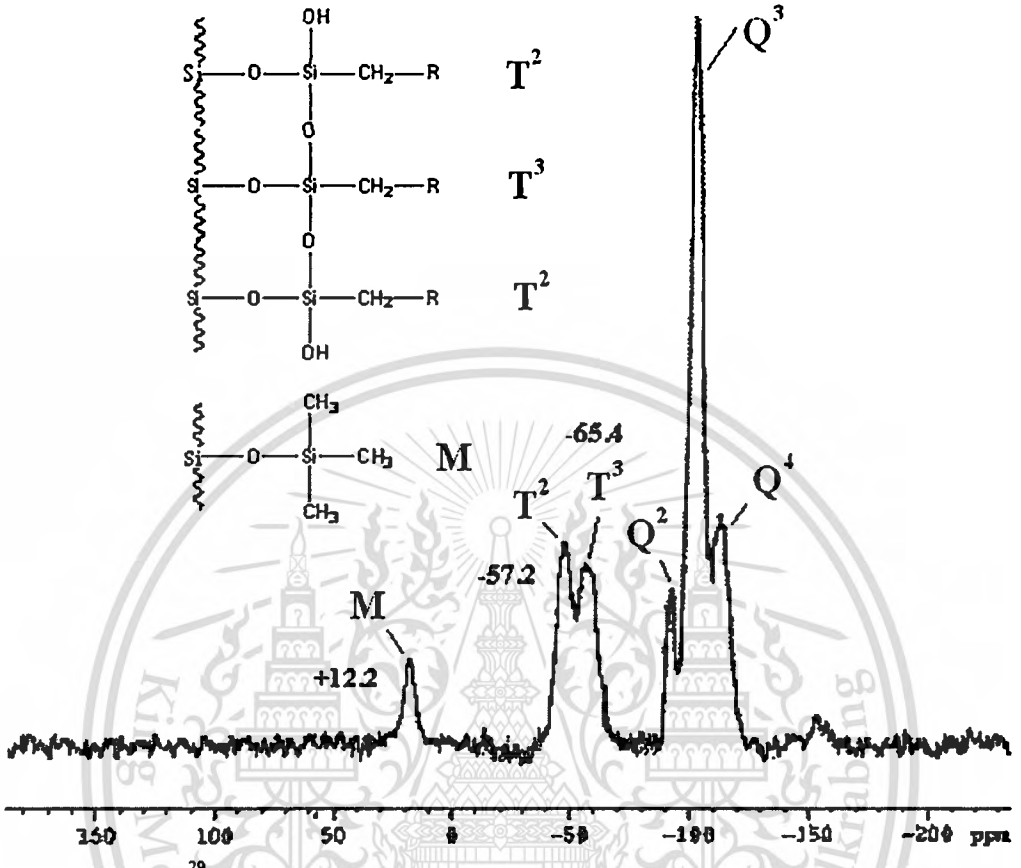

Fig. 4.16 Solid state ^{29}Si CP-MAS-NMR of silica-ODS with endcapping.

4.4 DETERMINATION OF CHROMATOGRAPHIC PARAMETERS

4.4.1 HPLC COLUMN TESTING

The first chromatographic evaluation was preformed using a standard phenol for compared Van Deemter's plot testing both of rice husk column (particle size 14.92 µm, I.D. 4.6 x 250 mm) and HiQ sil C18V column (particle size 5 µm, I.D. 4.6 x 150 mm). Van Deemter curve of rice husk column was shown in Fig. 4.17. The optimum flow rate for rice husk column and HiQ sil column are 0.3 ml/min (H_{min} = 0.0467 cm) and 0.7 ml/min (H_{min} = 0.0113 cm) respectively. Linearity testing of rice husk column was tested by varying the concentration of standard phenol (40 to 200 ppm). Fig. 4.18 shows the linearity testing of rice husk column.

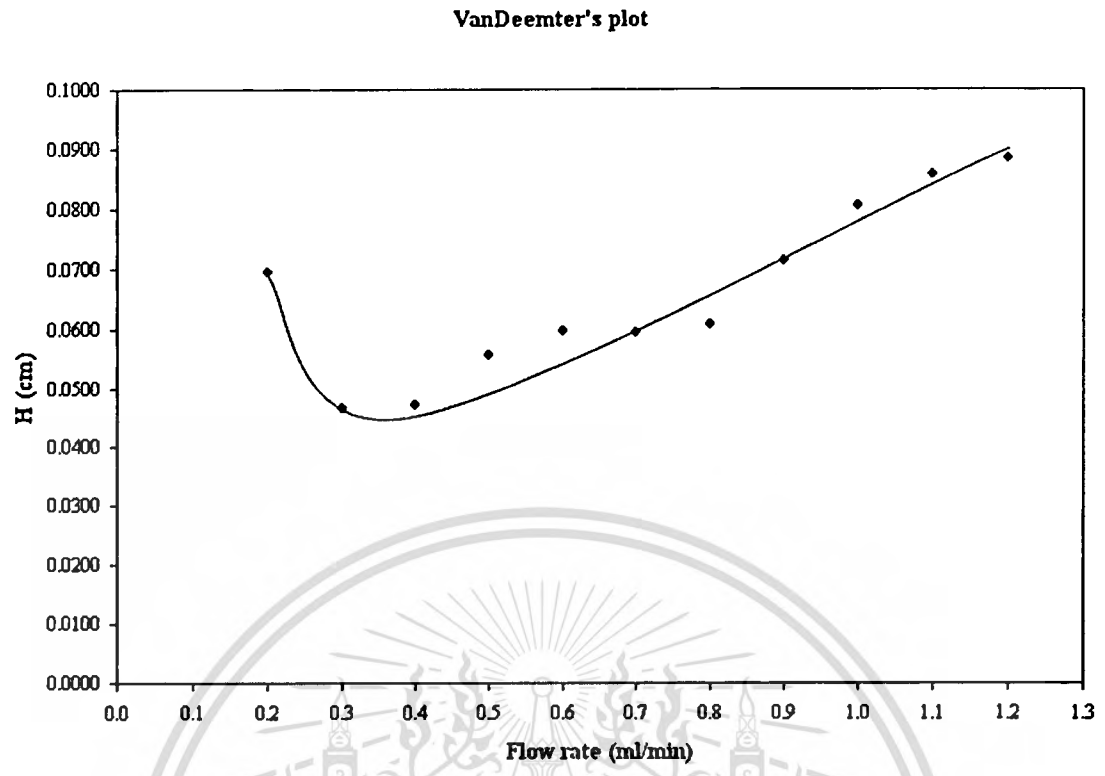

Fig. 4.17 Plots of *H* (plate height) for phenol 5000 ppm: 1.0 µl at different flow-rate of 100% methanol for rice husk column; maximum flow rate is 1.2 ml/min for 100% MeOH.

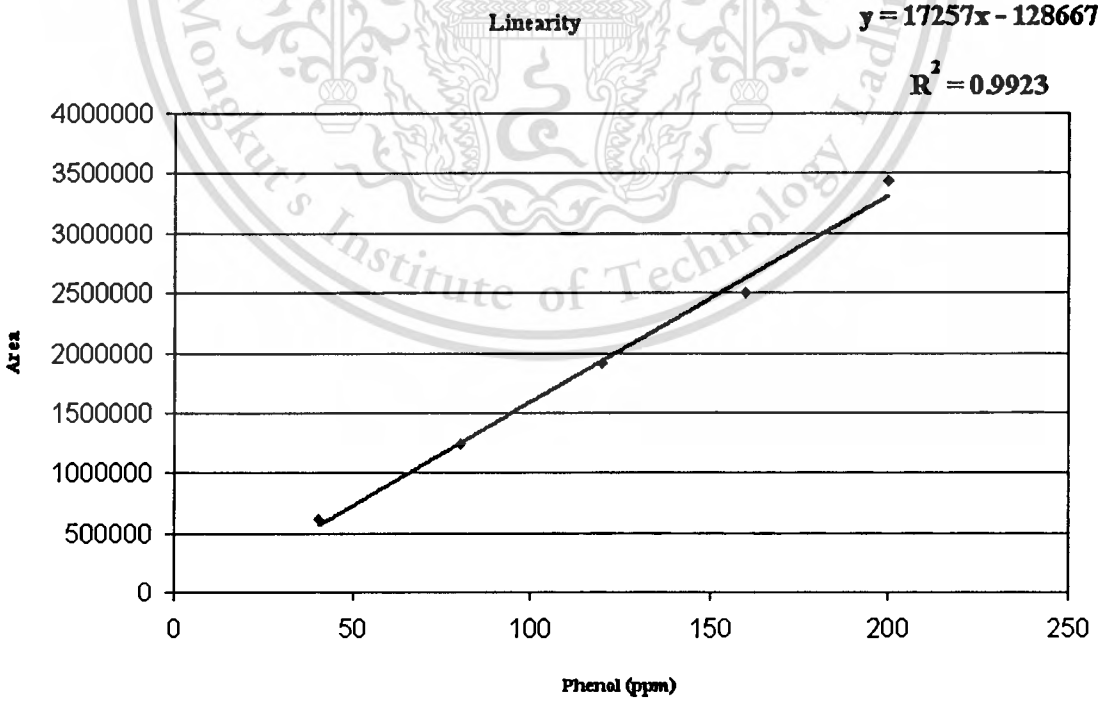

Fig. 4.18 Plots of linearity for phenol (40-200 ppm): 5.0 µl at 0.3 ml/min of 100% methanol.

* Note: For linearity testing was performed with 3-times for each concentration.

For linearity testing, the rice husk column was exhibited the R^2 of 0.9923 that shown good characteristic for quantitative analysis used. For separation efficiency testing of rice husk column was performed using 3-standard components (toluene/phenol/2-nitrophenol) and compared with HiQ sil C18V column. Fig. 4.19 and Fig. 1.20 shows the chromatograms of 3-components (toluene/phenol/2-nitrophenol) for HiQ sil C18V column at flow rate of 0.5 ml/min and 1.0 ml/min, respectively, using 100% methanol as a mobile phase.

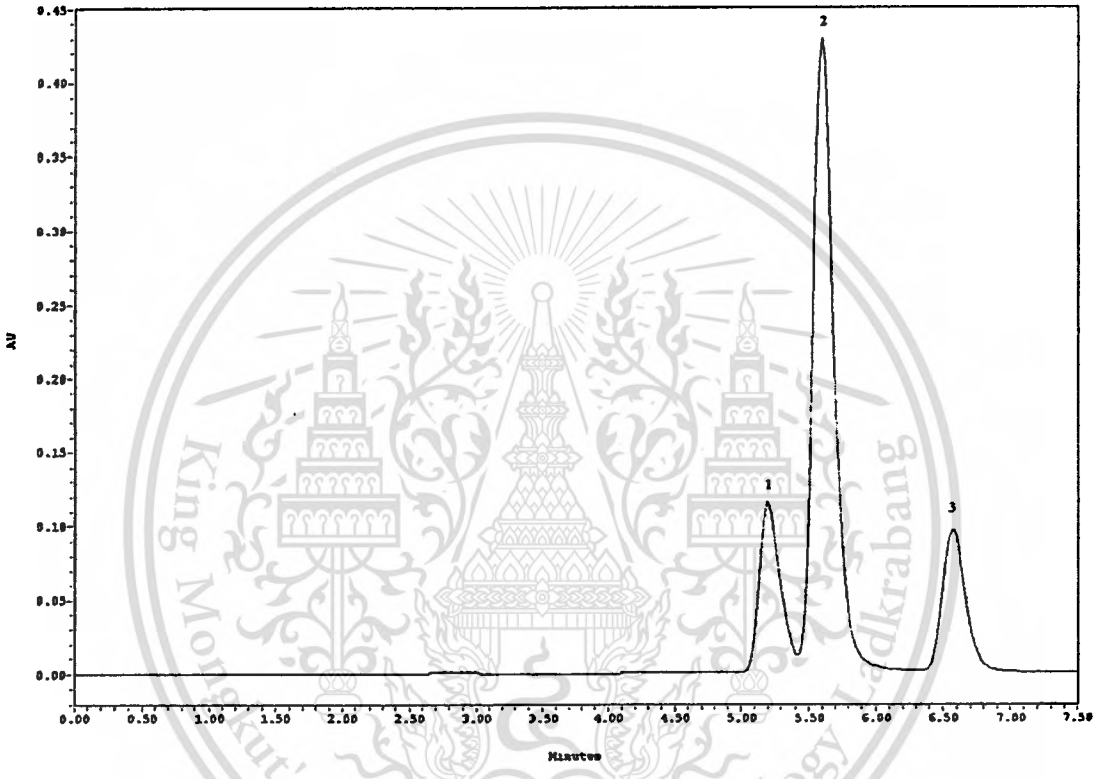

Fig. 4.19 Chromatogram for the separation of the test mixture composed of phenol (1), 2-nitrophenol (2), and toluene (3) (200 ppm for each standard) on HiQ sil C18V column. Mobile phase: 100% methanol at 0.5 ml/min, detection: UV at 254 nm and injection volume: 5 µl.

At the same conditions, but used for rice husk column, the chromatograms were showed in Fig. 4.21 and Fig. 4.22, respectively. This 3-components can not separated using rice husk column, therefore there must be varying of mobile phase composition into water and methanol mixture and it successful by using methanol:water (50:50), this 3-components was separated on rice husk column as shown in Fig. 4.23.

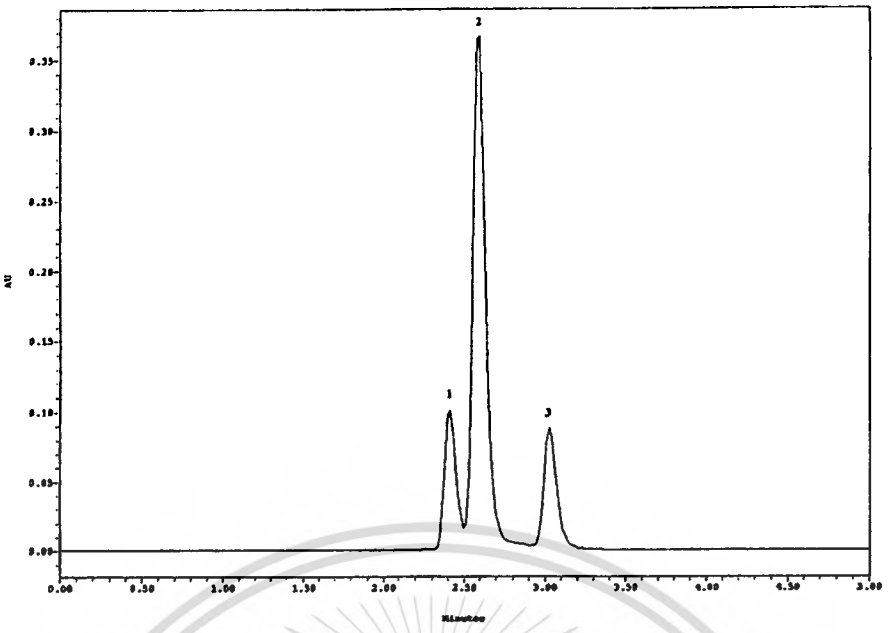

Fig. 4.20 Chromatogram for the separation of the test mixture composed of phenol (1), 2-nitrophenol (2), and toluene (3) (200 ppm for each standard) on HiQ sil C18V column. Mobile phase: 100% methanol at 1.0 ml/min, detection: UV at 254 nm and injection volume: 5 µl.

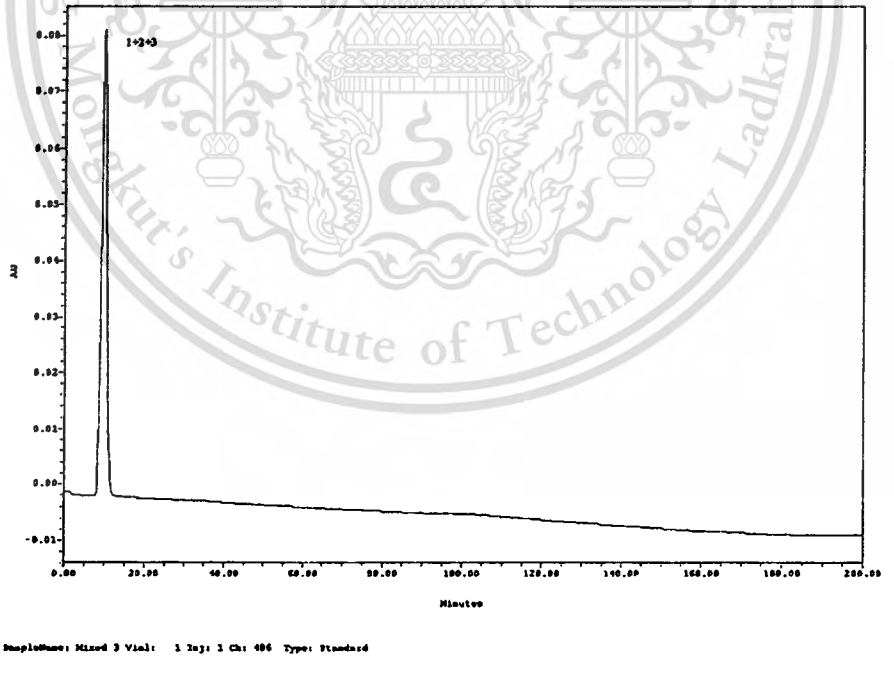

Fig. 4.21 Chromatogram for the separation of the test mixture composed of phenol (1), 2-nitrophenol (2) (200 ppm for each standard), and toluene (3) on rice husk column. Mobile phase: 100% methanol at 0.5 ml/min, detection: UV at 254 nm and injection volume: 5 µl.

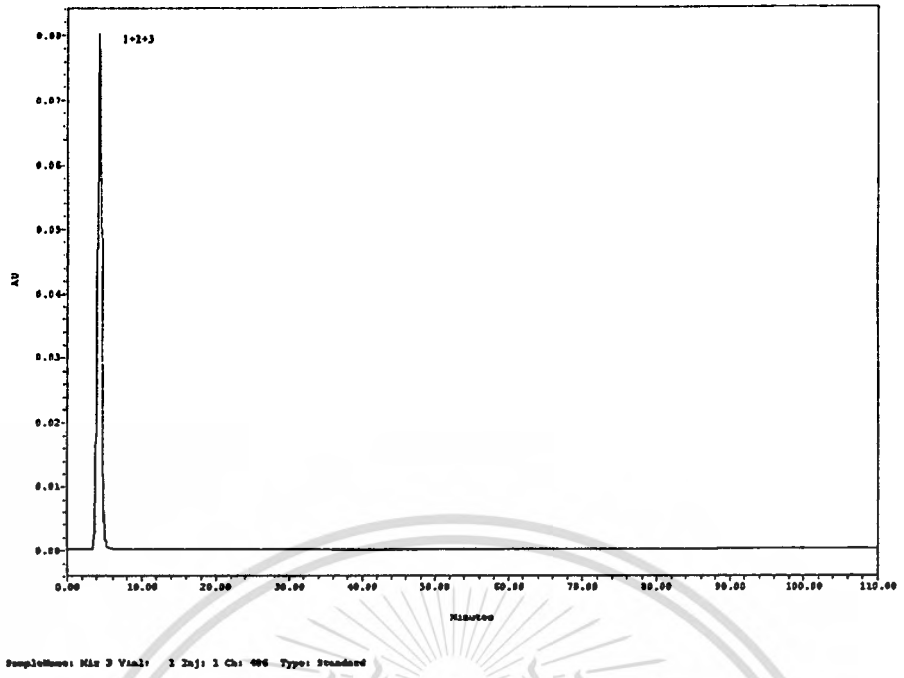

Fig. 4.22 Chromatogram for the separation of the test mixture composed of phenol (1), 2-nitrophenol (2), and toluene (3) (200 ppm for each standard) on rice husk column. Mobile phase: 100% methanol at 1.0 ml/min, detection: UV at 254 nm and injection volume: 5 µl.

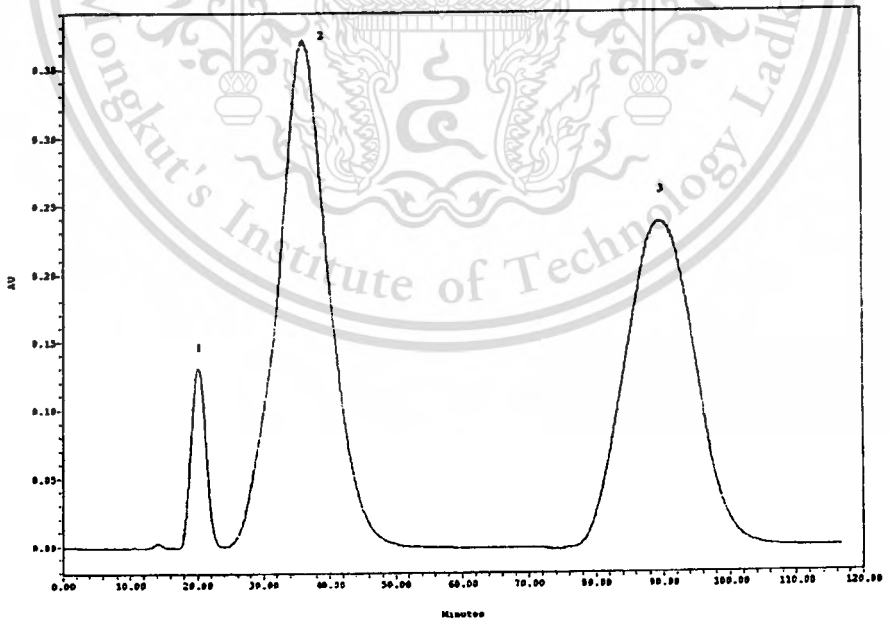

Fig. 4.23 Chromatogram for the separation of the test mixture composed of phenol (1), 2-nitrophenol (2), and toluene (3) (200 ppm for each standards) on rice husk column. Mobile phase: methanol:water (50:50) at 0.7 ml/min, detection: UV at 254 nm and injection volume: 5 µl.

4.4.2 GC COLUMN TESTING

The first chromatographic evaluation was preformed using a n-pentane for Van Deemter's plot of rice husk column (particle size 150-180 μm, O.D. 1/8" x 6').

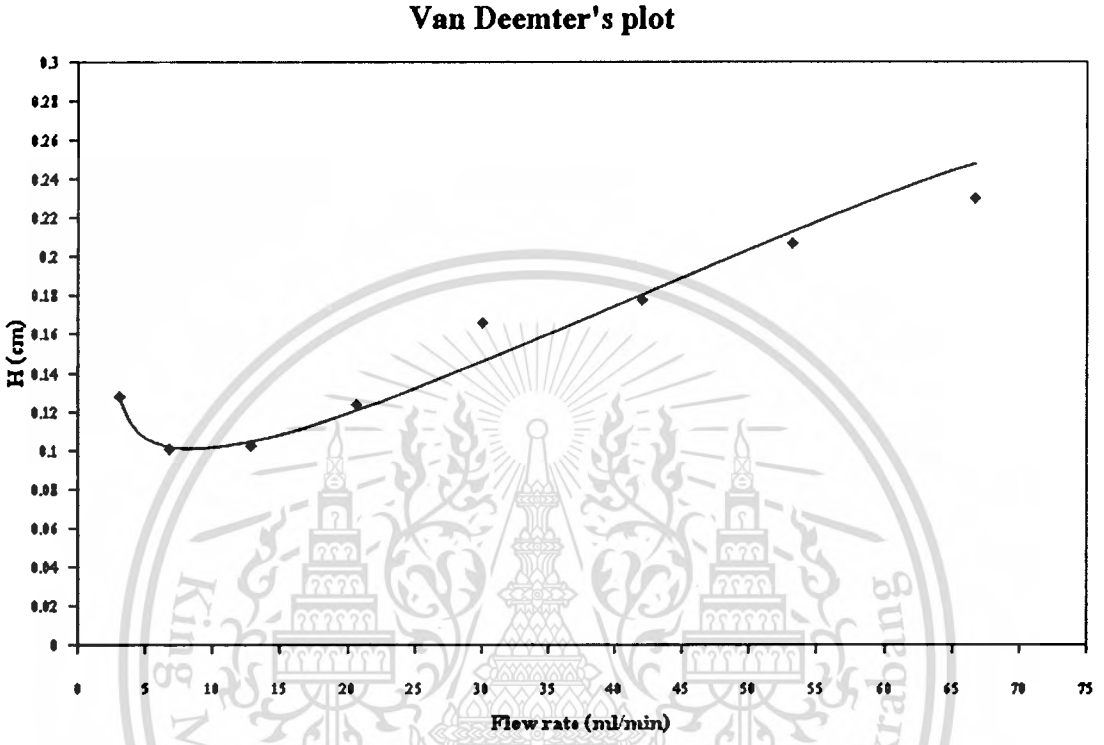

Fig. 4.24 Plots of *H* (plate height) for n-pentane. Injection volume:0.2 μl; carrier gas: N_2; inject port temperature: 180°C; oven temperature: isocratic at 150°C; detector: FID; detector temperature: 250°C; maximum operating pressure is 40 psi.

Fig. 4.24 shows Van Deemter's plot for n-pantane. The optimum flow rate for rice husk column is 6.76 ml/min (10 psi.) (H_{min} = 0.1003 cm).

The efficiency for mixture separation was performed using n-pentane (C5) and n-hexane (C6) as shown in Fig. 4.25.

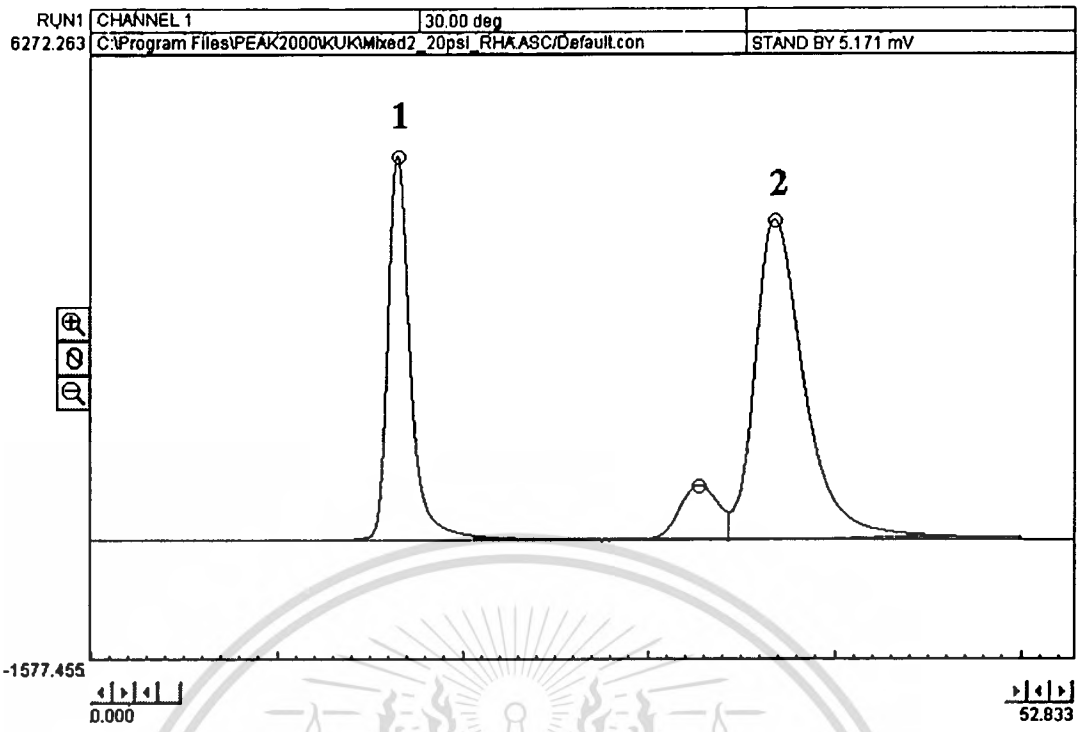

Fig. 4.25 Chromatogram for mixture separation of n-pentane (1) and n-hexane (2) (1:1). Injection volume:0.2 µl; carrier gas: N_2 at 20.70 ml/min (20 psi.); inject port temperature: 180°C; oven temperature: isocratic at 150°C; detector: FID; detector temperature: 250°C.

The H_{min} value for rice husk column can be accepted for analytical analysis, because in typically GC packed column, it has the H_{min} in range between 1 and 3 mm [35]. The H_{min} of rice husk is 0.1003 cm (1.003 mm) that was in range of general packed GC column.

CHAPTER 5

CONCLUSIONS

The objective of the present thesis was to study on the potential, limitation and suitable route for usage of rice husk in chromatographic application (GC and HPLC). Because these two columns are very expensive and can be imported from foreign countries. In this thesis, rice husk has been shown to have a very high potential to be used as starting material for high purity silica for use in HPLC and GC column.

From results obtained, the silica has a high specific surface area and high purity. However, the silica particles obtained from the spray dryer were not perfect used in HPLC column, because the particle production technique can not control the particle size and shape into targeted size and shape. This problem was a very serious factor affects on column efficiency. Generally, the particle size distribution should be as narrow as possible with a ratio of diameters of the smallest and the largest particles of 1:1.5 or 1:2 [13]. This is because the smallest particles determine the column permeability and the largest particles fix the plate number. Small particles produce a high flow resistance and large particles are responsible for a high degree of band broadening. For this research, the silica-ODS has $d_{0.9}$ of 31.21 μm and $d_{0.1}$ of 3.93 μm. Therefore the ratio of $d_{0.1}$:$d_{0.9}$ is 1:7.94, which is far from recommended value. The maximum flow rate of mobile phase is 1.2 ml/min (for 100% methanol) and 0.7 ml/min (for methanol:water (50:50)). These values depends on the allowed limitation of operating pressure. In this case, the allowed limitation of operating pressure is 3000 psi. It was very clear from the results that a lot of small size particles can not be removed from useful particle, thus these the small size particles were pushed into a frit that makes the high back pressure. Comparing the maximum flow rate of methanol and methanol-water mixture, the flow rate of 100% methanol was higher than methanol-water mixture. This is because of very high differential polarity between stationary phase (ODS, C18) and mobile phase (methanol-water mixture). The silica-ODS surface was highly hydrophobic, it can not wet with water. Therefore, to push the methanol-water mixture pass through the column must be given the higher pressure than 100% methanol.

The results from Van Deemter's plot, the H_{min} for commercial HPLC (HiQ sil C18V, i.d. 4.6 x 150 mm, average particle size of 5 μm) and rice husk column (i.d. 4.6 x 250 mm, average particle size of 14.92 μm) can not be accepted for HPLC application. Because of the H_{min} for

generally HPLC column should be in range of 5,000-10,000 plates per column [13]. It should be occurred from too much extra-column volume in the HPLC instrument, so that the peaks are broadened in the column.

For GC column, the GC column efficiency is acceptable for packed GC column technique. Because of, generally packed GC column should give the H_{min} in range of 1-3 mm [32]. From the results obtained, the rice husk GC column has the H_{min} of 1 mm. However, the silica particles are not perfect for used in GLC technique, because they precipitated from sol-gel synthesis route and would have very high surface area (generally for packed GLC column, the solid support has a surface area about 1-4 m^2/g (silica in this research has average surface area of 135.56 m^2/g)).

As future work, the silica particle size should be controlled within a range of 3 to 10 μm, with uniform size and shape. The author would like to suggest that the controlled size of silica particles can be synthezied from precipitation of sodium silicate in emulsion medium, e.g. water in oil techniques, used of surfactant, etc.

Finally, the author hopes that this work gives the initiating idea, information and guideline for develop and use of rice husk for another applications.

REFERENCES

[1] สมศักดิ์ โพธิ์ถวิลเกียรติ์, นิวัติ พิริยะรุ่งโรจน์ และ พงษ์เจต พรหมวงศ์. 2544. "อิทธิพลของขนาดของแกลบต่อคุณลักษณะการเผาไหม้." **วารสารพระจอมเกล้าลาดกระบัง**. 9(1) : 1-6.

[2] James J. and Rao M.S. 1986. "Silica from rice husk through thermal decomposition." **Thermochimica Acta**. 97 : 329-336.

[3] RiceWeb. 2004. **The Plant and How It Grows**. [Online]. Available : http://www.riceweb.org/Plant.htm.

[4] Geos 306. 2003. **Mineralogy of the Earth's Crust**. [Online]. Available : http://www.geo.arizona.edu/xtal/geos306/Geos306,Fall2002,Lecture17,TheCrust.htm.

[5] Iler R.K. 1979. **The Chemistry of Silica: Solubility, Polymerization, Colloid and Surface Properties and Biochemistry**. USA. : John Wiley & Sons, Inc.

[6] Birch D.J.S. and Geddes C.D. 2000. "Fluorescence metrology of silica sol-gels- The effect of D_2O and inorganic salts." **Proc. Indian Acad. Sci. (Chem. Sci.)**. 112(3) : 311–322.

[7] Berthod A. 1991. "Silica: backbone material of liquid chromatographic column packings." **J. of Chromato**. 549 : 1-28.

[8] Scott R.P.W. 1995. **Techniques and Practic of Chromatography**. New York : Marcel Dekker, Inc.

[9] Sheffield Hallam University. 2004. **Chromatography: Introductory theory**. [Online]. Available : http://www.shu.ac.uk/schools/sci/chem/tutorials/chrom/chrom1.htm.

[10] Carleton. 2004. **Analytical Separations**. [Online]. Available : http://www.carleton.ca/~bhollebo/Chem2303/Extraction.htm.

[11] Weigand R.J. 2004. **Practical Aspects of HPLC Theory**. [Online]. Available : http://www.alltechweb.com.

[12] Christian G.D. and O'Reilly J.E. 1986. **Instrumental Analysis**. 2nd ed. London : Allyn and Bacon, Inc.

[13] Meyer V.R. 1988. **Practical High-Performance Liquid Chromatography**. 3rd ed., New York : John Wiley & Sons, Inc.

[14] Sheffield Hallam University. 2003. **High Performance Liquid Chromatography**.

[Online]. Available : http://www.shu.ac.uk/schools/sci/chem/tutorials/chrom/hplc.htm.

[15] ANSYS Technologies. 2001. **HPLC Column Design.** [Online]. Available : http://www.metachem.com/tech/column.html.

[16] Melander W.R. and Horvath C. 1980. **Reversed-Phase Chromatography, in HPLC Advances and Perspectives vol. 2.** London : Academic Press.

[17] Unger K.K. 1979. **Porous silica.** London : Elsevier.

[18] Introduction into GC. 2002. **The GC system.** [Online]. Available : http://www.mn-net.com/web/MN-WEB-Webkatalog.nsf/WebframesE/Introduction into GC.htm.

[19] Neue U.D. 2001. **HPLC Columns : Theory, Technology, and Practice.** Milford : John Wiley & Sons, Inc.

[20] Katz E., Eksteen R., Schoenmakers P. and Miller N. 1999. **Chromatographic Science Series: Handbook of HPLC vol. 78.**

[21] Packing of HPLC columns. 2002. **Information for packing in LC.** [Online]. Available : http://www.mn-net.com/web/MN-WEB-Webkatalog.nsf/WebframesE/Information for packing in LC.htm.

[22] Snyder L.R. and Kirkland J.J. 1979. **Introduction to Modern Liquid Chromatography.** 2nd ed. New York : John Wiley & Sons, Inc.

[23] Ibrahim D.M. and Helmy M. 1981. "Crystallite growth of rice husk ash silica." **Thermochimica Acta.** 45 : 79-85.

[24] อุไรวรรณ ลีลาอดิศร. 2535. "การเตรียมและศึกษาคุณลักษณะของซิลิกาคุณภาพสูงจากแกลบ." วิทยานิพนธ์วิทยาศาสตรมหาบัณฑิต ภาควิชาวัสดุศาสตร์ บัณฑิตวิทยาลัย, จุฬาลงกรณ์มหาวิทยาลัย.

[25] Khunthon S., Tangwiwat S. and Roengsumran S. 1997. "The Application of Rice Husk Ash for Silica Production." **J. of Metals, Materials and Minerals.** 7(1) : 21-30.

[26] สรินทร ลิ่มปนาท, กฤษณา ศิรเลิศมุกุล และ ศรีไฉล ขุนทน. 2542. "การเตรียมแผ่นกรองซิลิกาจากขี้เถ้าแกลบ." หน้า 1-55. ใน **รายงานผลการวิจัยเสนอสำนักงานคณะกรรมการวิจัยแห่งชาติ (งบประมาณแผ่นดินประจำปีงบประมาณ 2542).** กรุงเทพฯ : สถาบันวิจัยโลหะและวัสดุจุฬาลงกรณ์มหาวิทยาลัย.

[27] Kalapathy U., Proctor A. and Shultz J. 2000. "Silica xerogels from rice hull ash: structure, density and mechanical strength as affected by gelation pH and silica concentration." **J. of Chem Technol Biotechnol.** 75 : 464-468.

[28] Souza M.F. de, Batista P.S., Regiani I., Souza D.P.F. de. 2000. "Rice Hull-Derived Silica: Applications in Portland Cement and Mullite Whiskers." **Materials Research**. 3(2) : 25-30.

[29] Nakbanpote W., Thiravetyan P. and Kalambaheti C. 2000. "Preconcentration of gold by rice husk ash." **Minerals Engineering**. 13(4) : 391-400.

[30] Jones K. 1987. "Optimization procedure for the silanization of silicas for reversed-phase high-performance liquid chromatography." **J. of Chromato**. 392 : 11-16.

[31] Altech. 2002. **GC FAQ's**. [Online]. Available : http://www.alltechweb.com/productinfo/Technical/faq/11 gc FAQ.htm.

[32] Christian G.D., and O'Reilly J.E. 1986. **Instrumental Analysis**. London : Allyn and Bacon, Inc.

[33] Joseph J.P., Maria T.M., and Riad R.A. 1996. **Chemically Modified Surfaces: Recent Developments**. London : The Royal Society of Chemistry.

[34] SEM-EDS Laboratory. 2002. **About EDS**. [Online]. Available : http://www2.arnes.si/~sgszmera1/.

[35] Braithwaite A. and Smith F.J. 1996. **Chromatographic Methods**. 5th Ed. London : Blackie Acadeemic & Professional.

[36] Silva C.R., Bachmann S., Schefer R.R., Albert K., Jardim I.C.S.F. and Airoldi C. 2002. "Preparation of a new C_{18} stationary phase containing embedded urea groups for use in high-performance liquid chromatography." **J. of Chromato. A.** 948 : 85-95.

[37] Blaaderen A.V. and Kentgens A.P.M. 1992. "Particle morphology and chemical microstructure of colloidal silica spheres made from alkoxysilanes." **J. of Non-Crystalline Solids**. 149 : 161-178.

[38] Zhao X.S., Lu G.Q., Whittaker A.K., Millar G.J. and Zhu H.Y. 1997. "Comprehensive Study of Surface Chemistry of MCM-41 Using 29Si CP/MAS NMR, FTIR, Pyridine-TPD, and TGA." **J. Phys. Chem. B**. 101 : 6525-6531.

[39] Huang X., Wang J. and Liu X. 2002. "A Simple Preparation of Stationary Phase of Alkylamide Reversed-Phase Liquid Chromatograph for the Separation of Basic Substances." **Analytical Sciences**. 18 : 69-72.

APPENDICES

APPENDIX A

CHARACTERIZATION OF SILICA

Table A-1 Chemical composition in rice husk ash determined using XRF after burning of rice husk 50 g at 700°C for 1 hr.

Na_2O	MgO	Al_2O_3	SiO_2	P_2O_5	SO_3	Cl
0.2 KCps	1.5 KCps	0.2 KCps	275.0 KCps	1.6 KCps	1.1 KCps	1.4 KCps
0.130 %	0.491 %	0.0965 %	94.2 %	1.03 %	0.369 %	0.199 %

K_2O	CaO	TiO_2	MnO	Fe_2O_3	ZnO	Rb_2O
17.9 KCps	6.7 KCps	0.1 KCps	2.5 KCps	1.5 KCps	0.8 KCps	2.8 KCps
2.25 %	0.857 %	0.0123 %	0.184 %	0.0583 %	0.0123 %	0.0103 %

WO_3	Au	Compton	Rayleigh	Sum
3.0 KCps	1.0 KCps			
0.129 %	0.00643 %	0.91	1.12	100.00 %

Table A-2 Chemical composition in rice husk ash determined using XRF after burning of rice husk 50 g at 700°C for 1.5 hrs.

Na_2O	MgO	Al_2O_3	SiO_2	P_2O_5	SO_3	Cl
0.2 KCps	1.2 KCps	0.3 KCps	284.5 KCps	1.7 KCps	1.3 KCps	1.7 KCps
0.122 %	0.371 %	0.100 %	94.3 %	1.04 %	0.408 %	0.222 %

K_2O	CaO	TiO_2	MnO	Fe_2O_3	CoO	ZnO
18.3 KCps	6.9 KCps	0.1 KCps	2.6 KCps	1.6 KCps	0.2 KCps	0.8 KCps
2.20 %	0.841 %	0.0102 %	0.176 %	0.0567 %	0.00621 %	0.0118 %

Rb_2O	SrO	Pd	WO_3	Au	Compton	Rayleigh
2.9 KCps	0.5 KCps	0.2 KCps	1.9 KCps	1.8 KCps		
0.00854 %	0.00207 %	0.0114 %	0.0778 %	0.0269 %	0.91	1.12

Sum
100.00 %

Table A-3 Chemical composition in rice husk ash determined using XRF after burning of rice husk 50 g at 700°C for 2 hrs.

Na_2O	MgO	Al_2O_3	SiO_2	P_2O_5	SO_3	Cl
0.2 KCps	1.2 KCps	0.2 KCps	289.0 KCps	1.6 KCps	1.2 KCps	1.9 KCps
0.125 %	0.351 %	0.0797 %	94.6 %	0.962 %	0.363 %	0.244 %

K_2O	CaO	MnO	Fe_2O_3	ZnO	Rb_2O	WO_3
18.1 KCps	6.8 KCps	2.5 KCps	1.6 KCps	0.9 KCps	2.7 KCps	1.5 KCps
2.14 %	0.807 %	0.165 %	0.0581 %	0.0125 %	0.00945 %	0.0603 %

Compton	Rayleigh	Sum
0.92	1.11	100.00 %

Table A-4 Chemical composition in silica gel after washed with conc. HCl determined using XRF.

SiO_2	CaO	Fe_2O_3	CuO	Compton	Rayleigh	Sum
64.9 KCps	0.3 KCps	2.8 KCps	3.0 KCps			
99.5 %	0.0872 %	0.154 %	0.109 %	0.82	0.97	100.00 %

File: MC-866.DI 8-Nov-2002

Philps Analytical X-Ray B.V. PC-APD, Diffraction software

Sample identification: SiO2 powder
Data measured at: 8-Nov-2002 19:56:00
Diffractometer type: PW3710 BASED
Tube anode: Cu
Generator tension [kV]: 40
Generator current [mA]: 30
Wavelength Alpha1 []: 1.54060
Wavelength Alpha2 []: 1.54439
Intensity ratio (alpha2/alpha1): 0.500
Divergence slit: 1½
Receiving slit: 0.1
Monochromator used: YES
Start angle [2θ]: 5.020
End angle [2θ]: 79.980
Step size [2θ]: 0.040
Maximum intensity: 967.2100
Time per step [s]: 1.000
Type of scan: CONTINUOUS
Peak positions defined by: Minimum of 2nd derivative of peak
Minimum peak tip width: 0.00
Maximum peak tip width: 1.00
Peak base width: 2.00
Minimum significance: 0.75
Number of peaks: 8

Angle [2θ]	d-value α1 []	d-value α2 []	Peak width [2θ]	Peak int [counts]	Back. int [counts]	Rel. int [%]	Signif.
27.310	3.2629	3.2710	0.200	69	46	7.1	1.79
31.675	2.8225	2.8295	0.160	967	35	100.0	5.86
36.180	2.4808	2.4869	0.800	4	22	0.5	0.75
45.385	1.9967	2.0016	0.240	412	22	42.6	7.91
53.815	1.7021	1.7063	0.320	12	16	1.2	0.77
56.380	1.6306	1.6346	0.120	102	17	10.5	1.18
66.195	1.4106	1.4141	0.400	40	17	4.1	2.49
75.230	1.2621	1.2652	0.120	94	15	9.7	1.61

Fig. A-1 XRD data for silica gel before acid washed, contaminated with NaCl.

Reference pattern: 05-0628 8-Nov-2002

Name	: Sodium Chloride
Name	: Halite, syn
Formula	: NaCl
Elements	: Na, Cl
Groups	: --
Subfiles	: Inorganic, Minerals, Common phases, NBS patterns, Forensics, Educational patterns
Pattern deleted	: NO
Radiation	: Cu Kα1
Wavelength	: 1.54060

d value	Angle	Rel. Int.
3.2600	27.335	13
2.8210	31.693	100
1.9940	45.450	55
1.7010	53.854	2
1.6280	56.479	15
1.4100	66.229	6
1.2940	73.066	1
1.2610	75.304	11
1.1515	83.973	7
1.0855	90.409	1
0.9969	101.193	2
0.9533	107.809	1
0.9401	110.046	3
0.8917	119.505	4
0.8601	127.170	1
0.8503	129.894	3
0.8141	142.240	2

Fig. A-2 XRD pattern of NaCl from XRD-instrument library.

Presentation: (2OHD) 1.330, 1.530 + i 0.10000
SiO2 Gel Run No. 2
Polydisperse Volume Result

Source: Analysed Focus = 300 mm Beam Length = 2.4 mm
Obscuration = 31.7%

Operator: Kuk

Residual = 0.327% Concentration = 0.059%
Uniformity = 0.468 Span = 1.541
Specific S.A. = 0.4968 sq. m. / gm
d (v, 0.5) = 21.52 um Mode = 26.24 um D [4, 3] = 21.75 um
d (v, 0.1) = 4.80 um d (v, 0.9) = 37.97 um D [3, 2] = 12.08 um

Size Um	Result Below %	Size um	Result Below %	Size Um	Result Below %	Size Um	Result Below %
0.100	0.00	0.562	0.00	3.162	3.64	17.783	38.30
0.107	0.00	0.603	0.00	3.388	4.50	19.055	42.13
0.115	0.00	0.646	0.00	3.631	5.45	20.417	46.43
0.123	0.00	0.692	0.00	3.890	6.48	21.878	51.18
0.132	0.00	0.741	0.00	4.169	7.58	23.442	56.30
0.141	0.00	0.794	0.00	4.467	8.74	25.119	61.66
0.151	0.00	0.851	0.00	4.786	9.93	26.915	67.14
0.162	0.00	0.912	0.00	5.129	11.15	28.840	72.54
0.174	0.00	0.977	0.00	5.495	12.36	30.903	77.65
0.186	0.00	1.047	0.00	5.888	13.55	33.113	82.31
0.199	0.00	1.122	0.00	6.310	14.73	35.481	86.46
0.214	0.00	1.202	0.00	6.761	15.89	38.019	90.06
0.229	0.00	1.288	0.00	7.244	17.00	40.738	93.08
0.245	0.00	1.380	0.00	7.762	18.03	43.651	95.43
0.263	0.00	1.479	0.00	8.318	18.98	46.773	96.97
0.282	0.00	1.585	0.01	8.913	19.88	50.118	98.11
0.302	0.00	1.698	0.05	9.550	20.80	53.703	99.05
0.324	0.00	1.820	0.15	10.233	21.80	57.544	99.67
0.347	0.00	1.950	0.32	10.965	22.92	61.659	99.94
0.371	0.00	2.089	0.54	11.749	24.21	66.069	100.00
0.398	0.00	2.239	0.82	12.589	25.71	70.794	100.00
0.427	0.00	2.399	1.19	13.490	27.48	75.857	100.00
0.457	0.00	2.570	1.66	14.454	29.57	81.283	100.00
0.490	0.00	2.754	2.22	15.488	32.04	87.096	100.00
0.525	0.00	2.951	2.88	16.596	34.94	93.325	100.00
						100.000	100.00

Fig. A-3 Particle size distribution for silica after sieving with test sieve 400 mesh (48 μm).

Date: 03/27/2003

Quantachrome Corporation
Quantachrome Autosorb Automated Gas Sorption System Report
Autosorb for Windows® Version 1.19

Sample ID	SiO2		
Description	BET 39 points		
Comments			
Sample Weight	0.0123 g		
Adsorbate	NITROGEN	Outgas Temp 200°C	Operator kuk
Cross-Sec Area	16.2 Å²/molec	Outgas Time 15.9 hrs	
Analysis Time	316.6 min		
NonIdeality	6.580E-05	P/Po Toler 0	
End of Run	03/26/2003 06:54		
Molecular Wt	28.0134 g/mol	Equil Time 3	
File Name	460325_1.RAW		
Station #	1	Bath Temp. 77.40	

AREA-VOLUME-PORE SIZE SUMMARY

SURFACE AREA DATA

Multipoint BET	1.061E+03 m²/g
BJH Method Cumulative Adsorption Surface Area	1.181E+03 m²/g
BJH Method Cumulative Desorption Surface Area	1.468E+03 m²/g
DH Method Cumulative Adsorption Surface Area	1.225E+03 m²/g
DH Method Cumulative Desorption Surface Area	1.529E+03 m²/g
DR Method Micro Pore Area	1.928E+03 m²/g

PORE VOLUME DATA

BJH Method Cumulative Adsorption Pore Volume	1.759E+00 cc/g
BJH Method Cumulative Desorption Pore Volume	1.834E+00 cc/g
BJH Interpolated Cumulative Adsorption Pore Volume for pores in the range of 5000.0 to 0.0 Å Diameter	1.759E+00 cc/g
BJH Interpolated Cumulative Desorption Pore Volume for pores in the range of 5000.0 to 0.0 Å Diameter	1.834E+00 cc/g
DH Method Cumulative Adsorption Pore Volume	1.757E+00 cc/g
DH Method Cumulative Desorption Pore Volume	1.839E+00 cc/g
DR Method Micro Pore Volume	6.852E-01 cc/g
HK Method Cumulative Pore Volume	4.075E-01 cc/g
SF Method Cumulative Pore Volume	4.194E-01 cc/g

PORE SIZE DATA

BJH Method Adsorption Pore Diameter (Mode)	4.655E+01 Å
BJH Method Desorption Pore Diameter (Mode)	6.106E+01 Å
DH Method Adsorption Pore Diameter (Mode)	4.655E+01 Å
DH Method Desorption Pore Diameter (Mode)	6.106E+01 Å
DR Method Micro Pore Width	1.816E+02 Å
HK Method Pore Width (Mode)	1.788E+01 Å
SF Method Pore Diameter (Mode)	3.350E+01 Å

DATA REDUCTION PARAMETERS
Thermal Transpiration : ON
Effective Molecule Diameter (D) 3.5400 Å
Effective Cell Stem Inner Diameter (d) 4.0000 mm
Last Po Acquired 707.71 mm Hg
Additional Initialization Information Not Recorded.
BJH/DH Moving Average Size : 1
Interaction Constant (K) 2.9600 nm^3 x kJ/mol

Fig. A-4 Silica gel for HPLC determined by BET method.

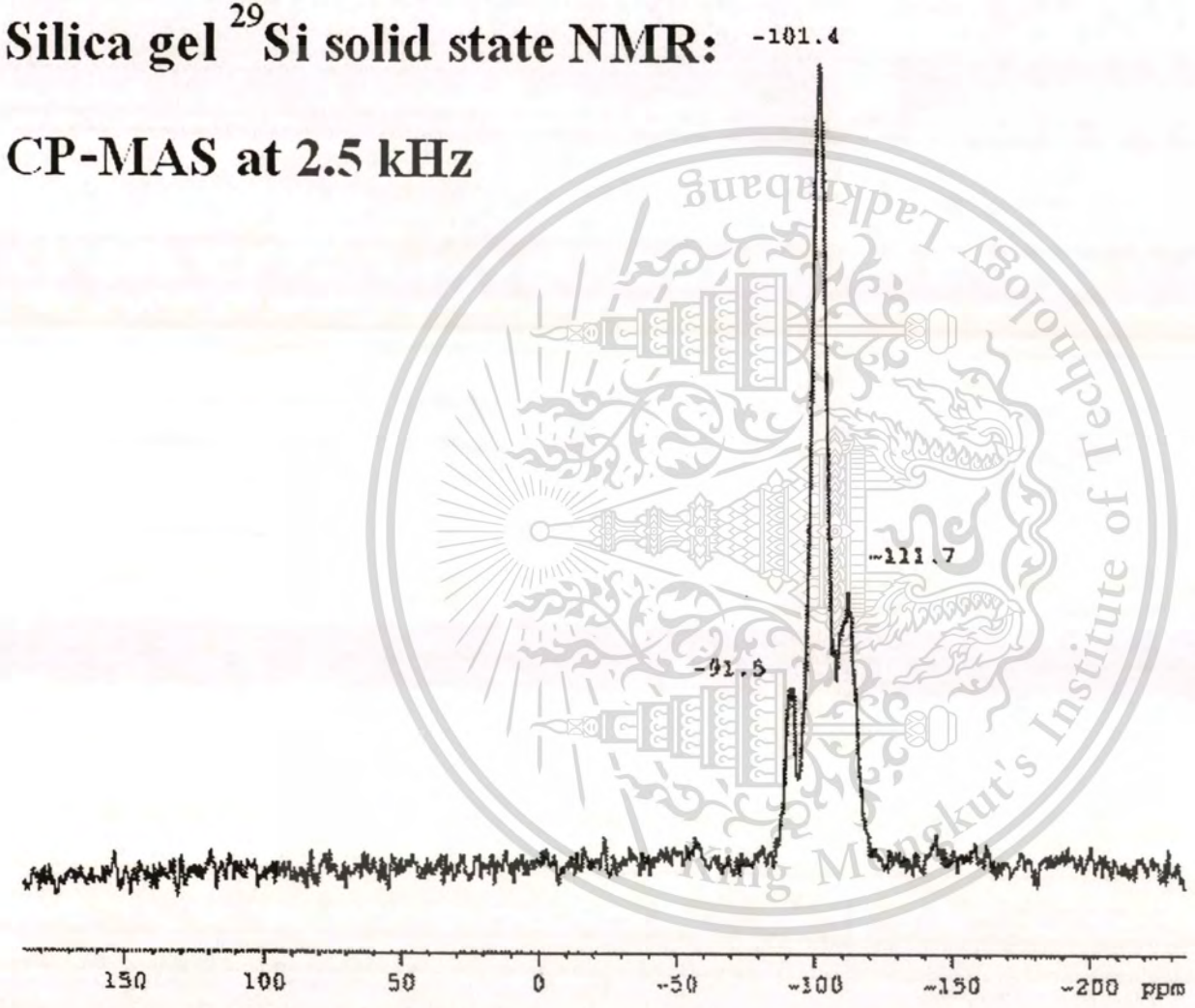

Fig. A-5 ^{29}Si solid state NMR: CP-MAS of silica gel.

```
Current Data Parameters
NAME          Silica_HPLC

F2 - Acquisition Parameters
Date           21/05/2003
Time                11.18
INSTRUM             drx300
PROBHD      5 mm Dual 13
PULPROG                 cp
TD                    1024
NS                    1024
DS                       0
SWH          25125.629 Hz
FIDRES       24.536747 Hz
AQ          0.0204276 sec
RG                    4096
DW           19.900 µsec
DE            6.00 µsec
TE             300.0 K
D1         3.00000000 sec
PL1            -2.45 dB
PL2            -6.00 dB
P3             5.50 µsec
SF02      300.1300000 MHz
NUC2                  1H
P15          2000.00 µsec
SF01       59.6261805 MHz
NUC1                29Si
PL12           -6.00 dB
DE            6.00 µsec

F1 - Acquisition parameters
ND0                     1
TD                     16
SF01          300.13 MHz
FIDRES       62.500000 Hz
SW            3.332 ppm

F2 - Processing parameters
SI                   2048
SF         59.627653 MHz
WDW                    EM
SSB                     0
LB                20.00 Hz
GB                      0
PC                   1.00

F1 - Processing parameters
SI                     16
MC2                    QF
SF        300.1300000 MHz
WDW                    no
SSB                     0
LB                0.30 Hz
GB                     0.1
```

Date: 10/30/2003

Quantachrome Corporation
Quantachrome Autosorb Automated Gas Sorption System Report
Autosorb for Windows® Version 1.19

Sample ID	Silica for GC column		
Description	20 Adsorption points, 20 Desorption point		
Comments			
Sample Weight	0.0462 g		
Adsorbate	NITROGEN	Outgas Temp 300°C	Operator kuk
Cross-Sec Area	16.2 Å²/molec	Outgas Time 27.0 hrs	
Analysis Time	543.7 min		
NonIdeality	6.580E-05	P/Po Toler 0	
End of Run	10/29/2003 04:59		
Molecular Wt	28.0134 g/mol	Equil Time 3	
File Name	461028_1.RAW		
Station #	1	Bath Temp. 77.40	

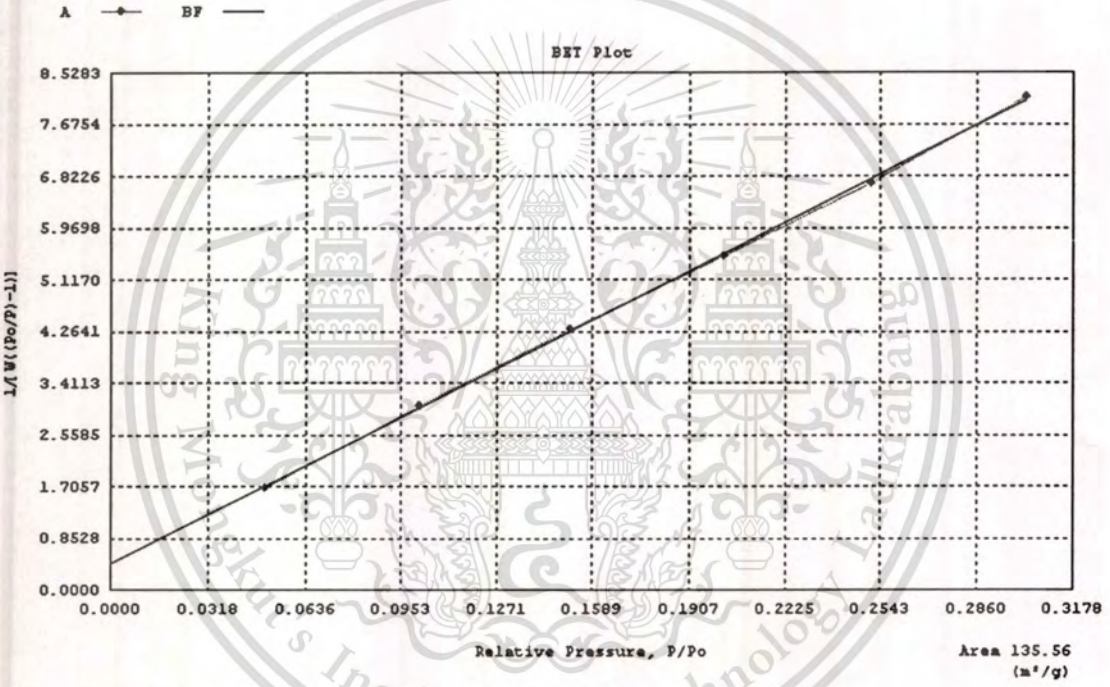

Fig. A-6 Silica gel for GC determined by BET method.

APPENDIX B

CHARACTERIZATION OF CHEMICALLY MODIFIED SILICA

QUANTACHROME CORPORATION
Ultrapycnometer 1000 Version 2.12
Analysis Report

Sample & User Parameters

Sample ID: Silica-ODS
Weight: 1.0176 grams
Analysis Temperature: 25.4 degC

Date: 04-25-03
Time: 11:17:14
User ID: Kuk

Analysis Parameters

Cell Size: Small
V added - Small:13.2408 cc
V cell: 14.1469 cc
Target Pressure: 17.0 psi
Equilibrium Time: Auto
Flow Purge: 2.00 min.
Maximum Runs: 5
Number of Runs Averaged: 5

Results

Deviation Requested: 0.005 % Deviation Achieved: +/- 0.2663 %
Average Volume: 0.6160 cc Std. Dev. : 0.0039 cc
Average Density: 1.6519 g/cc Std. Dev. : 0.0105 g/cc
Coefficient of Variation: 0.6390 %

Tabular Data

RUN	VOLUME (cc)	DENSITY (g/cc)
1	0.6224	1.6349
2	0.6178	1.6470
3	0.6153	1.6539
4	0.6139	1.6577
5	0.6107	1.6662

Fig. B-1 True density of silica-ODS determined using He-ultrapycnometer.

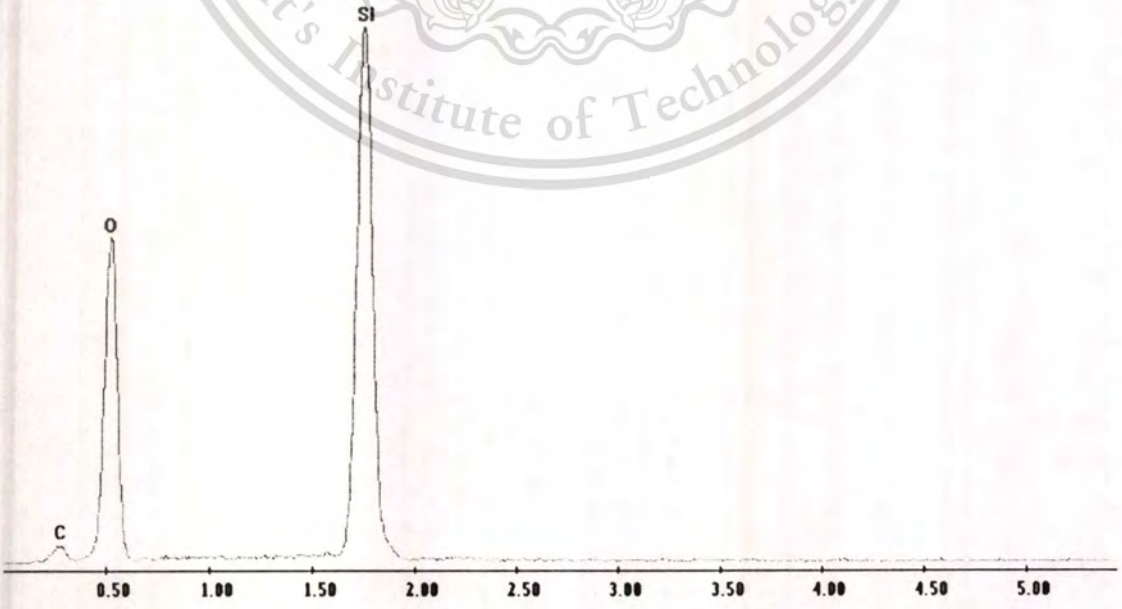

Fig. B-2 EDS spectra for silica-ODS determined using SEM-EDS.

EDAX ZAF Quantification (Standardless)
Element Normalized
SEC Table : Default

Elem	Wt %	At %	K-Ratio	Z	A	F
C K	16.22	26.47	0.0175	1.0428	0.1032	1.0002
O K	28.61	35.04	0.0596	1.0230	0.2036	1.0004
SiK	55.17	38.49	0.4599	0.9701	0.8593	1.0000
Total	100.00	100.00				

Element	Net Inte.	Backgrd Inte.	Error	P/B
C K	12.70	2.10	7.24	6.05
O K	126.35	2.80	2.03	45.13
SiK	1439.10	10.35	0.59	139.04

Elem	Wt %	At %	K-Ratio	Z	A	F
C K	17.93	25.30	0.0309	1.0283	0.1677	1.0005
O K	55.25	58.52	0.1540	1.0089	0.2761	1.0002
SiK	26.82	16.18	0.1940	0.9544	0.7581	1.0000
Total	100.00	100.00				

Element	Net Inte.	Backgrd Inte.	Error	P/B
C K	36.80	6.60	4.30	5.58
O K	533.55	6.80	0.98	78.46
SiK	993.15	8.40	0.72	118.23

Elem	Wt %	At %	K-Ratio	Z	A	F
C K	13.79	20.08	0.0219	1.0309	0.1537	1.0005
O K	55.79	60.98	0.1619	1.0114	0.2869	1.0002
SiK	30.42	18.94	0.2208	0.9572	0.7582	1.0000
Total	100.00	100.00				

Element	Net Inte.	Backgrd Inte.	Error	P/B
C K	24.05	3.40	5.16	7.07
O K	519.10	5.40	0.99	96.13
SiK	1045.35	7.90	0.70	132.32

Elem	Wt %	At %	K-Ratio	Z	A	F
C K	19.34	27.01	0.0344	1.0274	0.1730	1.0005
O K	55.03	57.69	0.1512	1.0081	0.2725	1.0002
SiK	25.62	15.30	0.1852	0.9535	0.7582	1.0000
Total	100.00	100.00				

Element	Net Inte.	Backgrd Inte.	Error	P/B
C K	43.30	3.55	3.67	12.20
O K	554.70	5.80	0.96	95.64
SiK	1003.30	10.30	0.71	97.41

c:\edax32\genesis\genesis.spc
Label :Spec10 Lower Al on Si 15 kV 9 kcps
Current Time : 16:46:16 Date : 2-Apr-2003

kV: 15.00 Tilt: 0.00 Take-off: 13.30 Tc: 35.0
Det Type:SUTW, Sapphire Res: 131.50 Lsec: 20

Fig. B-3 EDS data for carbon loading determined using SEM-EDS.

EDAX ZAF Quantification (Standardless)
Element Normalized
SEC Table : Default

Elem	Wt %	At %	K-Ratio	Z	A	F
C K	14.07	22.20	0.0168	1.0391	0.1152	1.0003
O K	38.83	46.01	0.0912	1.0195	0.2302	1.0003
SiK	47.10	31.79	0.3731	0.9661	0.8198	1.0000
Total	100.00	100.00				

Element	Net Inte.	Backgrd Inte.	Error	P/B
C K	15.25	1.95	6.42	7.82
O K	240.55	3.30	1.46	72.89
SiK	1453.80	12.90	0.59	112.70

Elem	Wt %	At %	K-Ratio	Z	A	F
C K	21.58	31.55	0.0307	1.0327	0.1377	1.0003
O K	41.12	45.13	0.0942	1.0132	0.2260	1.0003
SiK	37.30	23.32	0.2888	0.9592	0.8072	1.0000
Total	100.00	100.00				

Element	Net Inte.	Backgrd Inte.	Error	P/B
C K	34.50	2.50	4.07	13.80
O K	308.50	3.70	1.29	83.38
SiK	1397.05	8.55	0.60	163.40

Elem	Wt %	At %	K-Ratio	Z	A	F
C K	17.77	26.22	0.0255	1.0330	0.1388	1.0004
O K	45.93	50.88	0.1140	1.0135	0.2448	1.0003
SiK	36.30	22.90	0.2756	0.9595	0.7913	1.0000
Total	100.00	100.00				

Element	Net Inte.	Backgrd Inte.	Error	P/B
C K	27.55	2.00	4.56	13.77
O K	359.10	3.25	1.19	110.49
SiK	1282.10	9.45	0.63	135.67

Elem	Wt %	At %	K-Ratio	Z	A	F
C K	21.20	30.27	0.0333	1.0301	0.1522	1.0004
O K	46.88	50.24	0.1148	1.0107	0.2423	1.0002
SiK	31.92	19.49	0.2400	0.9564	0.7861	1.0000
Total	100.00	100.00				

Element	Net Inte.	Backgrd Inte.	Error	P/B
C K	40.15	2.50	3.74	16.06
O K	403.90	4.10	1.12	98.51
SiK	1246.55	12.10	0.64	103.02

c:\edax32\genesis\genesis.spc
Label :Spec10 Lower Al on Si 15 kV 9 kcps
Current Time : 16:46:16 Date : 2-Apr-2003

kV: 15.00 Tilt: 0.00 Take-off: 13.30 Tc: 35.0
Det Type:SUTW, Sapphire Res: 131.50 Lsec: 20

Fig. B-4 EDS data for carbon loading determined using SEM-EDS (continued).

EDAX ZAF Quantification (Standardless)
Element Normalized
SEC Table : Default

Elem	Wt %	At %	K-Ratio	Z	A	F
C K	19.04	27.13	0.0309	1.0296	0.1576	1.0004
O K	51.08	54.65	0.1337	1.0101	0.2591	1.0002
SiK	29.89	18.22	0.2206	0.9558	0.7721	1.0000
Total	100.00	100.00				

Element	Net Inte.	Backgrd Inte.	Error	P/B
C K	35.35	3.20	4.09	11.05
O K	445.65	5.30	1.07	84.08
SiK	1085.85	9.65	0.68	112.52

Elem	Wt %	At %	K-Ratio	Z	A	F
C K	20.16	28.50	0.0335	1.0289	0.1612	1.0004
O K	50.87	53.98	0.1317	1.0095	0.2564	1.0002
SiK	28.97	17.51	0.2137	0.9551	0.7723	1.0000
Total	100.00	100.00				

Element	Net Inte.	Backgrd Inte.	Error	P/B
C K	39.85	3.45	3.84	11.55
O K	457.10	5.10	1.06	89.63
SiK	1095.20	9.00	0.68	121.69

Elem	Wt %	At %	K-Ratio	Z	A	F
C K	13.79	20.28	0.0210	1.0320	0.1473	1.0005
O K	53.66	59.25	0.1513	1.0125	0.2784	1.0002
SiK	32.55	20.47	0.2388	0.9584	0.7656	1.0000
Total	100.00	100.00				

Element	Net Inte.	Backgrd Inte.	Error	P/B
C K	22.35	3.25	5.37	6.88
O K	469.85	5.45	1.04	86.21
SiK	1095.65	10.55	0.68	103.85

c:\edax32\genesis\genesis.spc
Label :Spec10 Lower Al on Si 15 kV 9 kcps
Current Time : 16:46:16 Date : 2-Apr-2003

kV: 15.00 Tilt: 0.00 Take-off: 13.30 Tc: 35.0
Det Type:SUTW, Sapphire Res: 131.50 Lsec: 20

Fig. B-5 EDS data for carbon loading determined using SEM-EDS (continued).

Silica-ODS :Run Number 3

Silica-ODS

Source: Analyzed

Measured on: Tue, May 06, 1003 2:51 PM

Presentation: (2OHD) 1.330, 1.530+i0.10000
Polydisperse model Volume Result Focus = 300 mm.
Residual = 1.151% Concentration = 0.013% Obscuration = 10.83%
d (0.5) = 14.92 µm d (0.1) = 3.93 µm d (0.9) = 31.21 µm
D [4, 3] = 17.97 µm Span = 1.83
Sauter Mean (D[3, 2]) = 9.20 µm Mode = 17.70 µm
Specific Surface Area = 0.6521 sq. m. / gm Density = 1.00 gm. / cc.

Size (Lo), µm	Result In, %	Size (Hi), µm	Result, Below %
0.50	0.00	1.32	0.00
1.32	0.49	1.60	0.49
1.60	1.09	1.95	1.59
1.95	1.72	2.38	3.31
2.38	2.30	2.90	5.61
2.90	2.76	3.53	8.36
3.53	3.05	4.30	11.42
4.30	3.26	5.24	14.68
5.24	3.60	6.39	18.28
6.39	4.38	7.78	22.66
7.78	5.81	9.48	28.46
9.48	7.87	11.55	36.33
11.55	10.26	14.08	46.60
14.08	12.05	17.15	58.64
17.15	12.36	20.90	71.00
20.90	10.78	25.46	81.78
25.46	8.00	31.01	89.79
31.01	5.06	37.79	94.85
37.79	2.74	46.03	97.59
46.03	1.26	56.09	98.84
56.09	0.43	68.33	99.27
68.33	0.00	83.26	99.27
83.26	0.00	101.44	99.27
101.44	0.00	123.59	99.27
123.59	0.00	150.57	99.28
150.57	0.13	183.44	99.40
183.44	0.28	223.51	99.68
223.51	0.23	272.31	99.91
272.31	0.08	331.77	100.00
331.77	0.00	404.21	100.00
404.21	0.00	492.47	100.00
492.47	0.00	600.00	100.00

Fig. B-6 Particle size distribution of silica-ODS after selected with sedimentation and centrifugation.

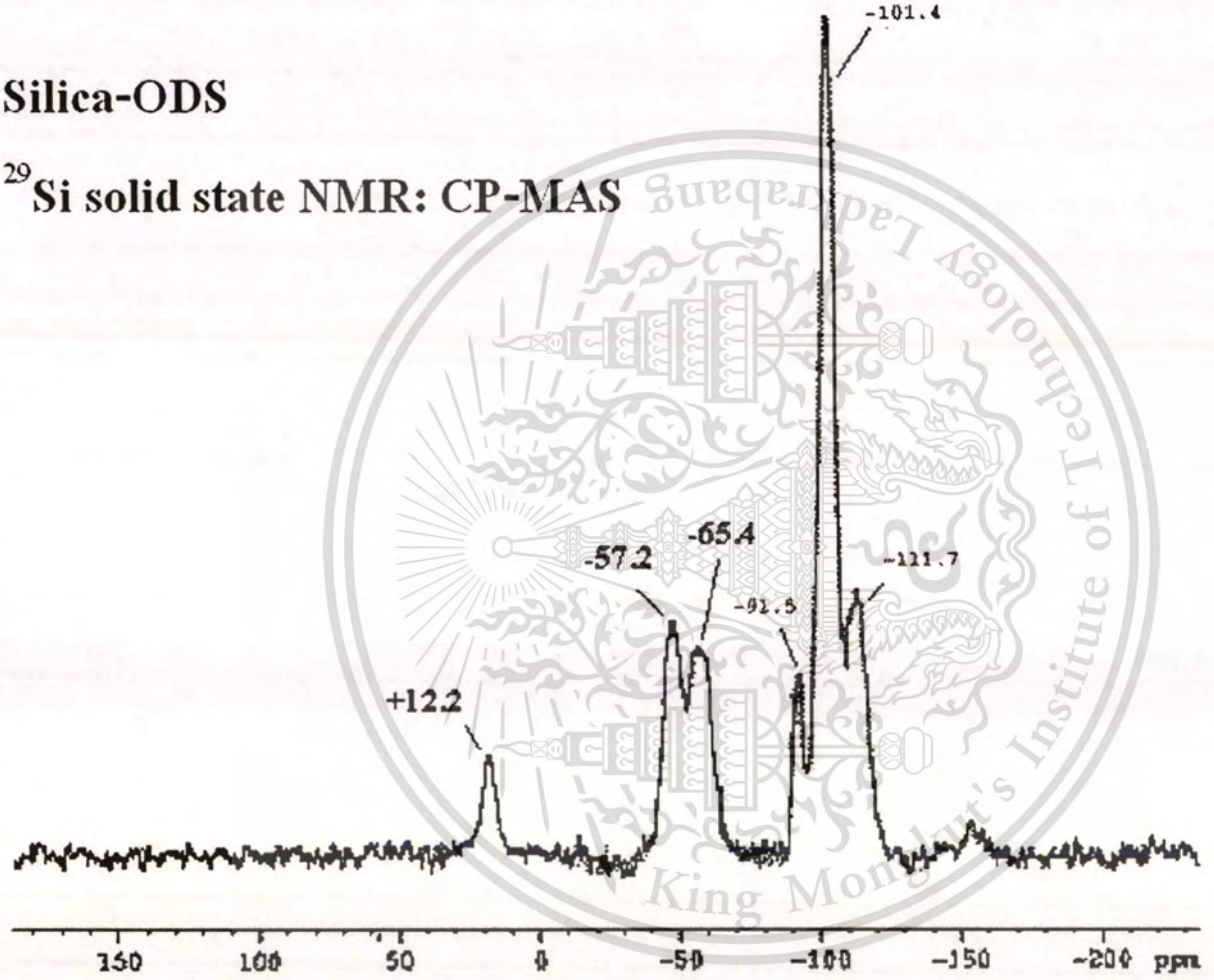


```
Current Data Parameters
NAME          Silica-ODS

F2 - Acquisition Parameters
Date          10/09/2003
Time              14.23
INSTRUM           drx300
PROBHD      5 mm Dual 13
PULPROG             cp
TD                1024
NS                1024
DS                   0
SWH         25125.629 Hz
FIDRES      24.536747 Hz
AQ          0.0204276 sec
RG                4096
DW           19.900 µsec
DE            6.00 µsec
TE             300.0 K
D1         3.00000000 sec
PL1           -2.45 dB
PL2           -6.00 dB
P3             5.50 µsec
SFO2     300.1300000 MHz
NUC2              1H
P15         2000.00 µsec
SFO1      59.6261805 MHz
NUC1             29Si
PL12          -6.00 dB
DE            6.00 µsec

F1 - Acquisition parameters
NDO                  1
TD                  16
SFO1        300.13 MHz
FIDRES    62.500000 Hz
SW          3.332 ppm

F2 - Processing parameters
SI                2048
SF        59.627653 MHz
WDW               EM
SSB                  0
LB           20.00 Hz
GB                   0
PC                1.00

F1 - Processing parameters
SI                  16
MC2                 QF
SF       300.1300000 MHz
WDW                 no
SSB                  0
LB           0.30 Hz
GB                 0.1
```

Fig. B-7 ^{29}Si solid state NMR: CP-MAS of silica-ODS.

Table B-1 Percent carbon loading (*%C*) and surface coverage (χ) of ligand on silica-ODS: 3 x 3 μm^2 determination area (rice husk HPLC column).

Carbon loading (*%C*)	Surface coverage (χ) (mol/m^2)
16.22	3.2424E-06
17.93	3.7121E-06
13.79	2.6280E-06
19.34	4.1254E-06
14.07	2.6958E-06
21.58	4.8361E-06
17.77	3.6668E-06
21.20	4.7105E-06
19.04	4.0354E-06
20.16	4.3775E-06
13.79	2.6280E-06
Average of *%C* = 17.72 ± 2.90	Average of surface coverage = 3.70 ± 0.81 $\mu mol/m^2$

APPENDIX C

CHROMATOGRAPHIC EVALUATION

Table C-1 Chromatographic parameter calculation for rice husk GC column.

Flow (ml/min)	t_r (min)	$W_{0.1}$	A	B	N^*	H (cm)
3.11	52.233	6.000	0.60	0.60	1404.562	0.128154
6.76	32.466	3.500	0.30	0.40	1794.021	0.100333
12.85	21.900	2.500	0.18	0.32	1765.494	0.101954
20.70	16.566	2.000	0.50	0.70	1456.487	0.123585
30.03	13.483	1.833	0.50	0.60	1082.992	0.166206
42.02	11.366	1.666	0.40	0.60	1012.639	0.177753
53.19	9.816	1.500	0.40	0.50	871.1015	0.206635
66.67	8.666	1.333	0.40	0.40	783.3045	0.229796

Note: N^* were calculated from equation 2.6 in chapter 2.

Table C-2 Chromatographic parameter calculation for rice husk HPLC column.

Flow rate(ml/min)	Retention time (min)	Peak width (min)	N^*	H (cm)
0.2	39.183	8.250	360.9171	0.0693
0.3	17.167	2.967	535.6409	0.0467
0.4	11.033	1.917	529.9843	0.0472
0.5	8.133	1.533	450.3366	0.0555
0.6	6.483	1.267	418.9081	0.0597
0.7	5.383	1.050	420.5234	0.0594
0.8	4.567	0.900	411.9998	0.0607
0.9	3.983	0.850	351.3199	0.0712
1.0	3.817	0.867	310.1174	0.0806
1.1	3.417	0.800	291.8972	0.0856
1.2	3.083	0.733	283.0473	0.0883

Note: N^* were calculated from equation 2.5 in chapter 2.

Table C-3 Data for linearity plot of phenol (40-200 ppm): 5.0 µl at 0.3 ml/min of 100% Methanol (rice husk HPLC column).

Concentration (ppm)	Peak area	Retention time (min)	Average peak area
40	602,963	17.022	616,728
	629,079	17.410	
	618,143	17.395	
80	1,237,587	17.102	1,243,960
	1,256,545	17.240	
	1,237,747	17.145	
120	1,919,594	17.064	1,912,286
	1,913,978	17.301	
	1,903,287	17.410	
160	2,526,263	16.952	2,495,811
	2,524,479	17.203	
	2,436,691	16.983	
200	3,473,373	17.222	3,442,263
	3,324,706	17.065	
	3,528,710	17.365	

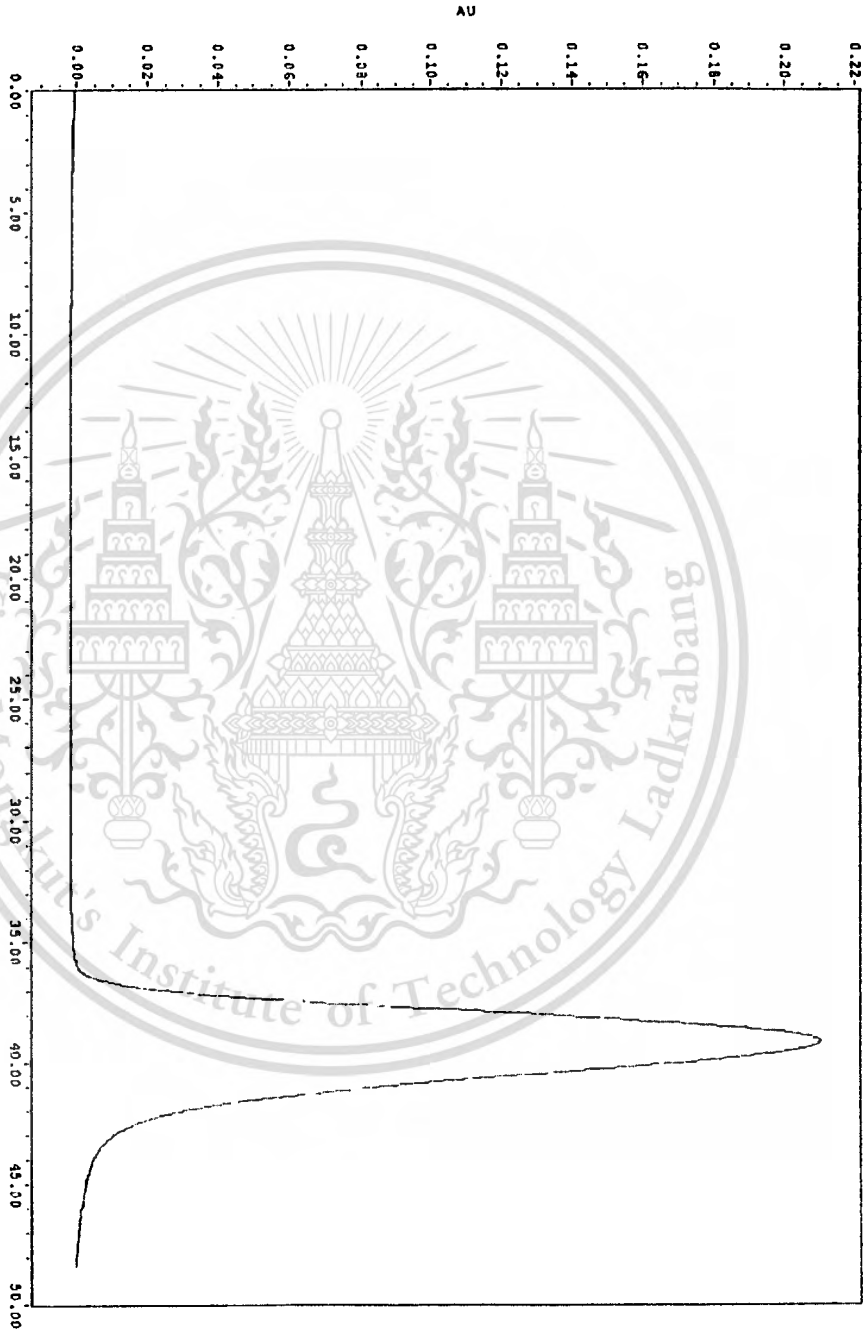

Fig. C-1 Chromatógram of phenol 5000 ppm; 1.0 µl; at 0.2 ml/min of 100% methanol (rice husk HPLC column).

Fig. C-2 Chromatogram of phenol 5000 ppm; 1.0 µl; at 0.3 ml/min of 100% methanol (rice husk HPLC column).

Fig. C-3 Chromatogram of phenol 5000 ppm; 1.0 µl; at 0.4 ml/min of 100% methanol (rice husk HPLC column).

Fig. C-4 Chromatogram of phenol 5000 ppm; 1.0 µl; at 0.5 ml/min of 100% methanol (rice husk HPLC column).

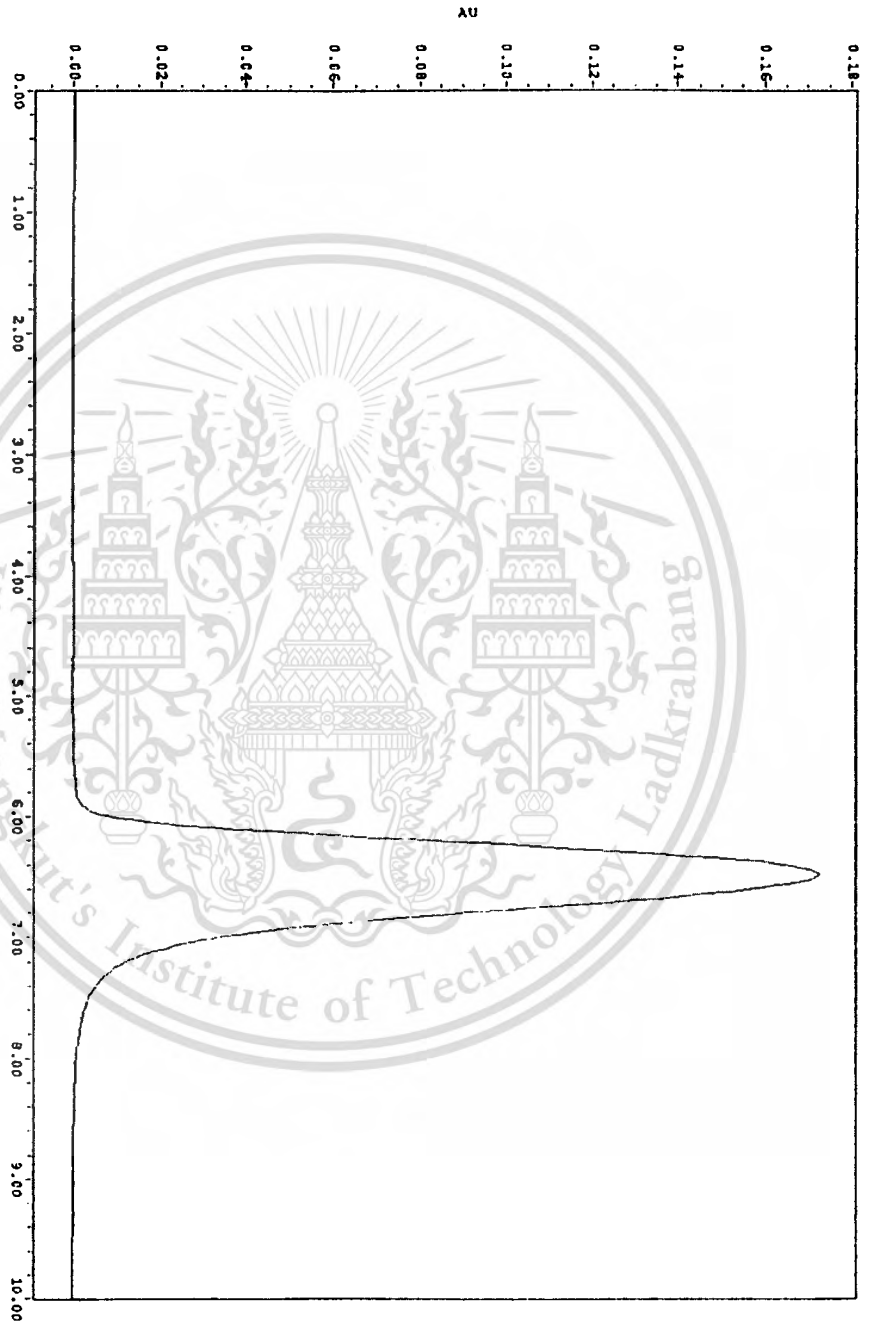

Fig. C-5 Chromatogram of phenol 5000 ppm; 1.0 µl; at 0.6 ml/min of 100% methanol (rice husk HPLC column).

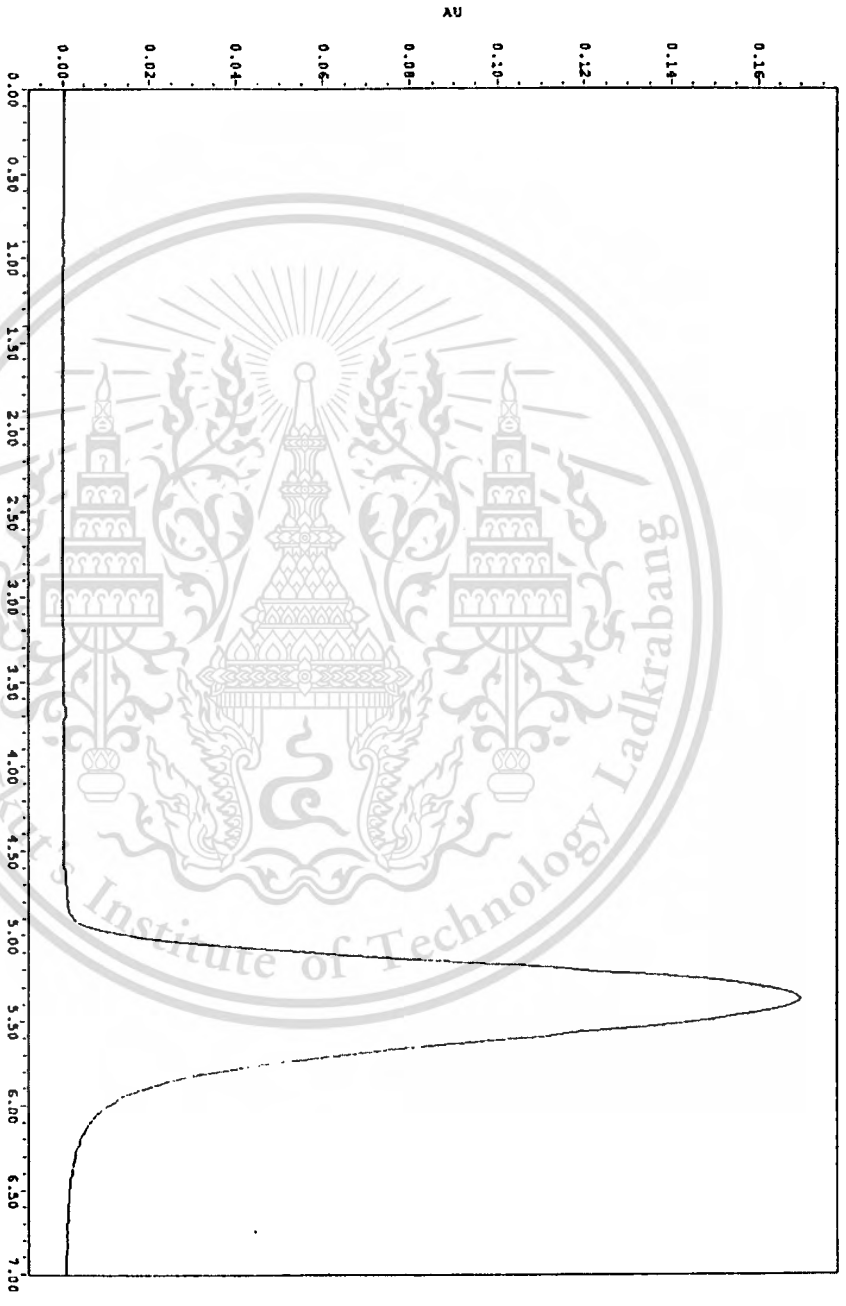

Fig. C-6 Chromatogram of phenol 5000 ppm; 1.0 µl; at 0.7 ml/min of 100% methanol (rice husk HPLC column).

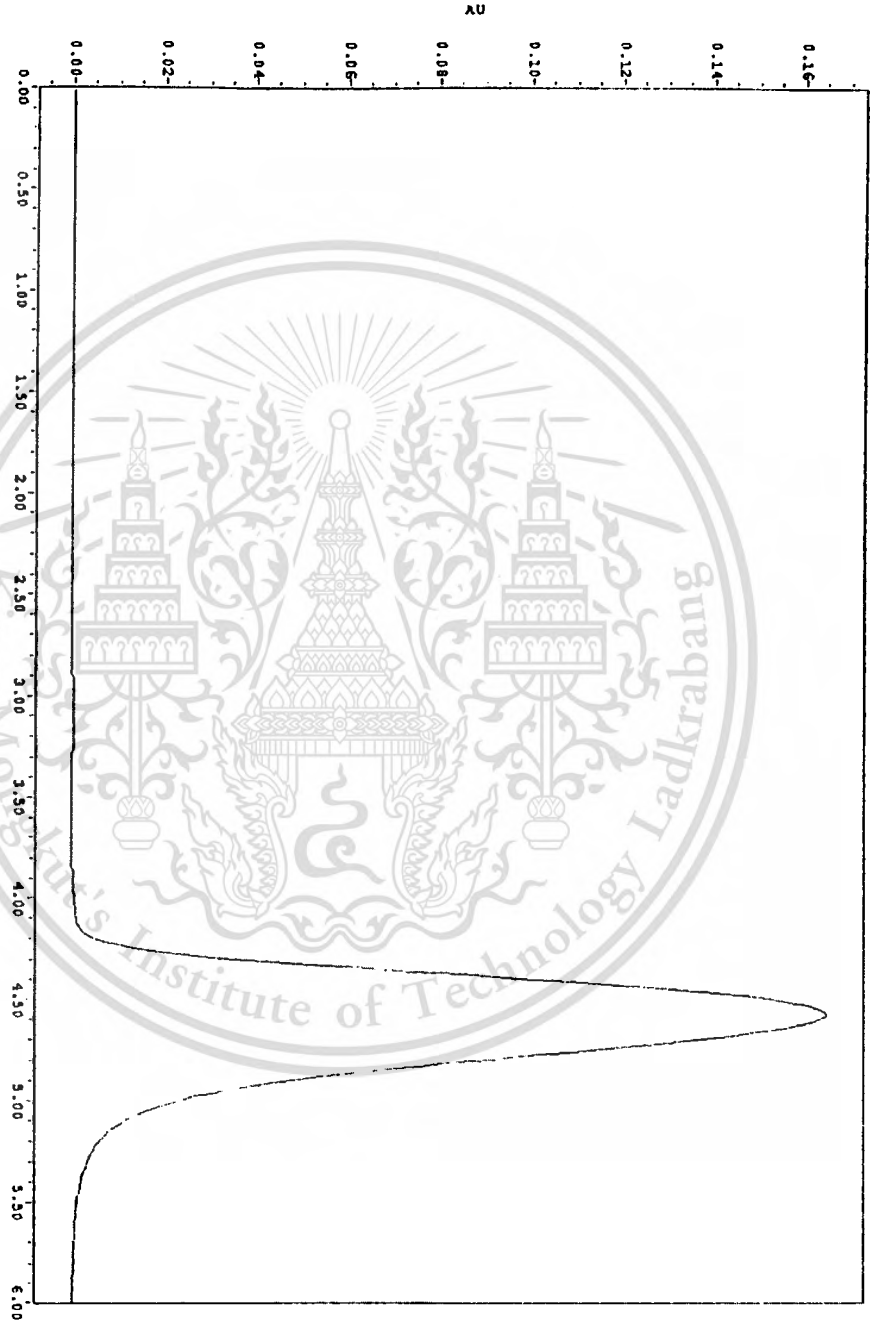

Fig. C-7 Chromatogram of phenol 5000 ppm; 1.0 µl; at 0.8 ml/min of 100% methanol (rice husk HPLC column).

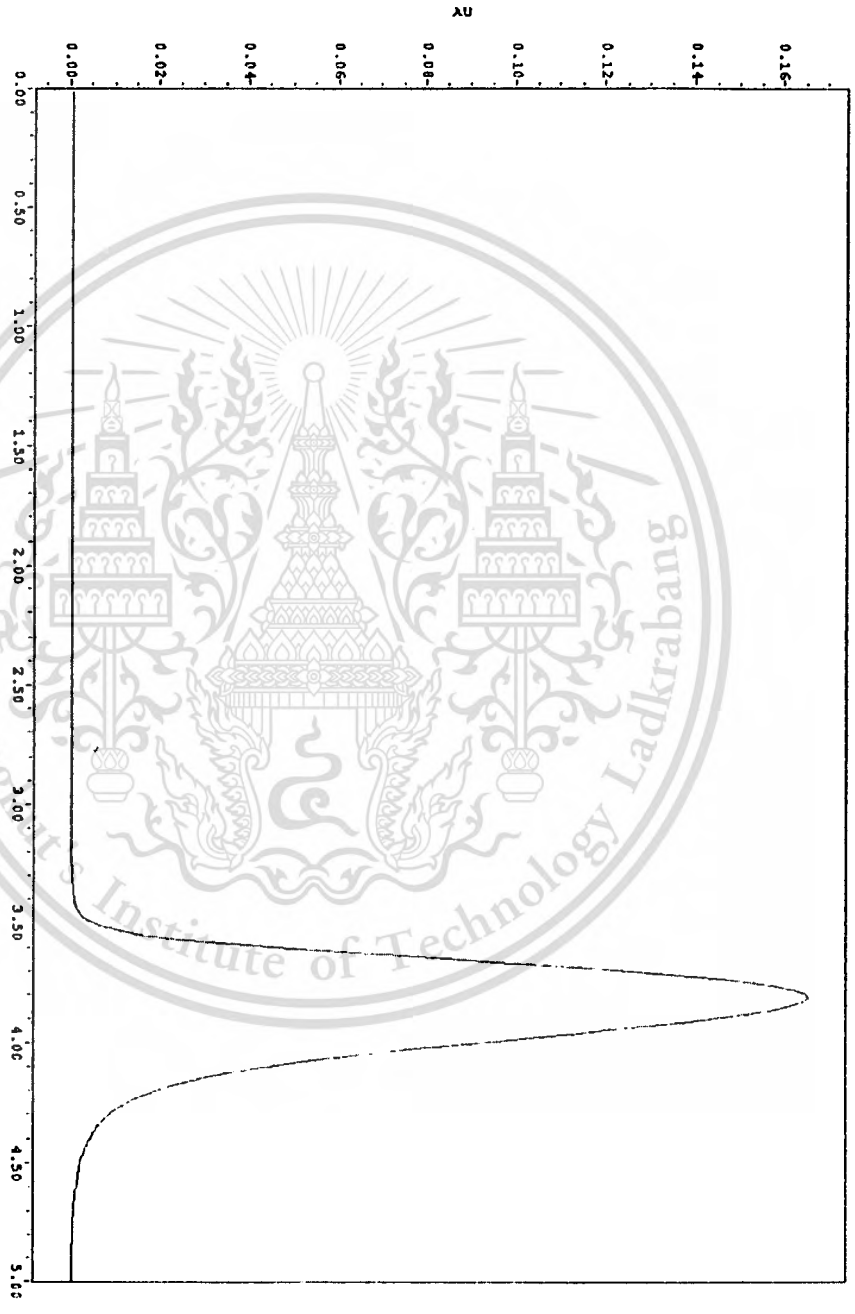

Fig. C-8 Chromatogram of phenol 5000 ppm; 1.0 µl; at 0.9 ml/min of 100% methanol (rice husk HPLC column).

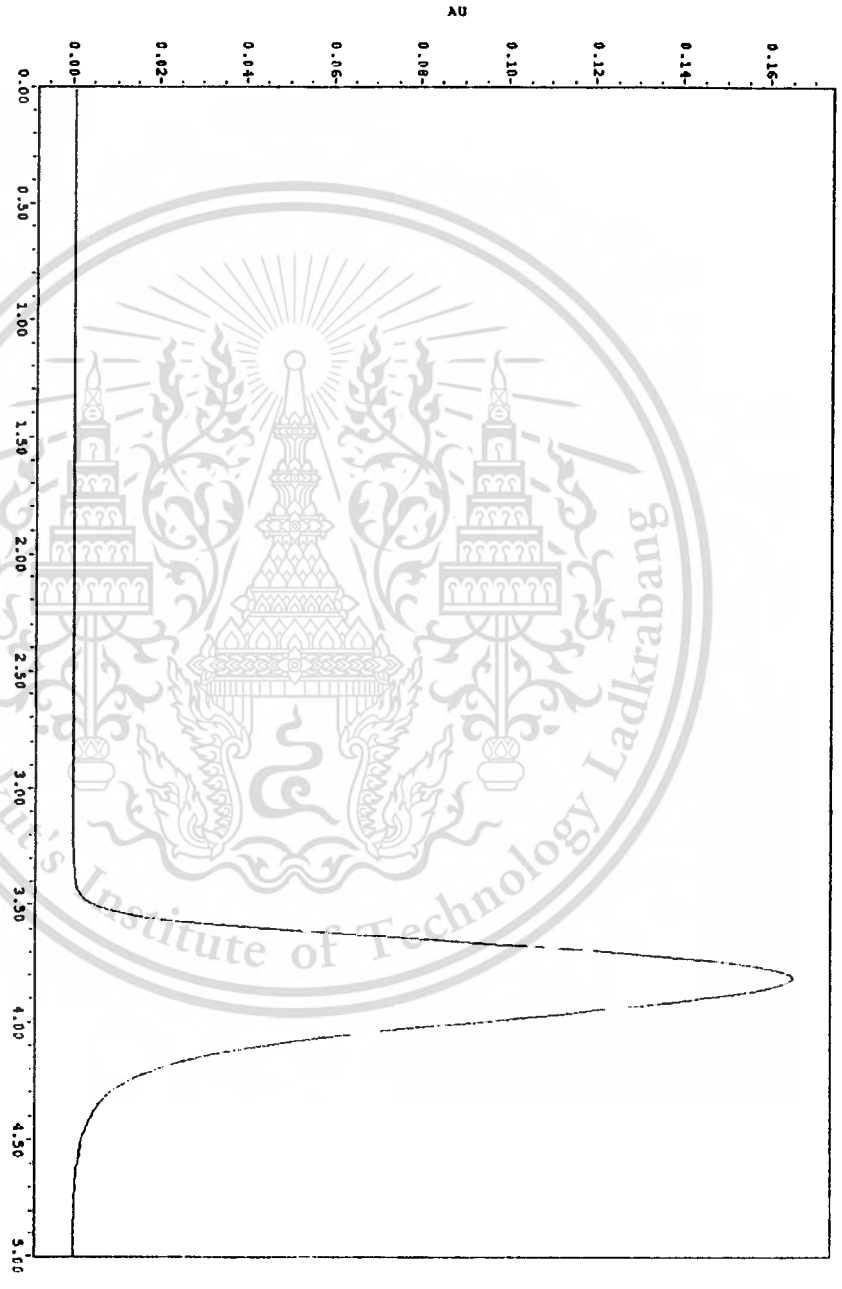

Fig. C-9 Chromatogram of phenol 5000 ppm; 1.0 µl; at 1.0 ml/min of 100% methanol (rice husk HPLC column).

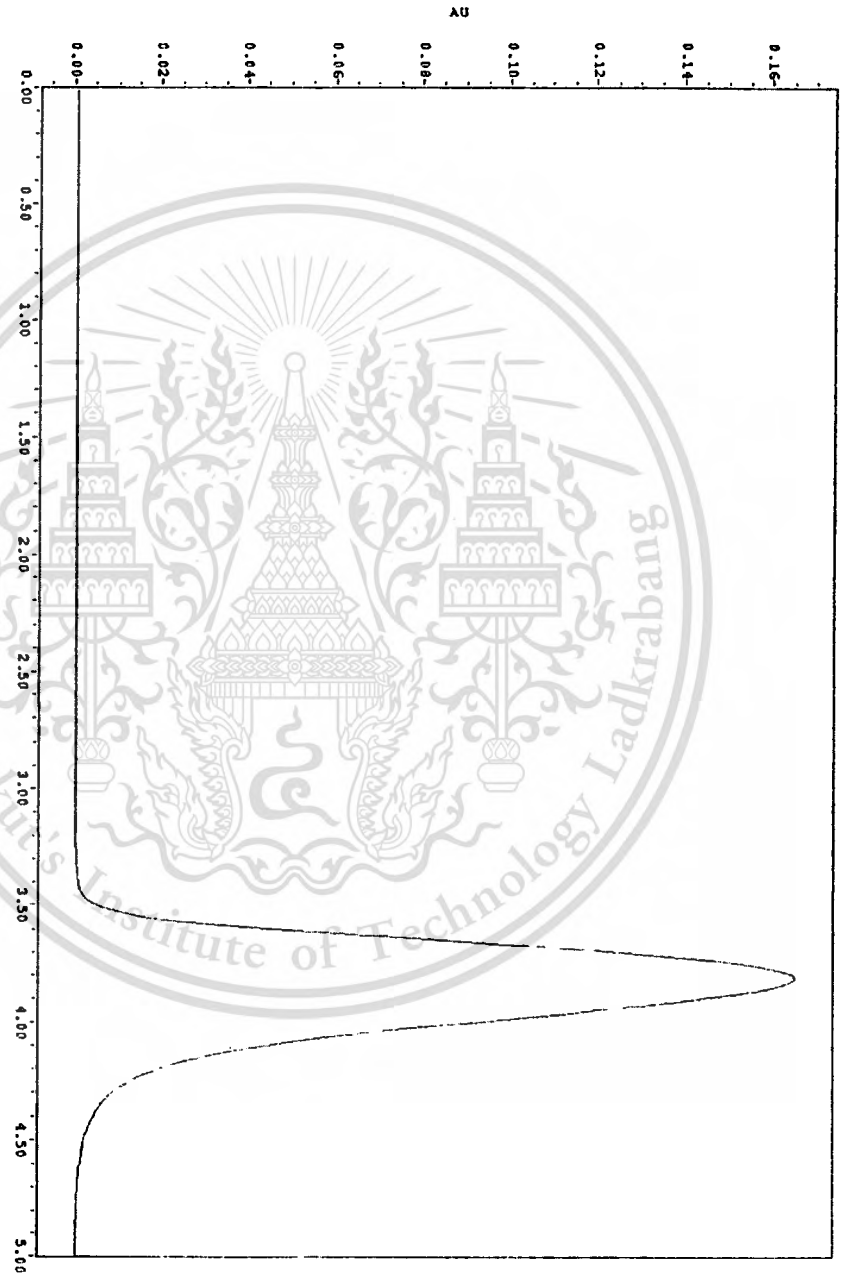

Fig. C-9 Chromatogram of phenol 5000 ppm; 1.0 µl; at 1.0 ml/min of 100% methanol (rice husk HPLC column).

Fig. C-11 Chromatogram of phenol 5000 ppm; 1.0 µl; at 1.2 ml/min of 100% methanol (rice husk HPLC column).

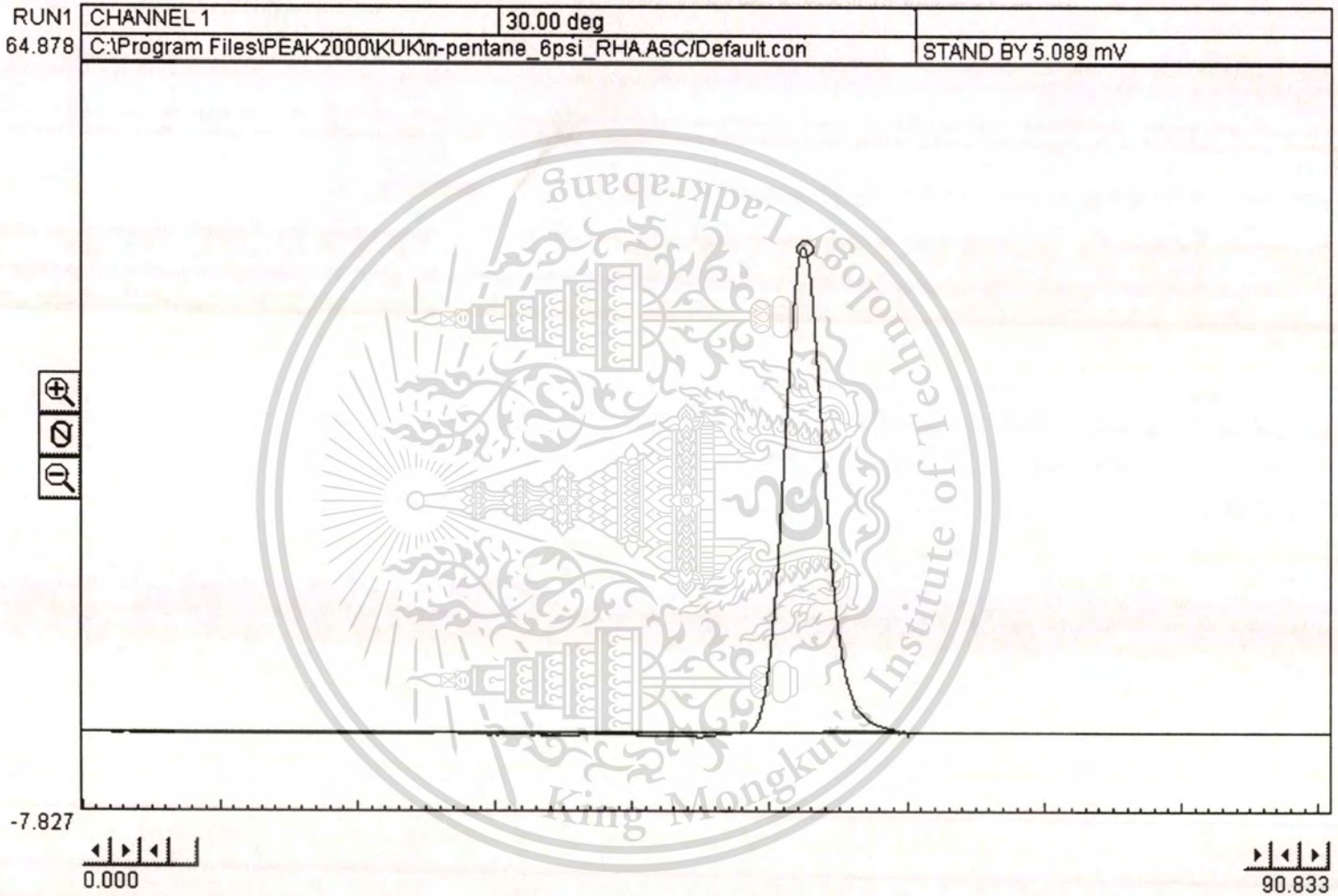

Fig. C-12 Chromatogram of n-pentane; 0.2 µl; at 6 psi of N_2 carrier gas (rice husk GC column).

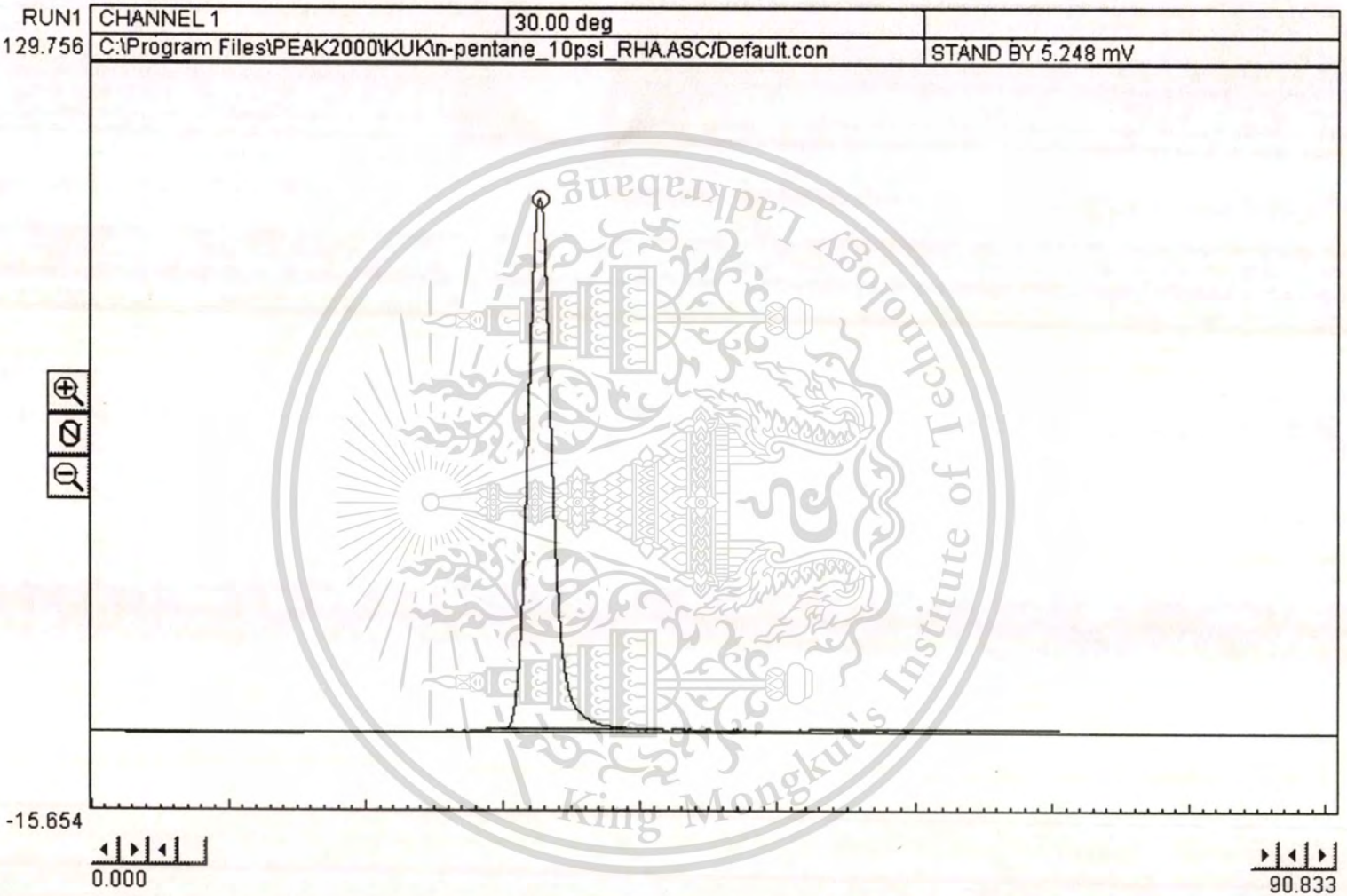

Fig. C-13 Chromatogram of n-pentane; 0.2 µl; at 10 psi of N_2 carrier gas (rice husk GC column).

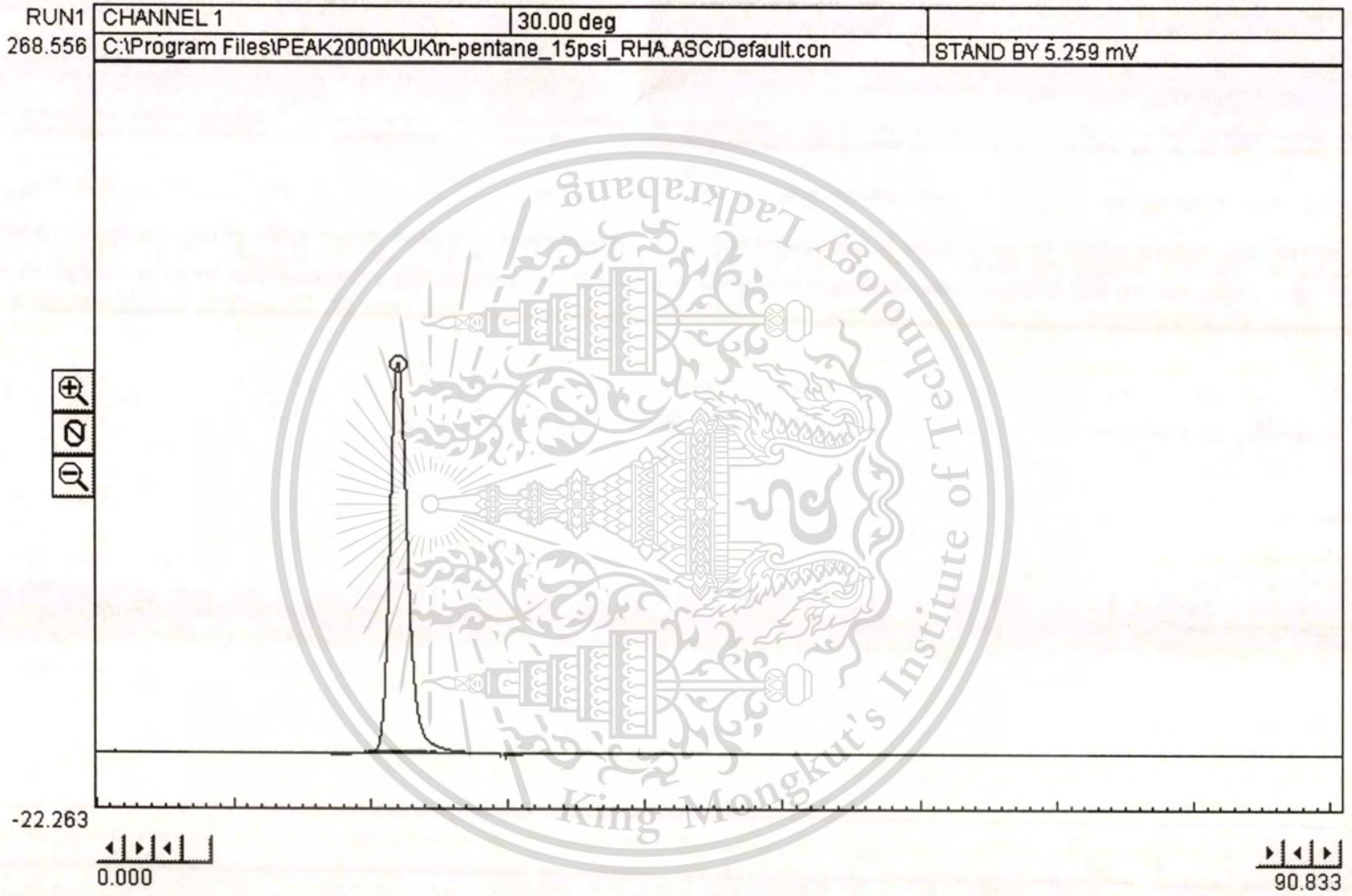

Fig. C-14 Chromatogram of n-pentane; 0.2 µl; at 15 psi of N_2 carrier gas (rice husk GC column).

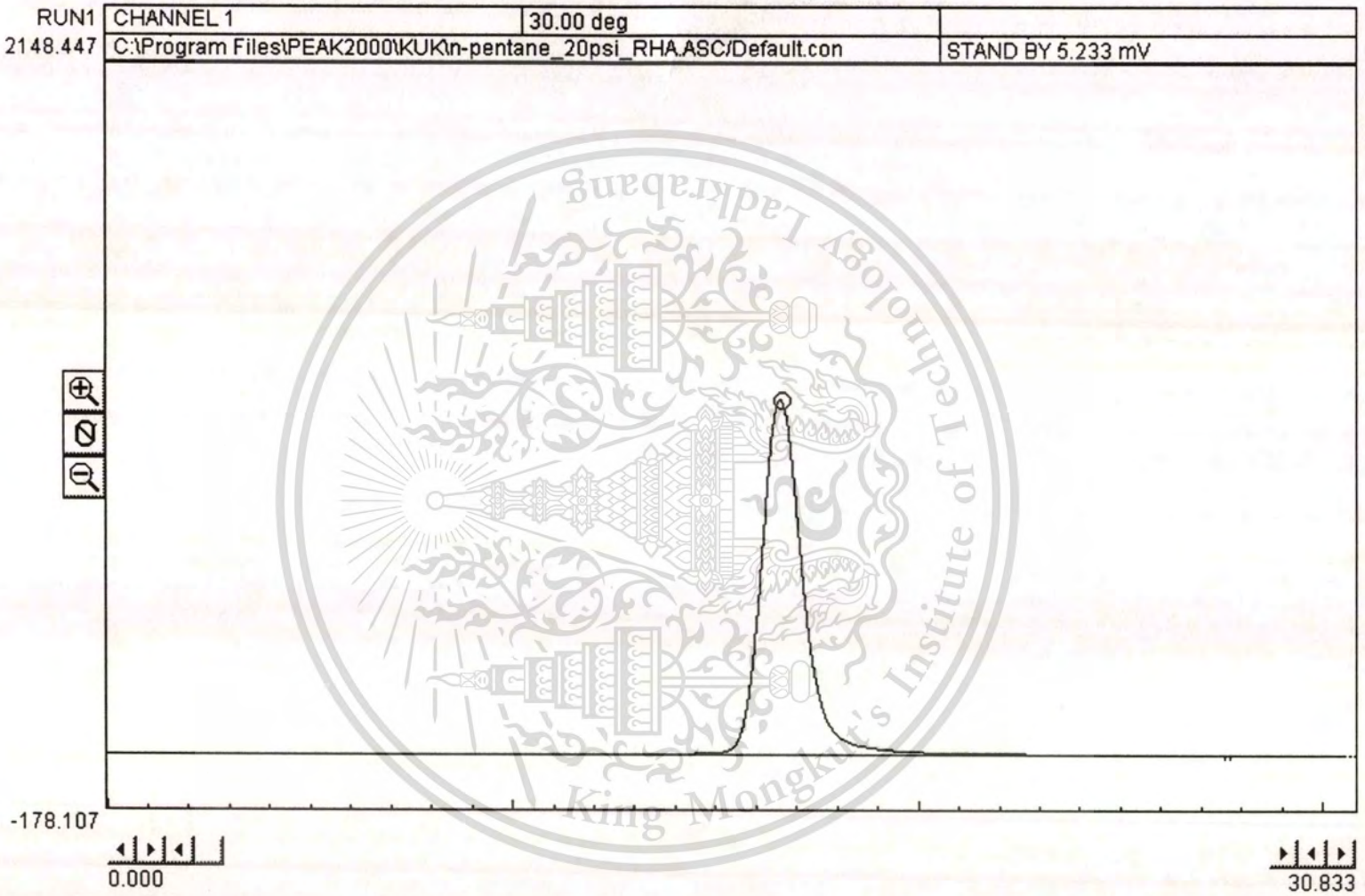

Fig. C-15 Chromatogram of n-pentane; 0.2 µl; at 20 psi of N_2 carrier gas (rice husk GC column).

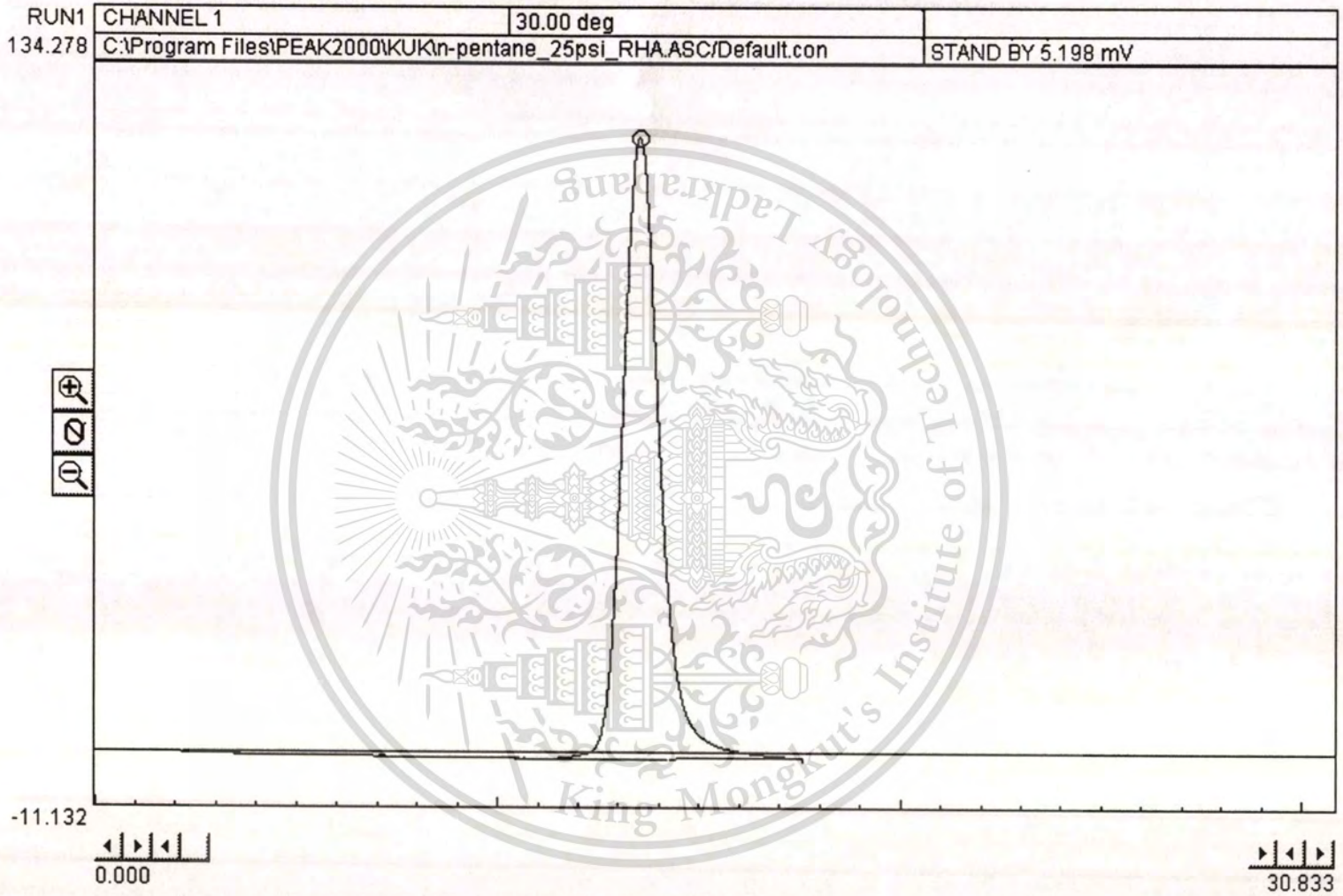

Fig. C-16 Chromatogram of n-pentane; 0.2 µl; at 25 psi of N_2 carrier gas (rice husk GC column).

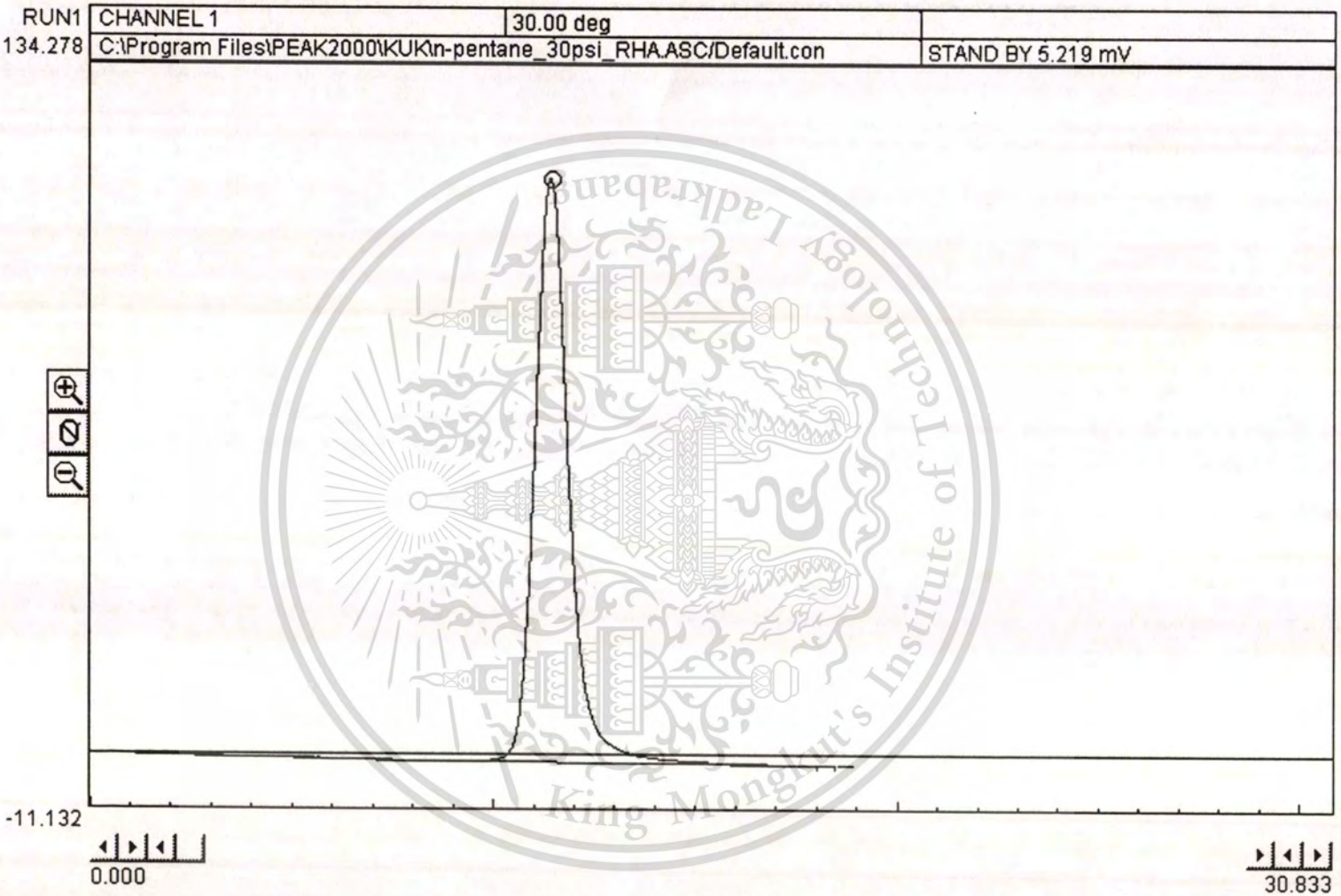

Fig. C-17 Chromatogram of n-pentane; 0.2 µl; at 30 psi of N_2 carrier gas (rice husk GC column).

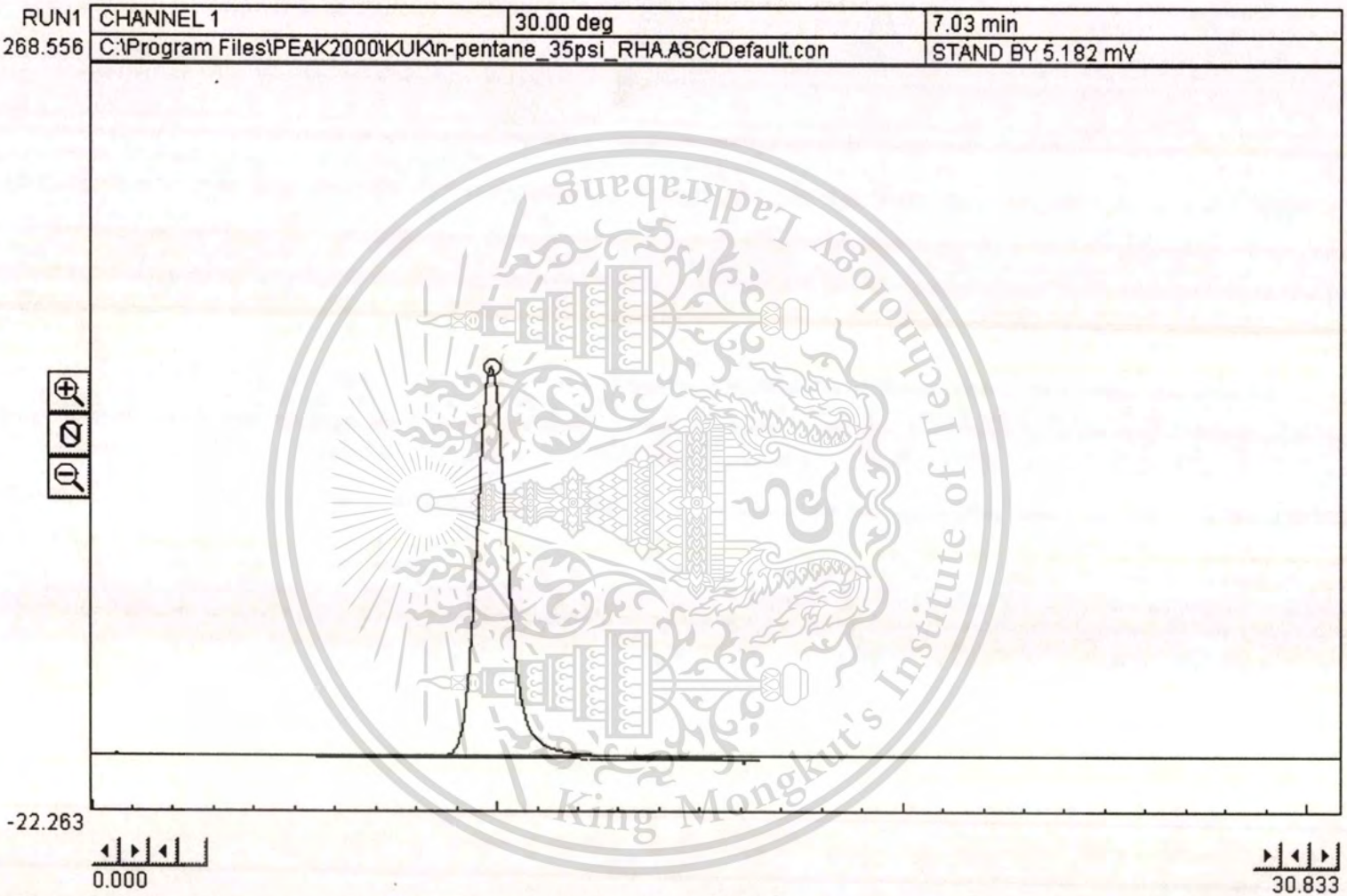

Fig. C-18 Chromatogram of n-pentane; 0.2 µl; at 35 psi of N_2 carrier gas (rice husk GC column).

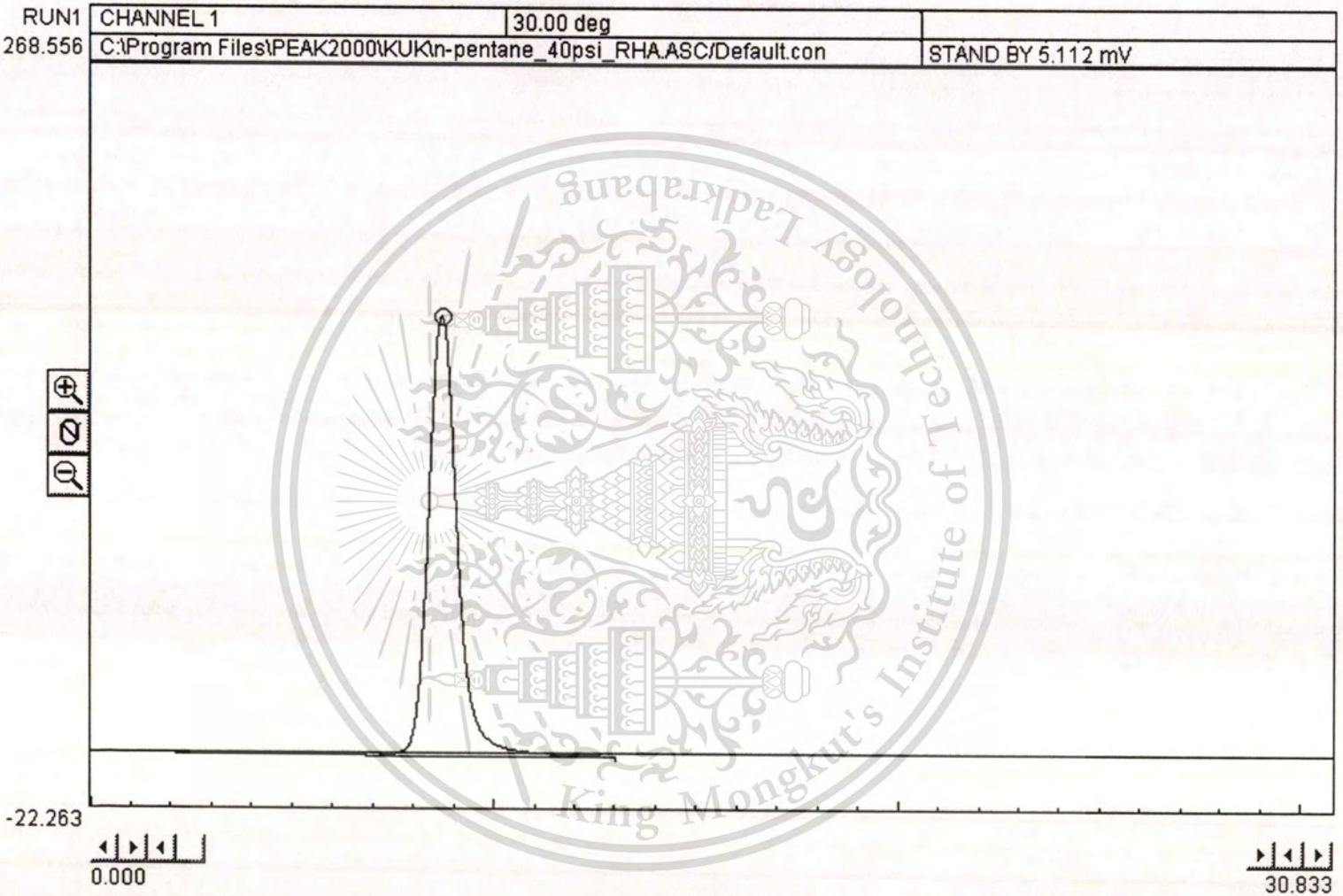

Fig. C-19 Chromatogram of n-pentane; 0.2 µl; at 40 psi of N_2 carrier gas (rice husk GC column).

APPENDIX D

EXPERIMENT FLOWCHARTS

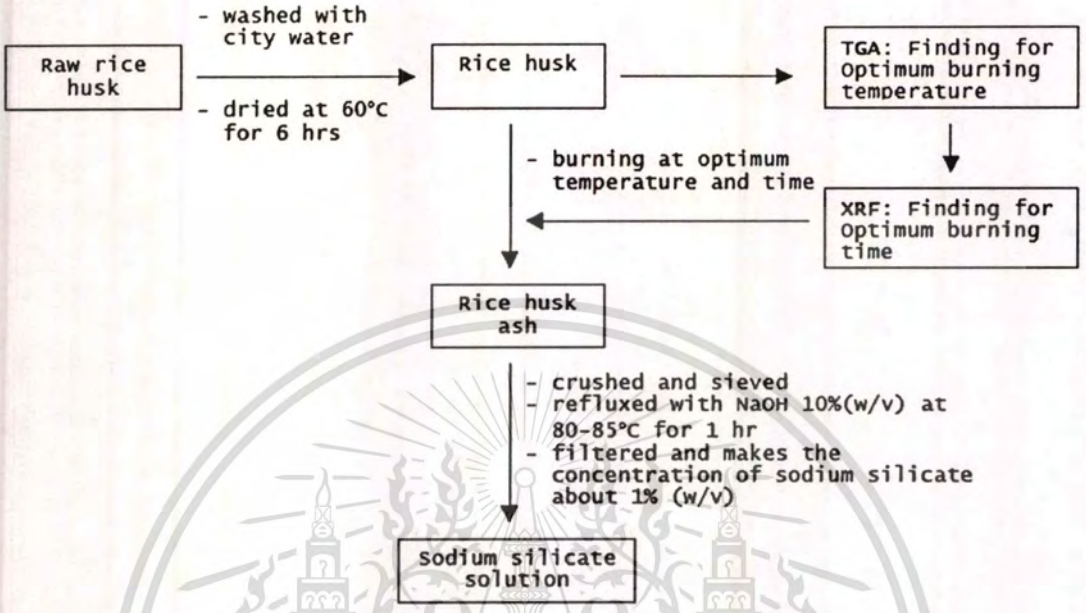

Fig. D-1 Sodium silicate synthesis process.

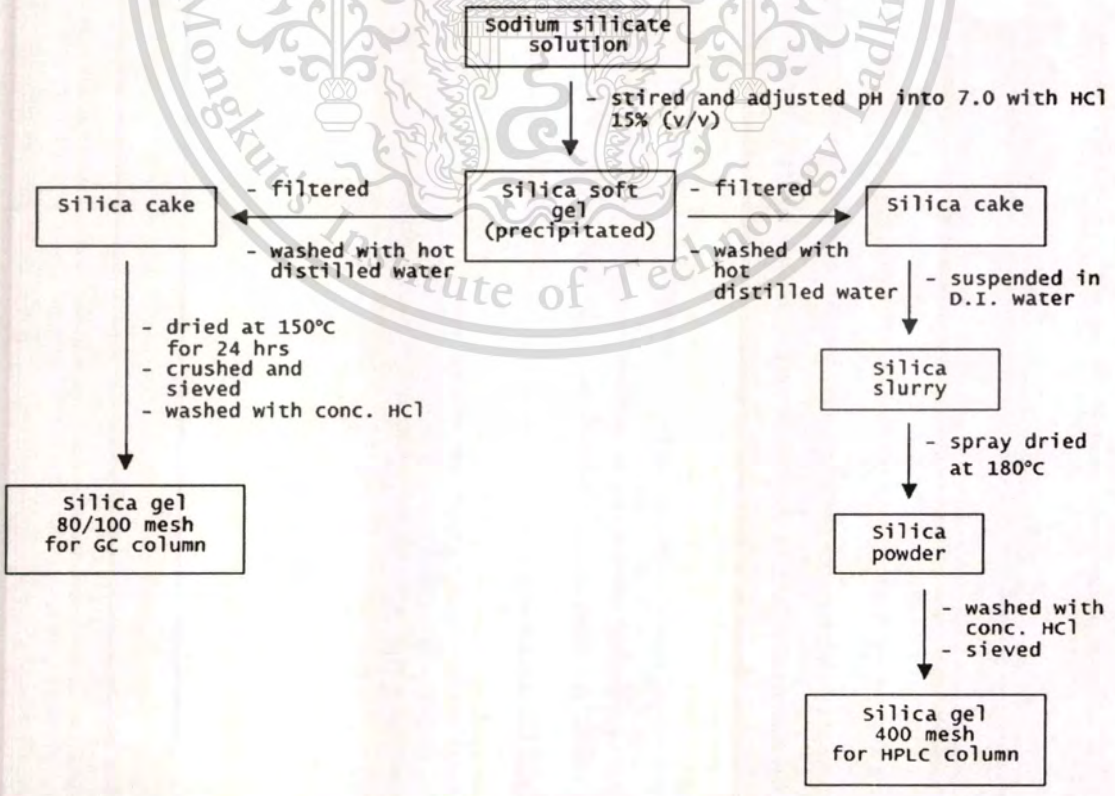

Fig. D-2 Silica particles for GC and HPLC column synthesis process.

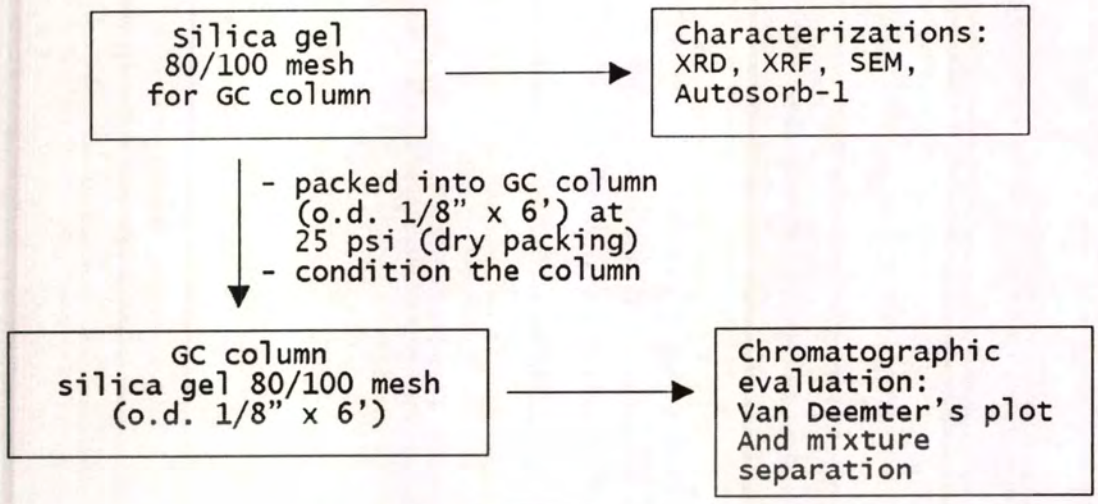

Fig. D-3 GC column preparation and testing processes.

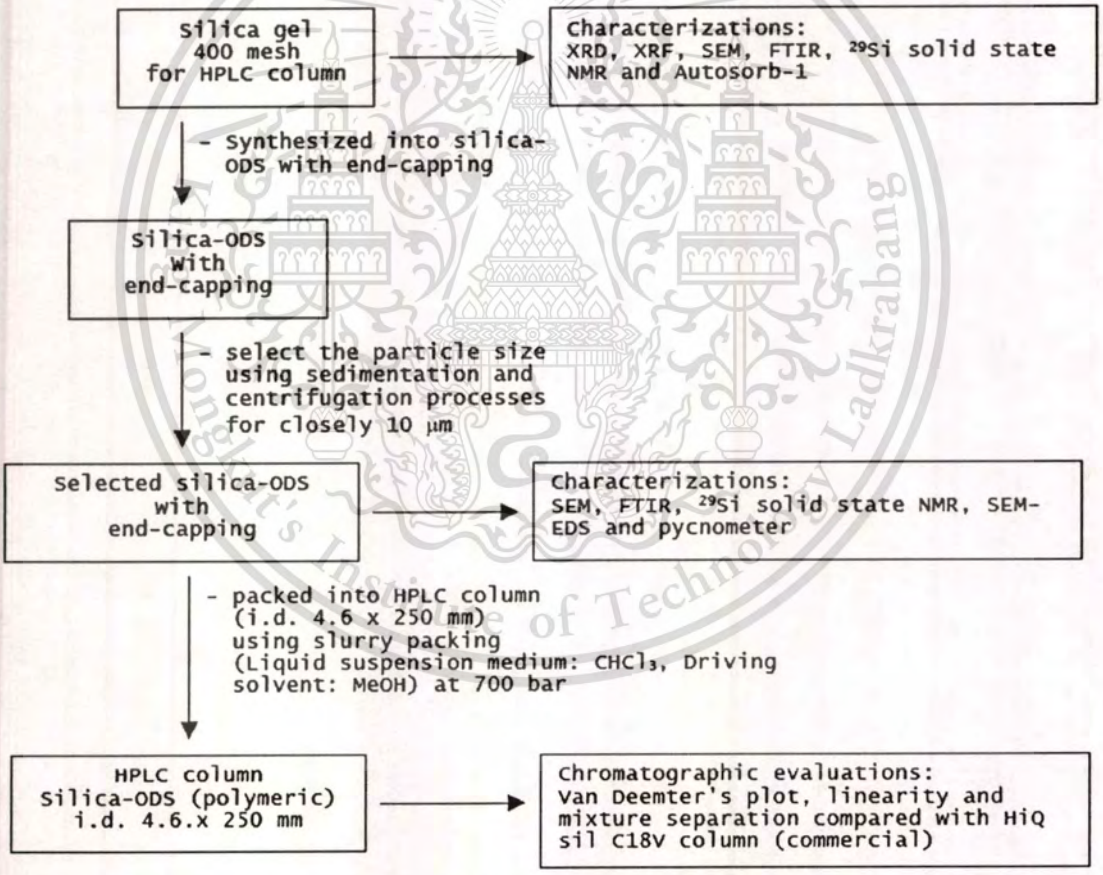

Fig. D-4 HPLC column preparation and testing processes.

BIOGRAPHY

Mr. Damrongsak Jadsadapattarakul was born on September 28, 1978 in Bangkok Thailand. He was graduated with Bachelor degree of Science in Chemistry from Prince of Songkla University, Hatyai, Thailand in 2000.

After graduated, he has worked in Technical and Lab Service (Chemist) position at Executive Chemical Co., Ltd. from 2000 to 2001. While he study in first year of Master degree at King Mongkut's Institute of Technology Ladkrabang, he has part-time worked at Semiconductor Technology Research Laboratory (STRL), The National Metals and Materials Technology Center (MTEC) with Assistant Researcher position from 2002 to 2003 in solar cell project. In the same time, he has worked in Teacher Assistant position at King Mongkut's Institute of Technology Ladkrabang. After that, he has part-time worked in Assistant Researcher position at The National Metals and Materials Technology Center (MTEC) in nanotechnology project from June. 2003 to Jan. 2004. Now, he has funding support for Ph.D. study in nanotechnology field (Thailand Graduate Institute of Science and Technology, TGIST) from The National Nanotechnology Center (NANOTEC), National Science and Technology Development Agency (NSTDA).